Structure-activity Relationships of Small Molecule Autotaxin Inhibitors with a Discrete Binding Mode

Lisa M. Miller,[a] *Willem-Jan Keune,*[b] *Diana Castagna,*[a] *Louise C. Young,*[c] *Emma L. Duffy,*[a] *Frances Potjewyd,*[a] *Fernando Salgado-Polo,*[b] *Paloma Engel García,*[a] *Dima Semaan,*[b] *John M. Pritchard,*[d] *Anastassis Perrakis,*[b] *Simon J. F. Macdonald,*[d] *Craig Jamieson,*[a] and Allan J. B. Watson*[a]*

[a] WestCHEM, Department of Pure and Applied Chemistry, University of Strathclyde, Thomas Graham Building, 295 Cathedral Street, Glasgow, UK.

[b] Division of Biochemistry, Netherlands Cancer Institute/Antoni van Leeuwenhoek, Plesmanlaan 121, 1066 CX, Amsterdam, Netherlands

[c] Strathclyde Institute of Pharmacy and Biomolecular Science, University of Strathclyde, John Arbuthnott Building (Hamnet Wing), 161 Cathedral Street, Glasgow, UK

[d] Fibrosis Discovery Performance Unit, GlaxoSmithKline, Medicines Research Centre, Gunnels Wood Road, Stevenage, UK

ABSTRACT

Autotaxin (ATX) is a secreted enzyme responsible for the hydrolysis of lysophosphatidylcholine (LPC) to the bioactive lysophosphatidic acid (LPA) and choline. The ATX-LPA signalling pathway is implicated in cell survival, migration, and proliferation; thus, the inhibition of ATX is a recognized therapeutic target for a number of diseases including fibrotic diseases, cancer, and inflammation, amongst others. Many of the developed synthetic inhibitors for ATX have resembled the lipid chemotype of the native ligand; however, a small number of inhibitors have

been described that deviate from this common scaffold. Herein, we report the structure-activity relationships (SAR) of a previously reported small molecule ATX inhibitor. We show through enzyme kinetics studies that analogues of this chemotype are noncompetitive inhibitors, and using a crystal structure with ATX we confirm the discrete binding mode.

INTRODUCTION

Autotaxin (ATX) is a secreted glycoprotein phosphodiesterase belonging to the ectonucleotide pyrophosphatase and phosphodiesterase family (ENPP).[1] ATX mediates the hydrolysis of lysophosphatidylcholine (LPC) **1** to the ubiquitous bioactive lipid mediator lysophosphatidic acid (LPA) **2** and choline **3** (Scheme 1).[2] **2** acts on the LPA receptors; a series of G-protein coupled receptors (GPCRs), of which six have been identified to date, termed LPA_{1-6}, with an additional three pending the publication of evidence to verify their categorization (GPR87, P2Y10, and GPR35).[3] Upon binding, a series of intracellular signaling pathways are invoked which could result in a range of cellular functions including differentiation, migration, proliferation, and survival.[4] Deregulation of the ATX-LPA signaling pathway is implicated in a variety of disease states and could lead to the development of several diseases including vascularization diseases, autoimmune diseases, cancer, fibrotic diseases, inflammation, and neurodegeneration, amongst others.[5-10] Accordingly, the use of ATX inhibitors has been and continues to be an attractive strategy for therapeutic intervention (for a recent review see Castagna *et al.*[11]).

Scheme 1. ATX-Mediated Hydrolysis of LPC Releasing LPA: Disease States via LPA Action on the GPCRs LPA_{1-6}. R group = fatty acid chain with varying degrees of unsaturation.

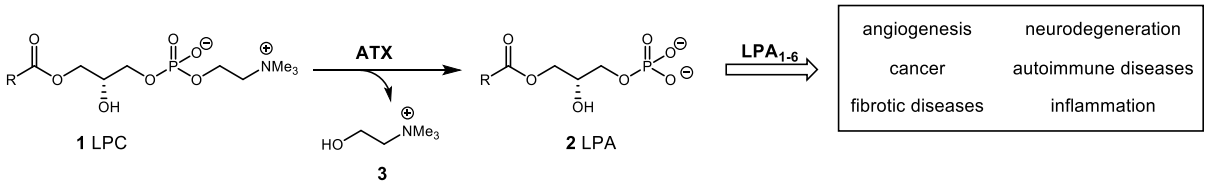

With respect to the endogenous ligand (**1**), it is perhaps unsurprising that many of the synthetic ligands developed for ATX have resembled the lipid chemotype: an acidic 'head' group linked through a variety of 'cores' to a lipophilic 'tail' (Figure 1: **4**, **5**, **6**, and **7**).[12] However, a comparatively smaller number of inhibitors have been described that deviate from this common scaffold, for example PAT-347 (**8**), reported by PharmAkea Therapeutics.[13] Lipid-based inhibitors have been previously reported to bind within the catalytic site of ATX and thus compete for the same region that the natural ligand is known to bind;[17] however, a recent report from PharmAkea found the small molecule inhibitor **8** to be a potent noncompetitive inhibitor of ATX, with a distinct mode of binding remote to the catalytic site.[13] This compound was noted to have a scaffold similar to our compound of interest, the indole-derived inhibitor **9** originally reported by Amira Pharmaceuticals.[18] The patent in which **8** and related analogues are claimed report the IC_{50} values in ≤0.5 μM, >0.5 but ≤3 μM, or >3 μM categories;[13] similarly, the patents in which analogues of **9** are reported also categorize the activities (IC_{50} <300 nM, 0.3-1 μM, or >1 μM).[18] From consideration of this data very little detailed SAR of these non-lipid-like ATX inhibitors can be extracted. Based on this, we generated a focused set of 50 analogues to explore the SAR of **9** in greater detail and to determine the features which contribute to its potency.

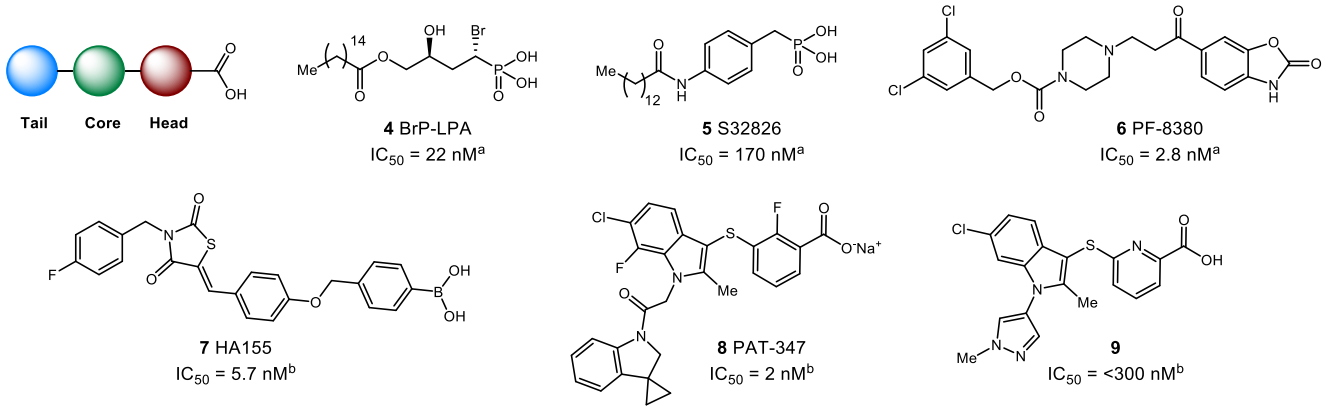

Figure 1. Lipid-Based Inhibitors and Small Molecule Inhibitors of ATX: **4**,[14] **5**,[15] **6**,[16] **7**,[17] **8**,[13] **9** (previously reported activity from patent literature).[18] [a] FS-3 assay; [b] LPC choline release assay.

Herein, we report the design, synthesis, and biological evaluation of our compound collection and describe the main determinants of potency regarding these indole-based compounds. We show that this chemotype has only limited activity in a bis-(*p*-nitrophenol) phosphate (bis-*p*NPP) based assay; however, using an LPC choline release assay a number of potent inhibitors were identified. Analysis of this data, combined with further kinetic studies into the mode of ATX inhibition, has furnished a new insight into the binding site of this chemotype. Furthermore, we report the crystal structure of ATX in complex with an analogue of **9**, confirming that this chemotype binds in the same discrete binding site identified by PharmAkea in the cocrystal of **8** with ATX.[13]

ATX Inhibition Assays. There are a number of *in vitro* assays that are currently used to evaluate ATX activity; these can be divided into two categories based on the type of substrate the assay utilizes (Table 1). The first category employs the natural ligand **1** and the second uses unnatural ATX substrates. As depicted in Scheme 1, ATX hydrolyzes **1** into **2** and **3**, thus the enzyme

activity can be determined by quantitative measurement of these products using liquid chromatography-tandem mass spectrometry (LCMS), radiometry, colorimetry, or fluorimetry.[19]

Table 1. Summary of ATX inhibition assays.

Category	**Substrate**	**Analysis**
Natural Substrate	LPC	LCMS,[19a] radiometry,[19b] colorimetry,[19c] fluorimetry[19d]
Unnatural Substrate	*p*NP-TMP[2]	Absorbance
	bis-*p*NPP[17]	Absorbance
	CPF4[20]	FRET
	FS-3[21]	Fluorescence
	TG-*m*TMP[22]	Fluorescence

Of assays based on **1**, a commonly used method measures the production of **3** using an enzyme-coupled colorimetric assay[19c] – choline oxidase converts **3** into betaine **10** and hydrogen peroxide, and then horseradish peroxidase (HRP) utilizes the hydrogen peroxide to oxidize a coloring substrate into its chromophoric state (Scheme 2). There is a risk of false positives associated with this assay as the molecules under analysis may inhibit the enzymes used in the coloring reactions;[23] however, control reactions can be employed to reveal any interference.

Scheme 2. ATX-mediated choline release colorimetric assay for ATX Inhibition. R group = fatty acid chain with varying degrees of unsaturation.

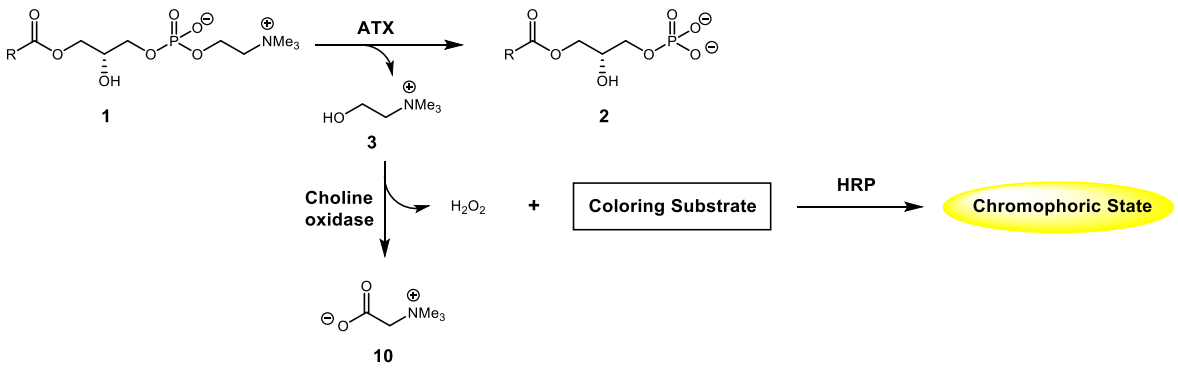

Accordingly, assays that employ synthetic substrates can appear to be advantageous over the LPC choline release assay as they do not require the use of these additional enzymes. There are a number of unnatural substrates widely used, including the nucleotide thymidine 5'monophosphate *p*-nitrophenyl ester (*p*NP-TMP),[2] the Förster resonance energy transfer (FRET) ligand CPF4,[20] the fluorogenic substrate 3 (FS-3),[21] and the fluorescence probe TokyoGreen *m*-thymidine monophosphate (TG-*m*TMP).[22] A particularly widely used method employs the unnatural substrate bis(*p*-nitrophenyl) phosphate (bis-*p*NPP) **11**. ATX catalyses the hydrolysis of **11** to release 4-nitrophenol **12** which, with an absorbance of 405 nm, is readily detected using colorimetry (Scheme 3). The popularity of this assay can be attributed to the low cost of this substrate and the direct readout the assay provides.[17]

Scheme 3. ATX-Mediated Hydrolysis of Bis-*p*NPP **11** Releasing 4-Nitrophenol **12**.

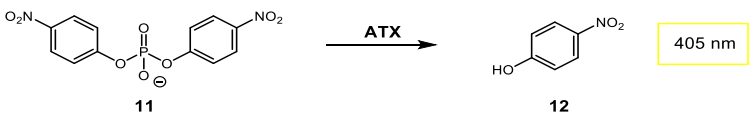

The recent report from PharmAkea Therapeutics described four structurally distinct ATX inhibitors that showed good inhibition using the LPC choline release assay but significantly lower potency when tested using the bis-*p*NPP or FS-3 substrates.[13] The differences in datasets of the three assays used were found to be a result of alternative binding modes within ATX, which was confirmed by crystallographic data identifying proximal binding sites. As stated above, these compounds were noted to have a scaffold similar to our compound of interest, the indole-derived inhibitor **9** originally reported by Amira Pharmaceuticals. In the choline release assay employed by Amira Pharmaceuticals, **9** is claimed to show an IC_{50} of <300 nM, however, no further detail was given.[18] In addition, **9** was reported to have activity in a mouse air pouch assay, collagen-induced arthritis, a rat model of neuropathic pain, and in lung melanoma metastasis, although the efficacy of **9** in these assays was not disclosed. Herein, we report that **9** and related analogues were found to display only limited activity in the bis-*p*NPP assay; however, using the LPC choline release assay a number of efficient inhibitors were identified, with IC_{50} values ranging from 4 nM to >30 μM for the complete series. The disconnect observed between the two assay datasets for this chemotype were hypothesized to be due to an alternative binding mode, remote to the catalytic site. We report enzyme kinetic studies and a co-crystal structure of ATX with an analogue of **9** to support this alternative binding site. Furthermore, we also report the exploration of the SAR associated with this chemotype.

Molecule Design. Using the limited data available, the key structural motifs of **9** were suspected to be (i) the chloro substitution at the 6-position of the indole, (ii) the substitution of the indole nitrogen, and (iii) the thiopyridine carboxylic acid. From this analysis we were able to infer the initial SAR shown in Figure 2. In the current study, we aimed to probe this emerging SAR further, to test our observations, and to more completely establish the contribution of each of

these principal structural motifs towards potency through the synthesis and biological evaluation of a series of analogues.

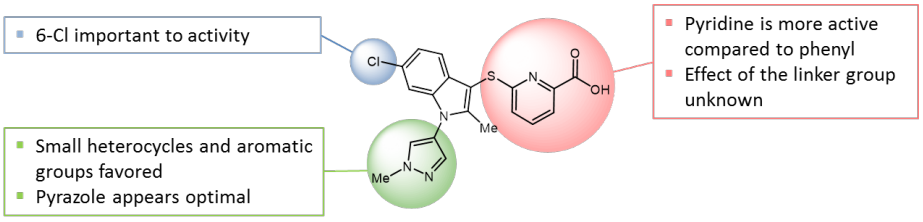

Figure 2. SAR of indole **9** extracted from data reported by Amira Pharmaceuticals.[18]

The first region of interest was the 6-Cl substitution of the indole ring. Analysis of the patent data had suggested this was an important region of the molecule, with changes to substituent or position on the ring having a direct effect on the activity observed. To explore this relationship in greater depth, a series of compounds were designed with alternative chloro regiochemistry, as well as removal or exchange of the chloro for alternative functional groups. Three alternatives were chosen to determine the optimal size and nature of the substituent: fluoro, methoxy, and methyl. The second region to be modified was at the *N*-1 position of the indole ring. The *N*-methyl pyrazole was replaced with a phenyl ring, cyclopentyl, and methyl to explore the tolerance of this region for a less polar aromatic ring as well as aliphatic groups. Finally, the thiopyridine carboxylic acid was modified, with changes made to the linker and the nature of the aromatic ring. The previously reported data in the patent literature contained little SAR around the linker area of the compound and therefore we were interested in converting the thioether to an ether or methylene linker, as well as exploring the difference between pyridyl and phenyl analogues.

Chemistry. The known ATX inhibitor indole **9** was prepared as shown in Scheme 4. Starting from ketone **13**,[24] the indole was synthesized using a Fischer synthesis as previously reported,

either according to or modified from literature procedures.[18] This reaction produced a mixture of the 4-Cl and 6-Cl substituted indoles, which were successfully separated on silica to isolate the desired 6-Cl regioisomer **16** as the major product. The 4-Cl analogue **14** was also carried through the synthesis as part of the SAR study around the indole substitution. Introduction of the 1-methyl-pyrazole substitution to the indole nitrogen proved to be challenging, requiring harsh conditions and long reaction times during which partial hydrolysis of the ester occurred. As a result, the substitution reaction was telescoped into the final step to fully hydrolyze the ester and produce the desired acid **9**.

Scheme 4. Synthesis of the Amira Compound **9**.[a]

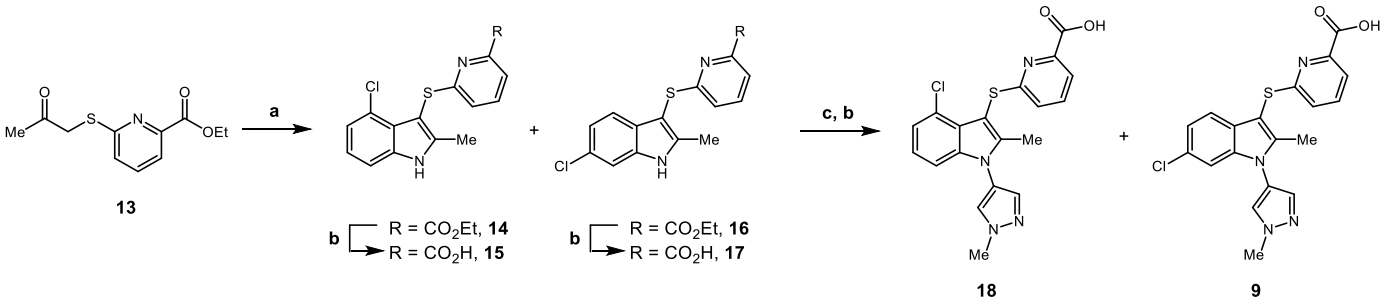

[a]Reagents and conditions: (a) (i) *t*BuOH, 3-chlorophenylhydrazine hydrochloride, reflux; (ii) HCl, AcOH; (b) 2 M aq. NaOH, THF, RT; (c) 4-iodo-1-methylpyrazole, K_2CO_3, CuO, pyridine, 170 °C.

Initial syntheses followed the reported methods from the Amira Pharmaceuticals patents to produce the desired indole **16** in good yield (71%, see experimental section) (Scheme 4). However, in the exploration of this key step it was discovered that a number of the Fischer indole reactions proceeded by refluxing the ketone with the respective hydrazine hydrochloride in EtOH without an additional acid catalyst (see experimental section). The synthesis of

analogues in which the chloro was exchanged for an alternative functionality (F, OMe, and Me) was achieved using the same synthetic strategy employed in the synthesis of compound **9**. Using this synthetic route, the analogues described in Figure 3 were accessed. Unfortunately, synthesis of the 7-Cl analogue with the 1-methyl-pyrazole *N*-substituent was not achieved, as efforts to introduce the 1-methyl-pyrazole were unsuccessful.

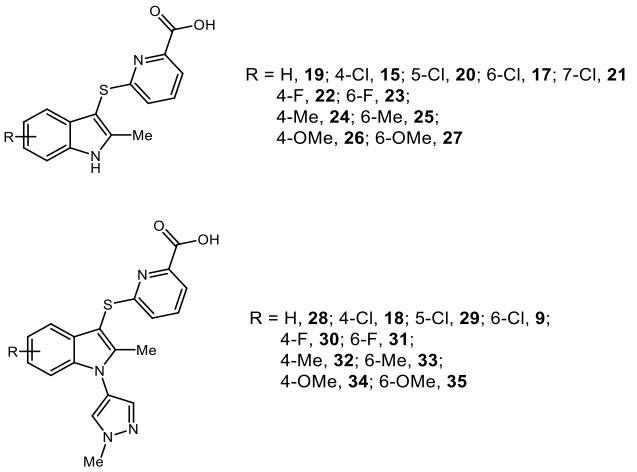

Figure 3. Substitution on the indole ring.

The next series was designed to investigate the SAR associated with the 1-methyl-pyrazole substituent on the indole nitrogen. In place of the 1-methyl-pyrazole three alternative substituents were used; methyl, cyclopentyl, and phenyl. The aliphatic substituents were introduced by an alkylation reaction using the corresponding alkyl halide and NaH (Scheme 5).

Scheme 5. Synthesis of Compound **37**.[a]

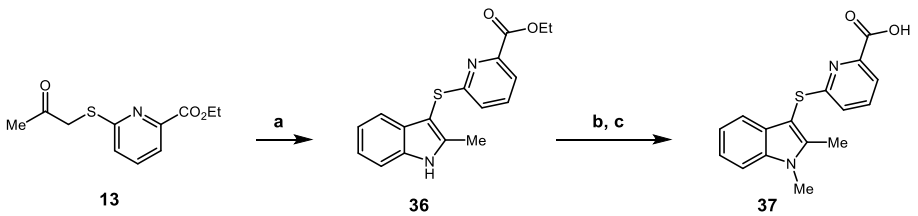

[a]Reagents and conditions: (a) (i) *t*BuOH, phenylhydrazine hydrochloride, reflux; (ii) HCl, AcOH; (b) NaH, MeI, THF, reflux; (c) 2 M aq. NaOH, THF, RT.

Following the alkylation step, hydrolysis of the corresponding ester revealed the desired carboxylic acid. The phenyl substituent was introduced using an alternative Ullmann coupling and the 1-methyl-pyrazole was introduced using the conditions described previously. Using these approaches, the analogues described in Figure 4 were successfully synthesized.

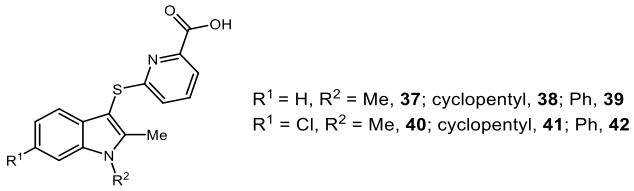

Figure 4. Substitution on the indole nitrogen.

The benzoic acid compounds were synthesized in a similar way to the pyridyl series with an additional step to introduce the ester functionality using a methoxycarbonylation reaction (Scheme 6). From this intermediate the desired alkyl or aryl *N*-substituent was introduced, followed by hydrolysis to gain the desired acid **47** in the final step of the synthesis. The ester **46**, and its deschloro counterpart **92** (not shown, see experimental section), then allowed access to the analogues described in Figure 5.

Scheme 6. Synthesis of Compounds **45-48**.[a]

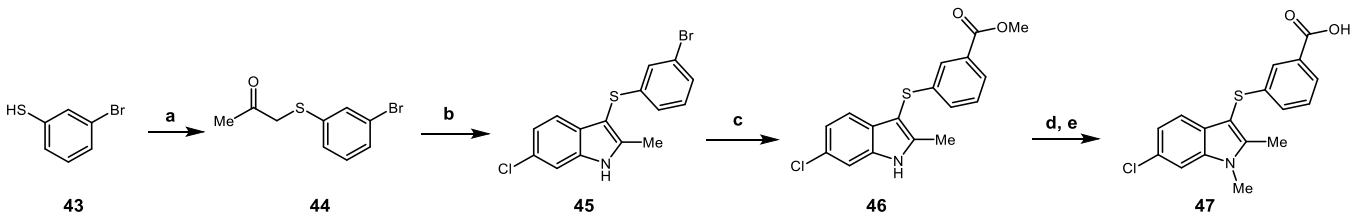

[a]Reagents and conditions: (a) chloroacetone, DIPEA, MeCN, reflux; (b) 3-chlorophenylhydrazine hydrochloride, EtOH, reflux; (c) Herrmann's catalyst, $Mo(CO)_6$, [tBu$_3$PH]BF_4, DBU, MeOH/MeCN (1:4), 70 °C; (d) NaH, MeI, THF, reflux; (e) 2 M aq. NaOH, THF, RT.

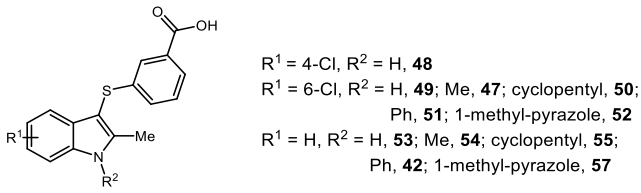

Figure 5. Substitution on the indole nitrogen, benzoic acid analogues.

The oxygen-linked benzoic acid subset (Figure 6) were synthesized using the Fischer indole reaction that was employed with previous analogues (Scheme 7). Efforts to synthesize the corresponding ether linked pyridyl compounds were unsuccessful (see Electronic Supporting Information (ESI)).

Scheme 7. Synthesis of Compounds **59**-**62**.[a]

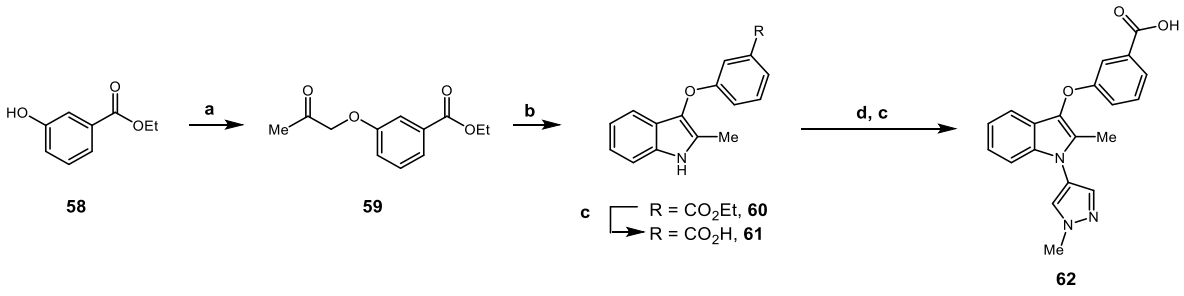

[a]Reagents and conditions: (a) chloroacetone, K_2CO_3, acetone, reflux; (b) phenylhydrazine hydrochloride, EtOH, reflux; (c) 2 M aq. NaOH, THF, RT; (d) 4-bromo-1-methylpyrazole, K_2CO_3, CuO, pyridine, 170 °C.

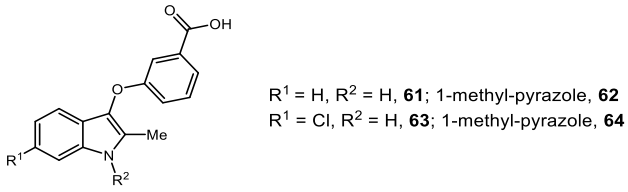

Figure 6. Ether linked analogues.

In order to access the methylene linked compounds an alternative synthetic strategy was required as efforts to employ a Fischer indole synthesis were unsuccessful. It was discovered that by reordering the synthetic steps to install the 1-methyl-pyrazole at an earlier stage, the *N*-substitution proceeded in a much improved yield than the late stage introduction used in previous syntheses (Scheme 8). A two-step alkylation of **66** using 6-bromopicolinaldehyde afforded the desired methylene linker in good yield. From the bromo intermediate **97** (not shown) the ester functionality was introduced via a methoxycarbonylation reaction to give **67**, followed by hydrolysis to reveal the desired acid **68**. Thus, this strategy was used to access the remaining compounds in this series (Figure 7).

Scheme 8. Synthesis of Compounds **66-68**.[a]

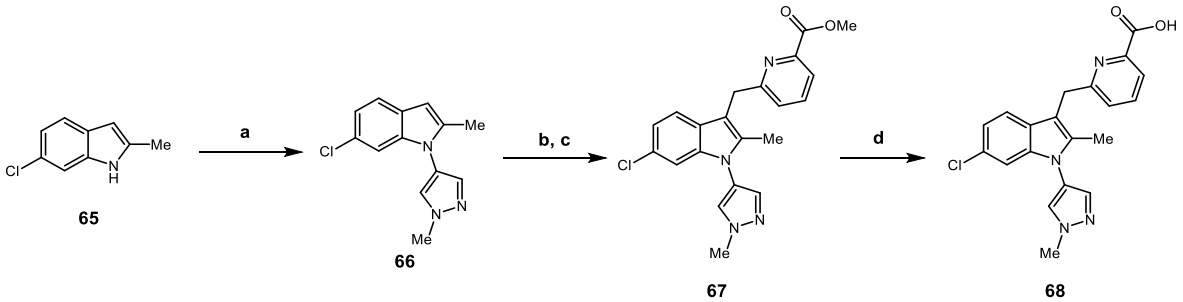

[a]Reagents and conditions: (a) 4-bromo-1-methylpyrazole, K_2CO_3, CuO, pyridine, 170 °C; (b) (i) 6-bromopicolinaldehyde, CH_2Cl_2 (ii) Et_3SiH, TFA, CH_2Cl_2; (c) Herrmann's catalyst, $Mo(CO)_6$, [tBu$_3$PH]BF_4, DBU, MeOH/MeCN (1:4), 70 °C; (d) 2 M aq. NaOH, THF, RT.

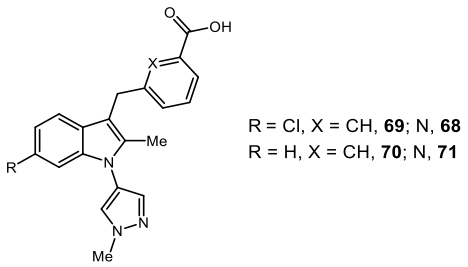

Figure 7. Methylene linked analogues.

To determine the importance of the indole core, this motif was removed and compound **75** was prepared featuring a phenyl at its center but retaining the 1-methyl-pyrazole motif. This compound was obtained from the commercial carboxylic acid **72** in four steps (Scheme 9). This required an alternative strategy, using a Suzuki-Miyaura reaction to introduce the 1-methyl-pyrazole via the coupling of **74** with 1-methylpyrazole-4-boronic acid pinacol ester.

Scheme 9. Synthesis of Analogue **75**.[a]

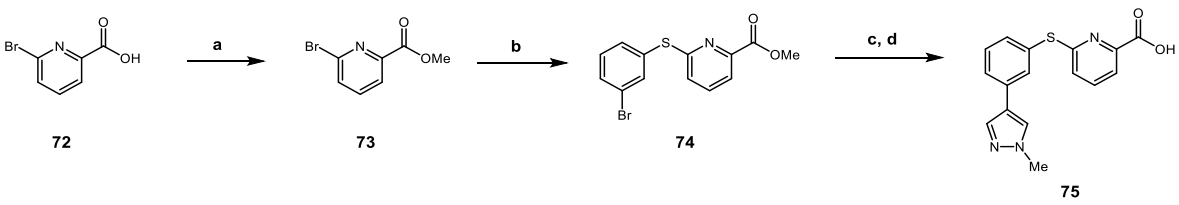

[a]Reagents and conditions: (a) conc. H_2SO_4, MeOH, reflux; (b) 4-bromothiophenol, DMF, 45 °C; (c) 1-methylpyrazole-4-boronic acid pinacol ester, K_3PO_4, $Pd(OAc)_2$, SPhos, THF/H_2O (7:1), 50 °C; (d) 2 M aq. NaOH, THF, RT.

The final deletion analogue was designed to remove one of the aromatic rings from the compound and replace it with an aliphatic carboxylic acid (Scheme 10). Starting from 4-bromobutyric acid **76** the thiol group was introduced by an *S*-alkylation of thiourea, which was subsequently hydrolyzed *in situ* to form the primary thiol **77**. This was then followed by a second alkylation using chloroacetone to access the Fischer indole precursor **78**. With **79** in hand, the 1-methyl-pyrazole was introduced at the indole nitrogen (Scheme 10). This route was also employed to access the 6-Cl analogue **81** (Figure 8).

Scheme 10. Synthesis of Aliphatic Carboxylic Acid Analogue **80**.[a]

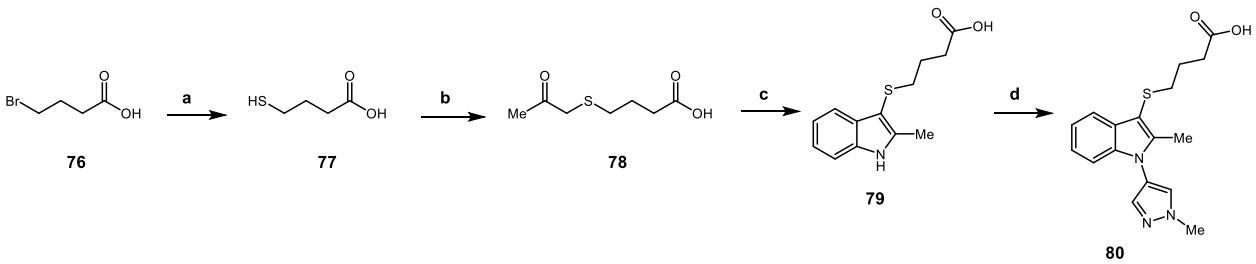

[a]Reagents and conditions: (a) thiourea, EtOH, reflux; (b) chloroacetone, DIPEA, THF, RT; (c) phenylhydrazine hydrochloride, EtOH, reflux; (d) 4-bromo-1-methylpyrazole, K_2CO_3, CuO, pyridine, 170 °C.

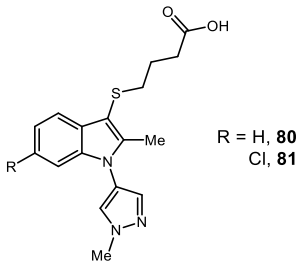

Figure 8. Aliphatic acid analogues.

Results and Discussion. To evaluate our compound library, the first screen was performed using the bis-*p*NPP assay. This was selected based on its broad application throughout the ATX literature.[11] An initial screen was carried out using 30 μM of inhibitor allowing a rapid evaluation of the compounds. The criteria of >60% inhibition was set for a compound to be termed active and therefore progressed to further testing. Based on this initial survey of the activity of Amira compound **9** along with the 49 analogues in the bis-*p*NPP assay, we identified 10 potential inhibitors, including the patent compound **9** (see ESI). These 10 compounds were tested again in the bis-*p*NPP assay using a concentration range of 30 nM – 30 μM inhibitor, to determine the IC_{50} for each of these compounds. Using the bis-*p*NPP assay, the Amira ATX inhibitor **9** was found to have an IC_{50} of 22 nM, which was consistent with the value of <300 nM claimed in the patent (LPC choline release assay);[18] however, the IC_{50} values observed in this set ranged from 22 nM to >30 μM (Table 2). These results demonstrated that our first screen at an inhibitor concentration of 30 μM had not been a reliable indicator of activity. Importantly, on further inspection of the dose response curves (Figure 9), it was noted that when using the bis-*p*NPP assay, compound **9** showed only 66% maximal inhibition of ATX at 30 μM (34% hydrolysis of **11**), indicating that this analogue was not fully inhibiting the ATX hydrolysis of **11**, potentially implying a discrete binding mode compared to that of the artificial substrate.

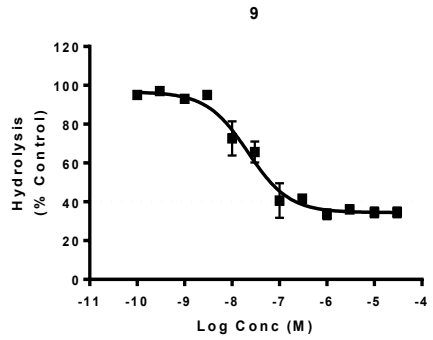

Figure 9. Testing of **9** in the bis-*p*NPP assay from 30 nM – 30 μM of inhibitor. Dashed line indicates 60% inhibition criteria of initial screen. Control reactions confirmed there was no hydrolysis of **11** in the absence of ATX (data not shown).

A further 20 analogues were tested in the bis-*p*NPP assay confirming that partial inhibition was a consistent feature associated with this series (data not shown, see ESI). Although the bis-*p*NPP assay has many advantages, there are risks associated with the use of unnatural substrates if the binding interactions with the target enzyme are dissimilar to those of the natural substrate. There are a number of reported examples where misleading results were observed when using ATX assays that employ the unnatural ligands FS-3, CPF4, and *p*NP-TMP.[17,25,26] The authors concluded that the discrepancies in assay datasets were the result of the inhibitor compounds and assay substrates binding to different regions of ATX. It has been well documented that the active site of ATX features three key regions with which small molecule inhibitors can interact: the catalytic site, the hydrophobic pocket, and the tunnel.[27-29] Comparing the likely binding of the unnatural substrate **11** with that of ATX in complex with **2**, it is noted that while both bind at the catalytic site, the acyl chain of **2** shows additional extensive interactions with the hydrophobic pocket (Figure 10). This suggests that it is possible for small molecules to bind outside the catalytic site without inhibiting, or only partially inhibiting, the hydrolysis of **11**, potentially resulting in false negative results in the bis-*p*NPP ATX assay.

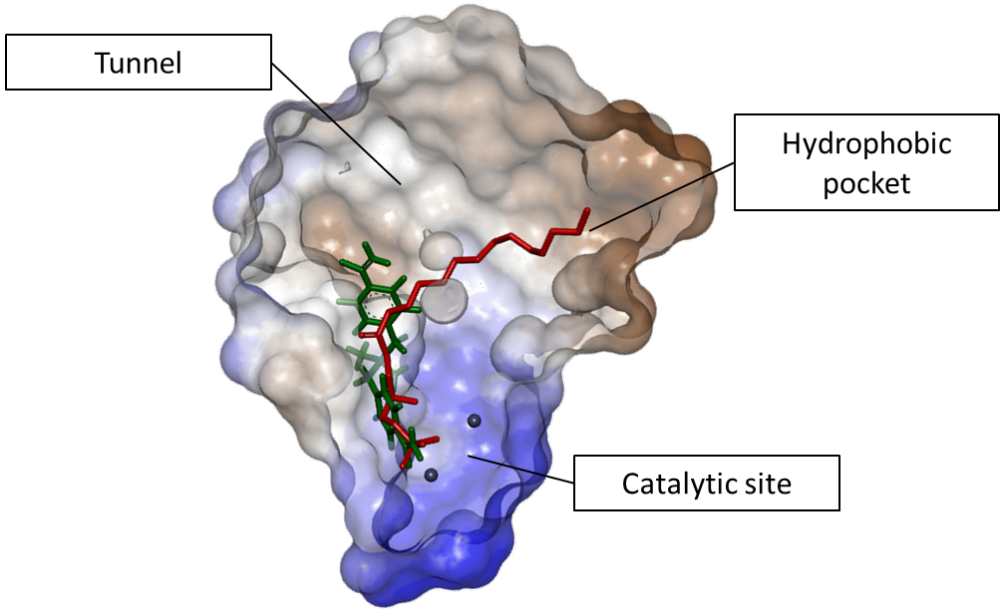

Figure 10. Three binding sites of ATX: Catalytic Site, Hydrophobic Pocket, and Tunnel. Complex of LPA 14:0 (red) in mouse ATX (PDB 3NKN) with the docked position of bis-*p*NPP **11** (green) overlaid. Docked using GOLD[30] and viewed using Discovery Studio Visualizer.[31]

Indeed, the noncompetitive inhibitor **8** from PharmAkea, which shares a number of structural similarities to **9**, has been reported to bind an allosteric site within the tunnel.[13] The authors observed that **8** inhibited the hydrolysis of **1** but not of **11**, showing that an inhibitor binding within the tunnel may not be detected using the bis-*p*NPP assay. Moreover, selected steroid analogues have recently been shown to bind the same site, with the activity of ATX in hydrolyzing LPC allosterically inhibited but not its activity on *p*NP-TMP.[29] These reports led us to employ the natural substrate **1** in the LPC choline release assay to further evaluate our inhibitors, gain a more complete understanding of the underlying SAR, and offer insight into potential binding modes. Prior to testing the inhibition of ATX, a control reaction was run using three exemplar compounds to ensure that there was no incompatibility with the two coupling

enzymes used in the assay: choline oxidase and HRP. Using choline chloride as the substrate, no inhibition was observed for the latter two reactions of the LPC assay, as shown in Scheme 2 (see ESI). Testing proceeded with an initial screen of all 50 compounds from 400 nM – 100 μM, to identify active inhibitors. From this dataset, compounds that exhibited an IC_{50} <1 μM were tested further across a concentration gradient of 0.3 nM – 10 μM, and the IC_{50} values were determined (compounds with IC_{50} >30 μM not shown, see ESI). This assay provided us with robust inhibition data, with the more potent compounds showing full inhibition of ATX. Of the 50 analogues described in the current study, only four had been previously reported by Amira Pharmaceuticals (**9**, **47**, **51**, **52**).[18] The IC_{50} values determined in our LPC choline release assay were consistent with the values claimed in the patents (Table 2). It is also important to note that substrate concentration can affect the IC_{50} value observed in an assay; for competitive assays such as bis-*p*NPP and the LPC choline release assay, the substrate concentration should be less than, or equal to, the Michaelis-Menten constant (K_M) for the given substrate.[32] The biological evaluations detailed in this current study were carried out using substrate concentrations equal to the K_M values of **1** (~150 μM) and **11** (~1 mM) for ATX previously reported by van Meeteren *et al*.[33]

Table 2. Bis-*p*NPP and LPC assay results.

Compound	Bis-*p*NPP IC_{50} (nM)	LPC IC_{50} (nM)
9	22 ±6.9	4 ±0.5[a]
17	604 ±113	25 ±13
23	-	>20 μM[b]
24	-	>8000[b]
28	5700 ±2500	1700 ±400

29	-	258 ±127
30	-	>3500[b]
31	816 ±564	349 ±125
32	-	>10 μM[b]
33	85 ±22	25 ±12
35	75 ±37	124 ±37
40	>4000[b]	31 ±11
41	2000 ±785	>2800[b]
42	-	- [c]
47	100 ±36	1200 ±800[d]
49	290 ±35	747 ±500
50	>4000[b]	>20 μM[b]
51	5 ±2.5	81 ±28[a]
52	-	11 ±7[a]
56	>30 μM	>5000[b]
64	204 ±88	726 ±155
68	89 ±43	339 ±190
69	33 ±16	660 ±224
80	-	>10 μM[b]

All tested from 0.3 nM – 10 μM, 10 point curves, n = 2. [a]Consistent with the value of < 300 nM claimed in the patent, LPC assay. [b]Incomplete curve observed. [c]Unable to determine IC_{50} due to solubility issues in the assay medium. [d]Consistent with the value of >1 uM claimed in the patent, LPC assay.

Structure-activity Relationship. Using the results from the LPC assay we were able to define the SAR around this chemotype and provide a better understanding of the features which contribute to its potency. During our examination of the patent data, it became apparent that the 6-Cl of compound **9** was of high importance to the potency. The deletion analogue **75**, in which the indole was removed with a phenyl ring used as the core, had resulted in a complete loss of activity (data not shown, see ESI), thus confirming the importance of the indole core. To investigate the SAR of the 6-Cl substitution on the indole, a series of analogues were made varying the position of the chloro around the benzenoid ring, as well as removing the substituent (Table 3). We also aimed to explore the significance of the chloro by exchanging this for alternative functionalities: F, OMe, and Me. The effect of this chloro on potency was apparent throughout our results, with its presence increasing the potency in every example. It was also identified that the 6-position of the indole ring was optimal for the chloro, with the other regioisomers resulting in lowered or a complete loss of activity (Table 3). This can be noted in the comparison of compounds **9**, **18**, and **29**, with the movement of the chloro substituent around the indole ring.

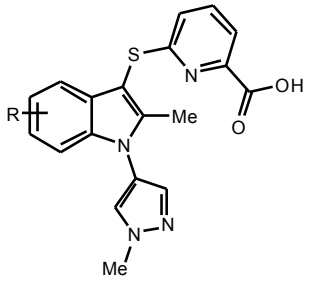

Table 3. SAR of indole ring.

Compound	**R**	**IC_{50} (LPC)**

28	H	1700 ±400 nM
18	4-Cl	>30 μM
29	5-Cl	258 ±127 nM
9	6-Cl	4 ±0.5 nM
30	4-F	>3 μM[a]
31	6-F	349 ±125 nM
32	4-Me	>10 μM[a]
33	6-Me	25 ±12 nM
34	4-OMe	>30 μM
35	6-OMe	124 ±37 nM

[a]Incomplete curve observed.

In order to rationalize the effect of the 6-Cl, docking studies were performed using the apo form of the ATX enzyme. From this work it was proposed that the 6-Cl projects into a nearby hydrophobic cleft (Leu160, Ala164, Trp207, Trp161), making a series of hydrophobic interactions (Figure 11B). The 6-Cl substituent is a vital motif for potency throughout this chemotype, therefore we hypothesize that the hydrophobic interactions of this substituent with the hydrophobic cleft are key contributors to the potency. It was possible to exchange the 6-Cl

for alternative substituents (F, **31**; Me, **33**; OMe, **35**) and retain the activity, although the chloro was optimal. Based on our *in silico* model, a conclusion was drawn that the 6-Cl substituent provides the optimal size to fit within the hydrophobic pocket with a larger (Me, **33**) or smaller (F, **31**) substituent resulting in a loss of potency.

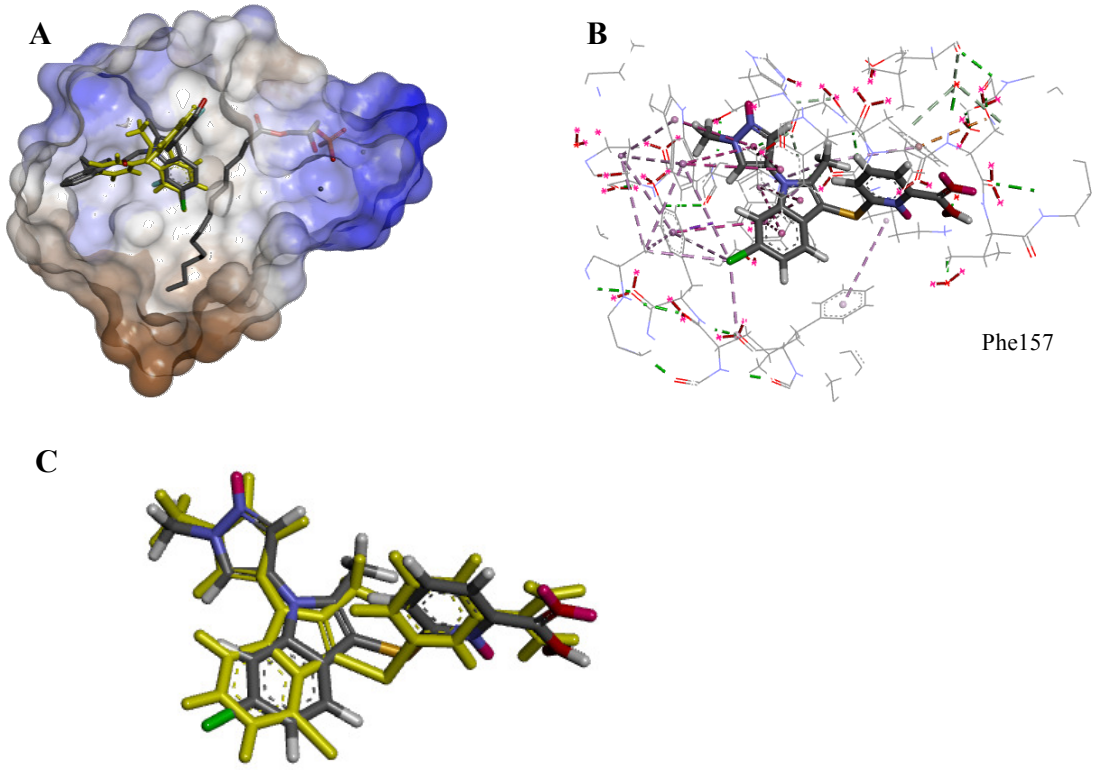

Figure 11. *In silico* studies created using co-crystal of ATX with **2** and **8** PDB 4ZG7. A: Model of **51** (yellow) overlayed with cocrystal of **8** (colored by atom type) and ATX, with **2** residing in the catalytic site and hydrophobic pocket. B: Model of ATX with **9** highlighting possible interactions. C: Shift observed when 4-Cl substituted **18** is docked (yellow) vs. 6-Cl substituted **9** (colored by atom type). Docked using GOLD[30] and viewed using Discovery Studio Visualizer[31] (see ESI).

Moving these alternative substituents from the 6- to the 4-position of the indole resulted in loss of activity, providing further support to the importance of the 6-position. It was noted that with no substituent on the indole some weak activity was observed with an IC_{50} of 1700 nM for compound **28**; however, introduction of a substituent to the 4-position resulted in loss of activity (**18**, **32**, **34**), with the exception of the 4-F which is tolerated (**30**), showing that substitution at this position prevents binding of these compounds. Using our *in silico* model, we suggest that a clash between the 4-position substituents and a nearby residue (Phe157) alters the binding of these analogues (Figure 11B). This shift in the binding position caused by the clash with the protein could explain the loss in potency observed when a substituent is introduced to the 4-position.

The next region to be explored was the substitution on the indole nitrogen. In order to establish whether the aromatic substituent was required for activity, and if the size of the substituent was important, three alternative substituents were used in place of the 1-methyl-pyrazole: methyl, cyclopentyl, and phenyl. Analogues with the unsubstituted indole were also synthesized to determine whether any substituent at this region was required for activity. Based on the patent data, the 1-methyl-pyrazole is important for activity and removal of this substituent did result in a reduction in potency; however, compound **17** with no decoration of the indole nitrogen, was a potent compound with an IC_{50} of 25 nM. Further analogues exploring the substitution of the indole nitrogen (methyl, cyclopentyl, phenyl) found that the 1-methyl-pyrazole remained the most active (Table 4). Unfortunately, we were unable to determine the IC_{50} of compound **42** due to poor solubility in the assay medium observed during the screening of this analogue. Our binding model had indicated possible π-π interactions for the 1-methyl-pyrazole of **9** with nearby residues (Trp207: pyrazole face to indole edge and Phe221: face to face). By changing the 1-

methyl-pyrazole to an aliphatic substituent these interactions are lost, thus resulting in a loss of activity. The methyl group of **40** was well tolerated, whereas the cyclopentyl substituent of **41** was found to cause a large drop in potency. These results suggest that the larger aliphatic substituent is detrimental, either through unfavorable interactions or by clashing with the protein; however, we did not observe either from consideration of our binding model.

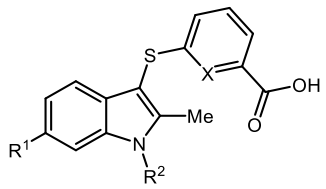

Table 4. SAR of indole nitrogen substituent, with 6-Cl.

Compound	X	R^1	R^2	IC_{50} (LPC)
9	N	Cl	1-methyl-pyrazole	4 ±0.5 nM
17	N	Cl	H	25 ±13 nM
40	N	Cl	Me	31 ±11 nM
41	N	Cl	cyclopentyl	>2800 nM[b]
42	N	Cl	Ph	- [a]
19	N	H	H	>30 μM
28	N	H	1-methyl-pyrazole	1700 ±400 nM

37	N	H	Me	>30 μM
38	N	H	cyclopentyl	>30 μM
39	N	H	Ph	>30 μM
52	CH	Cl	1-methyl-pyrazole	11 ±7 nM
49	CH	Cl	H	747 ±500 nM
47	CH	Cl	Me	1200 ±800 nM
50	CH	Cl	cyclopentyl	>25 μM[b]
51	CH	Cl	Ph	81 ±28 nM

[a]Unable to determine due to solubility issues in the assay medium. [b]Incomplete curve observed.

The relationship between the 1-methyl-pyrazole and the 6-Cl was highlighted by altering the substitution of the indole nitrogen in a series of compounds that did not feature the 6-Cl substitution. In this series of analogues (Table 4), only one compound exhibited weak activity, which was the 1-methyl-pyrazole **28**, thus showing that either the 6-Cl or the 1-methyl-pyrazole must be present for activity; however, the 6-Cl substituent has the most profound effect on activity.

This series of compounds was explored further via the synthesis of the analogous series with the nitrogen removed from the pyridine ring, thus allowing for the SAR of the pyridyl acid and the

phenyl to be determined. The benzoic acid analogues demonstrated the same SAR as the pyridyl sub-series, with the 1-methyl-pyrazole (**52**) giving the best inhibition (Table 4). Fortunately, compound **51** showed good solubility in the assay medium, allowing for the IC_{50} to be determined at 81 nM, unlike the pyridyl analogue **42** with which we had observed poor solubility during screening in the LPC assay. This set of analogues additionally supports our observation from the data in Table 4; that it is beneficial to have a substituent of aromatic nature on the indole nitrogen, and although a cyclopentyl is unfavorable (**50**), smaller aliphatic groups can be tolerated (**47**).

The acidic group of this chemotype was also found to be vital for ATX activity, as shown by the two deletion analogues in which the thioether linked pyridine was removed (**66**) or exchanged for an aliphatic acid (**81**) which resulted in loss of activity (Table 5). During our docking studies of **9**, it was noted that both the indole ring and the 1-methyl-pyrazole substituent could potentially contribute to binding through π-π interactions; however, with the pyridyl acid orientated towards the solvent it made no specific interactions with ATX, and only a potential H-bonding interaction with a crystallographic water molecule was identified. The loss of activity observed with **66** and **81** could indicate that the aromaticity is required for additional interactions not identified in our docking study, or that the increased number of rotatable bonds was unfavorable in the binding of this compound within ATX. By comparing the benzoic acid compound **52** with the corresponding pyridyl analogue **9** we observed no significant change in potency with removal of the pyridyl nitrogen; however, by comparing matched pair examples with *N*-substituents other than the 1-methyl-pyrazole, it can be noted that the pyridine in general improves potency (Table 4).

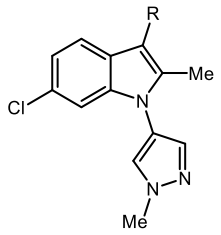

Table 5. SAR of the carboxylic acid region.

Compound	R	IC_{50} (LPC)
9	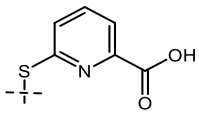	4 ±0.5 nM
52	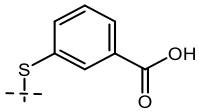	11 ±7 nM
81	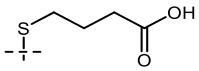	>30 μM
66	H	>30 μM

The thioether linker was then explored through replacement with an ether or a methylene. Previous reports from the patent literature had disclosed no analogues with the methylene, and only five with an ether linker, thus we sought to fill the SAR gap with a set of analogues using an ether and methylene with both the pyridyl and benzoic acids. A large drop in potency was observed as a result of changing the thioether (**9**) to a methylene spacer (**68**). We also noted this trend in the benzoic acid analogues with the thioether (**52**) being superior to an ether (**64**) or methylene (**69**) linker, though both alternatives were tolerated (Table 6). Our docking model provided little insight into the effects of changing the linker (see ESI); thus we hypothesize that the longer bond lengths of the thioether are beneficial to the binding of this chemotype.

Furthermore, this subset again demonstrates the importance of the 6-Cl for activity and the superiority of the pyridyl analogues over the corresponding phenyl analogues.

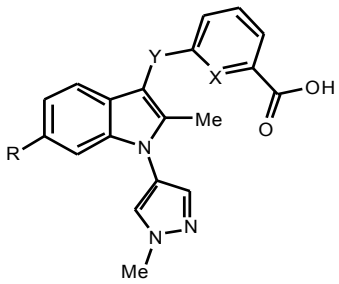

Table 6. SAR of the linker.

Compound	R	Y	X	IC_{50} (LPC)
28	H	S	N	1700 ±400 nM
9	Cl	S	N	4 ±0.5 nM
53	H	S	C	>30 μM
52	Cl	S	C	11 ±7 nM
62	H	O	C	>30 μM
64	Cl	O	C	726 ±155 nM
71	H	CH_2	N	>30 μM
68	Cl	CH_2	N	339 ±190 nM
70	H	CH_2	C	>30 μM

69	Cl	CH_2	C	660 ±224 nM

Mechanistic Studies. To explore the potential binding mode of this chemotype, enzyme kinetic studies were carried out in the presence of four representative inhibitors: compound **9**, **17**, **47**, and **51**. ATX activity for varying substrate concentrations (**1**) was measured in concentrations of each inhibitor. A mixed inhibition mathematical model was fitted to the original data to determine the value of alpha; values of alpha close to 1 indicate noncompetitive inhibition.[34] To graphically demonstrate the inhibition mode, we also present Lineweaver-Burk double reciprocal plots (Figure 12). These studies show that as the inhibitor concentration was increased, the V_{max} reduced but the K_M remained unchanged, which is indicative of noncompetitive inhibition. Consistently, the values of alpha for each of the compounds ranged between 0.6 and 2.6, characteristic of noncompetitive inhibition. Thus, all four exemplar compounds are strongly noncompetitive inhibitors. This data, along with the differences observed between the two ATX inhibition assays used, suggests that this chemotype has a distinct binding mode, remote to that of the catalytic site of ATX, similar to that reported for the three noncompetitive PharmAkea compounds.[13]

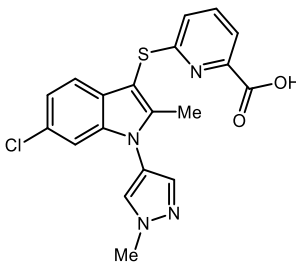

9 IC_{50} = 4 ±0.5 nM

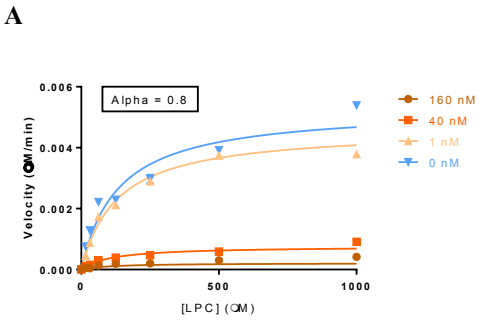

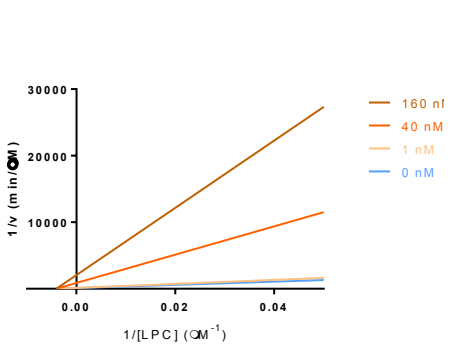

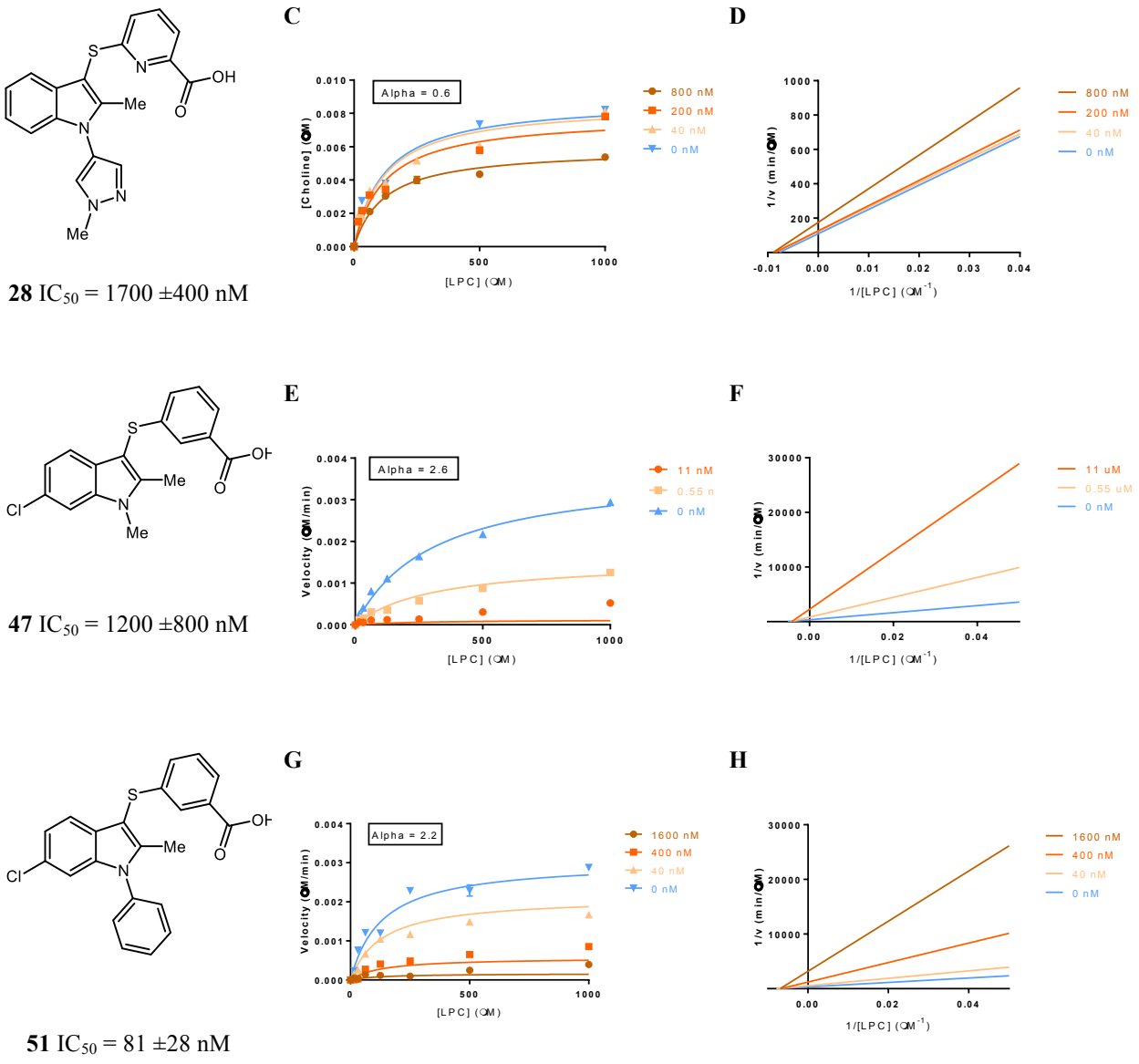

28 IC_{50} = 1700 ±400 nM

47 IC_{50} = 1200 ±800 nM

51 IC_{50} = 81 ±28 nM

Figure 12. Enzyme kinetic studies using compounds **9**, **28**, **47**, and **51**. Compound **9**: α = 0.8.

Compound **28**: α = 0.6. Compound **47**: α = 2.6. Compound **51**: α = 2.2. The data were plotted and the best fit values generated using GraphPad Prism 6 from nonlinear regression analysis to an equation corresponding to the mixed inhibition model allowing the determination of alpha.

The constant "alpha" defines the effect of an inhibitor binding has on the affinity of the enzyme for the substrate, a value close to 1 is indicative of noncompetitive inhibition.[34]

Crystallographic Data. In order to confirm the binding mode of this chemotype, the co-crystallization of a number of the inhibitors described herein with ATX was undertaken. Unfortunately, efforts to obtain a crystal structure of the most potent inhibitor **9** with ATX were unsuccessful; however, the co-crysallization of **51** (IC_{50} = 81 ±28 nM) with ATX was successful and the structure of this complex determined to 2.4 Å resolution, PDB 5LQQ. After molecular replacement and model adjustment difference, electron density in the tunnel close to the hydrophobic pocket could be observed, and compound **51** could be modelled in the difference density map. The docked position of **51** in our previously described *in silico* model with ATX (Figure 11) was found to be consistent with the binding mode observed in the cocrystal of **51** and ATX (Figure 13).

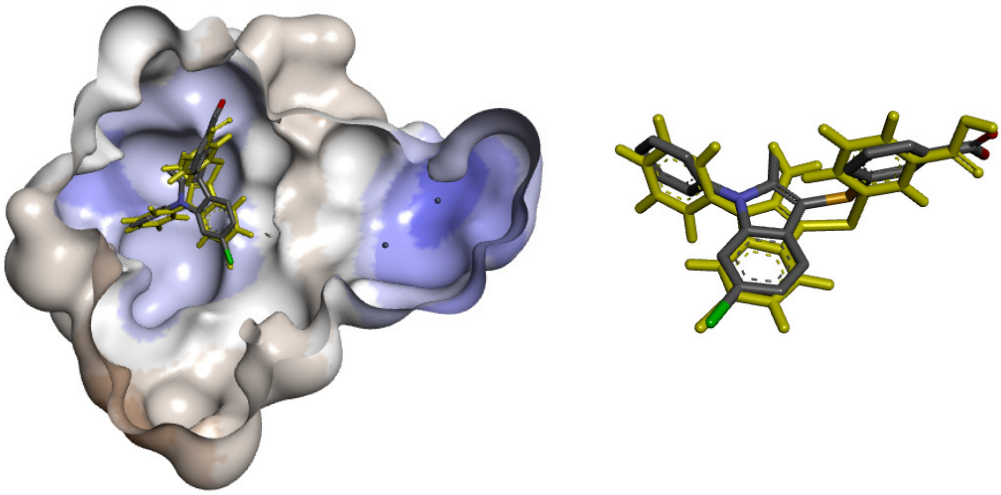

Figure 13. Crystal structure (PDB 5LQQ) vs docking model of **51** with ATX. Cocrystal structure of **51** (colored by atom type) overlayed with docking model of **51** (yellow). Docked using GOLD[30] and viewed using Discovery Studio Visualizer[31] (see ESI).

The thioether, indole, and *N*-phenyl are very clear in the electron map; however, the benzoic acid is not well resolved, possibly due to disorder (see ESI for density map). This structure allowed us to locate the binding mode of this chemotype and confirm a number of key binding interactions (Figure 14).

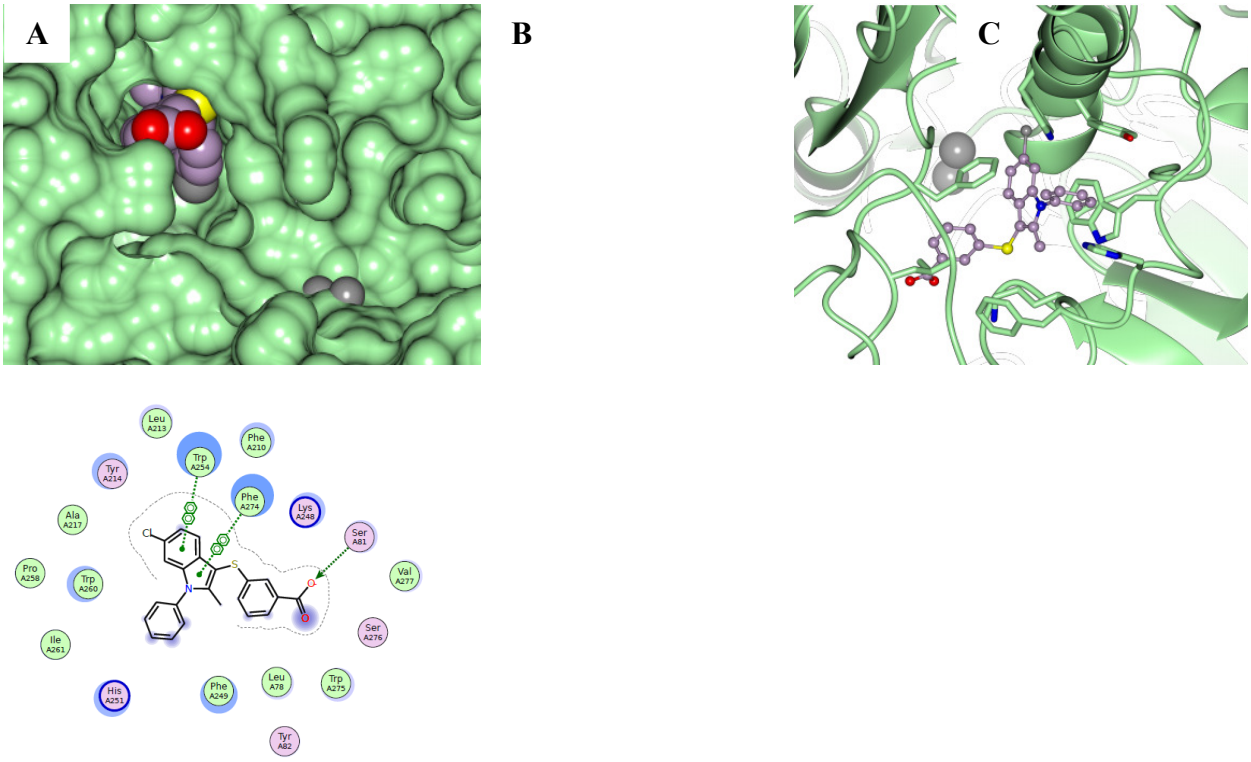

Figure 14. Crystallographic data of **51** with ATX. A: **51** bound within the tunnel, remote from the catalytic site. B: Stick and ball model of **51**. C: Ligand display for interaction and analysis (LIDIA) graph of **51**. Model and LIDIA graph built using COOT.[35] Images created using CCP4MG.[36]

Compound **51** binds in a very similar pose compared to the PharmAkea inhibitor **8** (PDB 4ZG7),[13] which shares a number of structural similarities to analogue **51**. The placement of the

thioether and indole moieties is nearly identical in the two structures, while the phenyl of **51** overlaps well with the cyclopropyl-dihydroindole in **8**. The 6-Cl substituent, shown to be vital for potency in our SAR studies, resides in a hydrophobic cleft, resulting in a series of interactions to nearby residues (Figure 11B). Both the indole ring and the *N*-phenyl substituent contribute to binding with a number of π-π interactions; however, the benzoic acid (**51**) appears to make few discernible interactions with ATX as it is orientated towards the solvent. In the case of compound **8**, however, the fluoro-benzoic acid makes interactions with the main chain amide of Val278, a well-ordered glycerol molecule, and a crystallographic water molecule (see ESI) and is thus very well defined in a single conformation in the electron density map. This is in sharp contrast to the benzoic acid in **51** that is clearly disordered, which suggests that the fluoro substituent of the benzoic acid ring may help to order it in a defined position within the tunnel. Alternatively, the presence of the phospholipid (**2**) in the structure of **8** bound to ATX, but not present in our structure with **51**, may help order this ring system. Docking studies result in an excellent overlay of **51** with **8** as expected, but the benzoic acid moiety was able to rotate around the thioether and project in a number of different vectors (see ESI). The disorder observed of the benzoic acid in the cocrystal structure of **51** with ATX supports the hypothesis that the thioether has rotational freedom.

Physicochemical Properties. ATX inhibitors that resemble the natural ligand have high molecular weight (MW) and high logD resulting in poor drug discovery potential. We were interested in the Amira compound **9**, not only due to its unique non-lipid chemotype, but also because its lower MW and improved lipophilicity it is potentially a more druglike inhibitor. With this in mind, we evaluated some key physicochemical properties as well as potency for a selected number of the analogues synthesized. Table 7 details the physicochemical properties of the

analogues in which the indole nitrogen substituent was varied (see ESI for further properties measured). Compounds **9**, **17**, and **40** all showed good ligand efficiency in terms of both ligand efficiency index (LEI) and lipophilic ligand efficiency (LLE); however, the introduction of the pyrazole in compound **9** improves both potency and LLE.

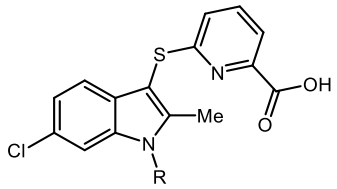

Table 7. Physicochemical properties of indole nitrogen substituent analogues.

Compound	R	MW	$logD_{7.4}$[a]	Sol.[b] (μM)	P_{app}[c] ($nm\ s^{-1}$)	PSA[d]	IC_{50}[e]	LEI[f]	LL
9	1-methyl-pyrazole	399	2.70	377	23	76	4 nM	0.31	6
17	H	319	2.19	≥395	11	69	25 nM	0.36	5
40	Me	333	2.68	300	32	58	31 nM	0.34	5
41	cyclopentyl	386	4.05	336	290	58	>2800 nM	0.21	1
42	Ph	395	4.30	485	155	58	- [h]	-	-

[a]logD, Chrom log D at pH 7.4; [b]Chemiluminescent nitrogen detection (CLND) kinetic aqueous solubility assay; [c]P_{app} permeability pH 7.4 assay;[46] [d]Topological polar surface area (PSA) determined using JChem for Office (Excel) 16.3.2100.656, 2008-2016, ChemAxon (http://www.chemaxon.com). [e]IC_{50} in LPC choline release assay; [f]Ligand efficiency index, LEI = pIC_{50}/HA, where HA denotes the number of non-hydrogen atoms; [g]Lipophilic ligand efficiency, LLE = pIC_{50} – logD. [h]Unable to determine due to solubility issues in the assay medium.

As expected, the compounds with the more lipophilic *N*-substituents, cyclopentyl (**41**) and phenyl (**42**), had increased $logD_{7.4}$, lowered PSA, and increased permeability. All the analogues in this series had reasonable aqueous solubility when measured using a high throughput screening solubility assay, including compound **42** with which we had observed poor solubility in the assay medium. By comparing compounds **9** and **52** we were able to determine the effects that the pyridine ring has on the physicochemical properties of this chemotype (Table 8). Although the activities and the LEI values of these two analogues are comparable, the lower $logD_{7.4}$ of **9** improves the LLE, giving it an excellent LLE value of 6. At first glance this can make **9** appear to be a more attractive molecule; however, the introduction of the pyridine increases the PSA and lowers permeability of **9** and thus **52** is perhaps the more attractive analogue. In particular, **52** has significantly improved solubility and permeability compared to the progenitor pyridine system **9**. This is not associated with any significant reduction in potency against ATX, as evidenced by the essentially conserved ligand efficiency value.

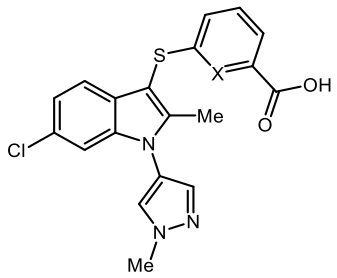

Table 8. Physicochemical properties of benzoic acid vs. pyridyl.

Compound	X	MW	$logD_{7.4}$[a]	Sol.[b] (μM)	P_{app}[c] ($nm\ s^{-1}$)	PSA[d]	IC_{50}[e]	LEI[f]	LLE
9	N	399	2.70	377	23	76	4 nM	0.31	6
52	CH	398	3.36	556	64	63	11 nM	0.30	5

[a]logD, Chrom log D at pH 7.4; [b]Chemiluminescent nitrogen detection (CLND) kinetic aqueous solubility assay; [c]P_{app} permeability pH 7.4 assay;[46] [d]Topological polar surface area (PSA) determined using JChem for Office (Excel) 16.3.2100.656, 2008-2016, ChemAxon (http://www.chemaxon.com). [e]IC_{50} in LPC choline release assay; [f] Ligand efficiency index, LEI = pIC_{50}/HA, where HA denotes the number of non-hydrogen atoms; [g]Lipophilic ligand efficiency, LLE = pIC_{50} – logD.

CONCLUSION

We designed and synthesized a series of analogues to explore the atypical ATX inhibitor **9**, previously reported by Amira Pharmaceuticals. In the current study, we have developed a robust SAR through the biological assessment of our compound library using two different ATX assays. This survey has established that some compounds inhibit hydrolysis of the natural substrate (LPC) but only partially inhibit activity with an artificial substrate. Based on this we can infer a binding mode outside of the orthosteric site and this was corroborated by kinetic studies, which identified this chemotype as a noncompetitive ATX inhibitor. In addition to this, a crystal structure of ATX bound to compound **51** confirmed that it binds within the tunnel, which is an underexploited and recently described allosteric binding site. We emphasize that cross screening with an assay using a natural substrate is important to determine the true inhibitory activity of compounds for this enzyme. Through the measurement of the physicochemical properties, we demonstrated that this chemotype had consistently good aqueous solubility, with the more potent analogues possessing excellent LLE. This combined biochemical, biostructural, and physicochemical work has provided a more detailed insight into the SAR and binding mode of these small molecule ATX inhibitors, which could aid the design of new novel ATX inhibitors with non-lipid-like scaffolds.

EXPERIMENTAL SECTION

General Procedures. All reagents and solvents were obtained from commercial suppliers and were used without further purification unless otherwise stated. Purification was carried out according to standard laboratory methods.[37] All solvents for dry reactions were distilled according to standard laboratory practice. These solvents were transferred to a septum-sealed oven-dried flask over previously activated 4 Å molecular sieves and purged with and stored under nitrogen. Dichloromethane, ethyl acetate, methanol, petroleum ether 40-60°, and cyclohexane for purification purposes were used as obtained from suppliers without further purification. Thin layer chromatography (TLC) was carried out using Merck silica plates coated with fluorescent indicator UV254. These were analyzed under 254 nm UV light or developed using potassium permanganate solution. Silica chromatography was carried out using ZEOprep 60 HYD 40-63 μm silica gel or IST Isolute Flash silica cartridges. Reverse-phase HPLC purification was carried out using a Gilson 151 preparative HPLC using an Agilent Zorbax SB-C18 column at room temperature. Purification was performed using a gradient method, eluting with 5-80% acetonitrile/water over 15 minutes at a flow rate of 10 mL/min. Fractions were collected automatically using a GX-271 liquid handler. Reverse-phase ultra-performance liquid chromatography (UPLC) purification was carried out using an Acquity UPLC CSH C18 column at 40 °C. Purification was performed using a gradient method, eluting with 5-97% acetonitrile/10 mM $(NH_4)HCO_3$ in water. Mass-directed automatic purification (MDAP) was carried out using a ZQ MS using alternate-scan positive and negative electrospray and a summed UV wavelength of 210-350 nm and an Xbridge C18 column (100 mm x 19 mm, 5 μm packing diameter, 20 mL/min flow rate) or Xbridge C18 column (150 mm x 30 mm, 5 μm packing diameter, 40 mL/min flow rate). Purification was performed using a gradient method at room temperature with the mobile

phases as (A) 10 mM aqueous ammonium bicarbonate solution, adjusted to pH 10 with 0.88 M aqueous ammonia and (B) acetonitrile. All compounds for testing were purified to at least 95% purity, as verified by HPLC, ^{1}H NMR, and high-resolution mass spectrometry (HRMS). Fourier Transformed Infra-Red (FTIR) spectra were obtained on one of three machines: (i) Shimadzu IRAffinity-1 machine; (ii) A2 Technologies ATR spectrometer; (iii) Agilent 5500a FTIR ATR. ^{1}H, ^{13}C, and ^{19}F NMR spectra were obtained on a one of four Bruker NMR spectrometers: (i) Advance III HD console, Ascend 500 MHz magnet, BBO smart probe; (ii) Advance III console, 400 MHz Ultrashield magnet, Prodigy BBO probe, BB-H&F-D-05 Z; (iii) Advance II console, 400 MHz 9.4 T Oxford unshielded magnet, BBFO-z-ATMA probe; (iv) Advance III console, 600 MHz 14.1 T Bruker Ultrashield magnet, TBI-z probe. Chemical shifts are reported in ppm and coupling constants are reported in Hz with $CDCl_3$ referenced at 7.26 (^{1}H) and 77.16 ppm (^{13}C), $CO(CD_3)_2$ at 2.05 (^{1}H) and 29.84 ppm (^{13}C), MeOD at 3.31 (^{1}H) and 49.00 ppm (^{13}C), and DMSO-d_6 at 2.50 (^{1}H) and 39.52 ppm (^{13}C), respectively. HRMS were obtained through analysis at the EPSRC National Mass Spectrometry Facility, University of Wales, Swansea or on a Micromass Q-Tof Ultima hybrid quadrupole time-of-flight mass spectrometer, with analytes separated on an Agilent 1100 Liquid Chromatograph equipped with a Phenomenex Luna C18(2) reversed phase column (100 mm x 2.1 mm, 3 μm packing diameter). LC conditions were 0.5 mL/min flow rate, 35 ºC, injection volume 2-5 μL. Gradient elution with (A) water containing 0.1% (v/v) formic acid and (B) acetonitrile containing 0.1% (v/v) formic acid. Gradient conditions were initially 5% B, increasing linearly to 100% B over 6 min, remaining at 100% B for 2.5 min then decreasing linearly to 5% B over 1 min followed by an equilibration period of 2.5 min prior to the next injection.

Materials. Ethyl 6-((2-oxopropyl)thio)picolinate (**13**) was obtained from GVK Biosciences Private Limited (ref. 25). Bromocyclopentane was distilled over anhydrous calcium carbonate under reduced pressure prior to use.

General Procedure 1: Fischer Indole synthesis. For example, ethyl 6-((6-chloro-2-methyl-1*H*-indol-3-yl)thio)picolinate (16). Prepared according to a modified version of the procedure described by Amira Pharmaceuticals.[18] To a round bottomed flask ethyl 6-((2-oxopropyl)thio)picolinate (**13**) (512 mg, 2.09 mmol, 1 equiv.) and (3-chlorophenyl)hydrazine hydrochloride (374 mg, 2.09 mmol, 1 equiv.) were added and dissolved in *t*BuOH (25 mL, 0.08 M) and stirred at 80 °C for 16 h. Following this, 1 M HCl in Et_2O (0.3 mL) was added to the reaction mixture and stirred for a further 2 h before adding AcOH (0.3 mL) and stirred for a further 1 h. The reaction mixture was then allowed to return to room temperature and concentrated under vacuum to a residue that was purified by reverse-phase UPLC to afford the title compound as a brown solid (517 mg, 71%).

General Procedure 2: Ullmann coupling. For example, 6-((6-chloro-2-methyl-1-(1-methyl-1*H*-pyrazol-4-yl)-1*H*-indol-3-yl)thio) picolinic acid (9). Prepared according to a modified version of a literature procedure for an Ullmann coupling.[38] To a microwave vial was added 1,10-phenanthroline (56 mg, 0.311 mmol, 1 equiv.), CuI (30 mg, 0.156 mmol, 0.5 equiv.), Cs_2CO_3 (203 mg, 0.622 mmol, 2 equiv.), 4-iodo-1-methyl-1*H*-pyrazole (129 mg, 0.622 mmol, 2 equiv.), and ethyl 6-((6-chloro-2-methyl-1*H*-indol-3-yl)thio)picolinate (**16**) (108 mg, 0.311 mmol, 1 equiv.). The reaction vessel was then sealed and purged with N_2 before addition of DMF (1 mL, 0.3 M). The reaction was then heated to 110 °C for 48 h. The reaction mixture was then diluted with water (15 mL) and extracted with EtOAc (3 x 10 mL). The combined organics

were dried (hydrophobic frit), and concentrated under vacuum to a residue that was purified using MDAP to afford the title compound as a pale yellow solid (10 mg, 8%).

General Procedure 3: Ester hydrolysis. For example, 6-((2-methyl-1*H*-indol-3-yl)thio)picolinic acid (19). To a round bottomed flask was added a solution of ethyl 6-((2-methyl-1*H*-indol-3-yl)thio)picolinate (**36**) (56 mg, 0.179 mmol, 1 equiv.) and 2 M aq. NaOH (0.5 mL) in THF (0.5 mL, 0.4 M) and the reaction stirred at room temperature until complete by TLC. The reaction mixture was then concentrated under vacuum to a residue that was purified using MDAP to afford the title compound as a brown amorphous solid (27 mg, 53%).

General Procedure 4: *N*-Arylation. For example, 6-((2-methyl-1-(1-methyl-1*H*-pyrazol-4-yl)-1*H*-indol-3-yl)thio)picolinic acid (28). Prepared according to a modified version of the procedure described by Amira Pharmaceuticals.[18] To a microwave vial was added ethyl 6-((2-methyl-1*H*-indol-3-yl)thio)picolinate (**36**) (198 mg, 0.635 mmol, 1 equiv.), 4-bromo-1-methyl-1*H*-pyrazole (198 μL, 1.90 mmol, 3 equiv.), K_2CO_3 (114 mg, 0.826 mmol, 1.3 equiv.), and CuO (102 mg, 1.27 mmol, 2 equiv.). The vial was then sealed and purged with N_2 before the addition of pyridine (2 mL, 0.3 M). The reaction mixture was then heated to 170 °C for 16 h. The reaction mixture was then allowed to return to room temperature, diluted with EtOAc (15 mL), and washed with water (3 x 10 mL). The organic layer was collected, dried (hydrophobic frit), concentrated under vacuum, and the residue purified using reverse-phase HPLC to afford the title compound as a yellow amorphous solid (15 mg, 6%).

General Procedure 5: Alternative Fischer Indole synthesis. For example, ethyl 6-((5-chloro-2-methyl-1*H*-indol-3-yl)thio)picolinate (82). A solution of ethyl 6-((2-oxopropyl)thio)picolinate (**13**) (1 g, 4.18 mmol, 1 equiv.) and (4-chlorophenyl)hydrazine hydrochloride (749 mg, 4.18 mmol, 1 equiv.) in EtOH (25 mL, 0.2 M) was refluxed until the

reaction was complete by TLC. The reaction mixture was then allowed to return to room temperature, concentrated under vacuum, and the residue purified using silica chromatography, eluting with 0-50% EtOAc/cyclohexane, to afford the title compound as a brown amorphous solid (460 mg, 32%).

General Procedure 6: *N*-Alkylation of the indole. For example, methyl 3-((1,2-dimethyl-1*H*-indol-3-yl)thio)benzoate (93). A solution of methyl 3-((2-methyl-1*H*-indol-3-yl)thio)benzoate (**92**) (200 mg, 0.673 mmol, 1 equiv.), and NaH 60% w/w (54 mg, 1.35 mmol, 2 equiv.) in THF (3 mL, 0.2 M) was heated to 60 °C for 1 h before adding MeI (84 µL, 1.35 mmol, 2 equiv.). The reaction mixture was heated to 60 °C for 16 h then allowed to return to room temperature, concentrated under vacuum, and the residue purified using silica chromatography, eluting with 10% EtOAc/petroleum ether, to afford the title compound as a pale yellow amorphous solid (71 mg, 34%).

General Procedure 7: Methoxycarbonylation. For example, **methyl 3-((2-methyl-1*H*-indol-3-yl)thio)benzoate (92).** *trans*-Bis(acetato)bis[*o*-(di-*o*-tolylphosphino)benzyl] dipalladium(II) (184 mg, 0.196 mmol, 5 mol%) was added to a solution of 3-((3-bromophenyl)thio)-2-methyl-1*H*-indole (**91**) (1.24 g, 3.91 mmol, 1 equiv.), $Mo(CO)_6$ (1 g, 3.91 mmol, 1 equiv.), [tBu$_3$PH]BF$_4$ (227 mg, 0.782 mmol, 20 mol%), and DBU (875 µL, 5.86 mmol, 1.5 equiv.) in MeCN/MeOH (20 mL, 1:4, 0.2 M). The reaction mixture was heated to 70 °C for 16 h then allowed to return to room temperature, concentrated under vacuum, and the residue purified using silica chromatography, eluting with 20% EtOAc/petroleum ether, to afford the title compound as a brown solid (1 g, 88%).

General Procedure 8: Two-step alkylation. For example, 3-(3-bromobenzyl)-6-chloro-2-methyl-1*H*-indole (101). 6-Bromopyridine-2-carbaldehyde (91 mg, 0.488 mmol, 1.03 equiv.)

was added to a solution of 2-methyl-1-(1-methyl-1*H*-pyrazol-4-yl)-1*H*-indole (**98**) (100 mg, 0.474 mmol, 1 equiv.) in CH_2Cl_2 (2 mL, 0.2 M) at 0 °C and stirred for 20 min. Et_3SiH (84 µL, 0.529 mmol, 1.1 equiv.) and TFA (47 µL, 0.610 mmol, 1.3 equiv.) were then added to the reaction mixture and stirred for a further 1 h, during which the reaction mixture was allowed to return to room temperature. The resulting solution was then quenched with sat. aq. $NaHCO_3$ and extracted using CH_2Cl_2 (20 mL). The organic layer was collected, dried (hydrophobic frit), concentrated under vacuum, and the residue purified using silica chromatography, eluting with 20-60% EtOAc/petroleum ether, to afford the title compound as a yellow gum (158 mg, 87%).

6-((6-Chloro-2-methyl-1-(1-methyl-1*H*-pyrazol-4-yl)-1*H*-indol-3-yl)thio) picolinic acid (9). Prepared according to General Procedure 2 using 1,10-phenanthroline (56 mg, 0.311 mmol, 1 equiv.), CuI (30 mg, 0.156 mmol, 0.5 equiv.), Cs_2CO_3 (203 mg, 0.622 mmol, 2 equiv.), 4-iodo-1-methyl-1*H*-pyrazole (129 mg, 0.622 mmol, 2 equiv.), and ethyl 6-((6-chloro-2-methyl-1*H*-indol-3-yl)thio)picolinate (**16**) (108 mg, 0.311 mmol, 1 equiv.) in DMF (1 mL, 0.3 M). Purified using MDAP to afford the title compound as a pale yellow solid (10 mg, 8%). ^{1}H NMR (400 MHz, MeOD) δ 8.06 (s, 1H), 7.90 – 7.79 (m, 1H), 7.78 (s, 1H), 7.73 – 7.61 (m, 1H), 7.46 (d, *J* = 8.3 Hz, 1H), 7.23 (d, *J* = 1.7 Hz, 1H), 7.16 (d, *J* = 7.1 Hz, 1H), 6.97 – 6.84 (m, 1H), 4.07 (s, 3H), 2.43 (s, 3H). CO_2H proton not observed. ^{13}C NMR (126 MHz, $CDCl_3$): δ 163.7, 161.5, 145.9, 144.9, 139.1, 138.6, 129.0, 127.9, 127.6, 127.5, 126.8, 124.0, 122.3, 119.4, 110.7, 97.8, 39.9, 11.6. One carbon not observed/coincident. υ_{max} (neat): 2947, 2924, 1712, 1577 cm^{-1}. HRMS: exact mass calculated for $[M+H]^+$ ($C_{19}H_{16}ClN_4O_2S$) *m/z* requires 401.0646, *m/z* found 401.0646.

Ethyl 6-((4-chloro-2-methyl-1*H*-indol-3-yl)thio)picolinate (14). Prepared according to General Procedure 1 using ethyl 6-((2-oxopropyl)thio)picolinate (**13**) (512 mg, 2.09 mmol, 1 equiv.) and (3-chlorophenyl)hydrazine hydrochloride (374 mg, 2.09 mmol, 1 equiv.) in *t*BuOH (25 mL, 0.1

M) with additional 1 M HCl in Et_2O (0.3 mL) and AcOH (0.3 mL). Purified using reverse-phase UPLC to afford ethyl 6-((4-chloro-2-methyl-1*H*-indol-3-yl)thio)picolinate (**14**) as a white amorphous solid (125 mg, 17%). Ethyl 6-((4-chloro-2-methyl-1*H*-indol-3-yl)thio)picolinate (**14**): ^{1}H NMR (600 MHz, MeOD): δ 7.75-7.71 (m, 1H), 7.58 (app t, *J* = 7.9 Hz, 1H), 7.33 (dd, *J* = 8.0, 0.5 Hz, 1H), 7.07 (app t, *J* = 7.9 Hz, 1H), 7.00 (dd, *J* = 7.6, 0.5 Hz, 1H), 6.82 (dd, *J* = 8.2, 0.6 Hz, 1H), 4.42 (q, *J* = 7.1 Hz, 2H), 2.49 (s, 3H), 1.41 (t, *J* = 7.1 Hz, 3H). NH proton not observed. ^{13}C NMR (151 MHz, MeOD): δ 165.8, 164.8, 147.2, 144.1, 137.7, 137.5, 125.4, 124.8, 122.7, 122.0, 121.2, 120.0, 109.9, 95.2, 61.6, 13.1, 10.4. υ_{max} (neat): 3267, 2980, 1720, 1572, 1537 cm^{-1}. HRMS: exact mass calculated for $[M+H]^+$ ($C_{17}H_{16}ClN_2O_2S$) *m/z* requires 349.0585, *m/z* found 349.05885.

6-((4-Chloro-2-methyl-1*H*-indol-3-yl)thio)picolinic acid (15). Prepared according to General Procedure 3 using ethyl 6-((4-chloro-2-methyl-1*H*-indol-3-yl)thio)picolinate (**14**) (50 mg, 0.144 mmol, 1 equiv.) and 2 M aq. NaOH (1 mL) in THF (1 mL, 0.1 M). Purified using MDAP to afford the desired product as a brown amorphous solid (40 mg, 87%). ^{1}H NMR (400 MHz, MeOD): 7.78 (d, *J* = 7.6 Hz, 1H), 7.63 (app t, *J* = 7.9 Hz, 1H), 7.36 (dd, *J* = 7.9, 0.7 Hz, 1H), 7.10 (app t, *J* = 7.8 Hz, 1H), 7.03 (d, *J* = 7.6 Hz, 1H), 6.85 (dd, *J* = 8.1, 0.7 Hz, 1H), 2.51 (s, 3H). NH and CO_2H protons not observed. ^{13}C NMR (101 MHz, MeOD): δ 166.0, 165.5, 147.1, 144.1, 137.7, 125.4, 124.8, 122.8, 122.0, 121.2, 119.9, 109.9, 95.1, 10.4. One carbon not observed/coincident. υ_{max} (neat): 3250, 3020, 2924, 1708, 1573, 1558, 1535 cm^{-1} HRMS: exact mass calculated for $[M+H]^+$ ($C_{15}H_{12}ClN_2O_2S$) *m/z* requires 319.0303, *m/z* found 319.0300.

Ethyl 6-((6-chloro-2-methyl-1*H*-indol-3-yl)thio)picolinate (16). Prepared according to General Procedure 1 using ethyl 6-((2-oxopropyl)thio)picolinate (**13**) (512 mg, 2.09 mmol, 1 equiv.) and (3-chlorophenyl)hydrazine hydrochloride (374 mg, 2.09 mmol, 1 equiv.) in *t*BuOH (25 mL, 0.1

M) with additional 1 M HCl in Et_2O (0.3 mL) and AcOH (0.3 mL). Purified using reverse-phase UPLC to afford ethyl 6-((6-chloro-2-methyl-1*H*-indol-3-yl)thio)picolinate (**16**) as a brown amorphous solid (517 mg, 71%). ^{1}H NMR (600 MHz, MeOD): δ 7.73 (dd, *J* = 7.6, 0.8 Hz, 1H), 7.59-7.54 (m, 1H), 7.39 (d, *J* = 1.8 Hz, 1H), 7.31 (d, *J* = 8.4 Hz, 1H), 7.02 (dd, *J* = 8.4, 1.8 Hz, 1H), 6.74 (dd, *J* = 8.2, 0.8 Hz, 1H), 4.42 (q, *J* = 7.1 Hz, 2H), 2.48 (s, 3H), 1.41 (t, *J* = 7.1 Hz, 3H). NH proton not observed. ^{13}C NMR (151 MHz, MeOD): δ 164.7, 163.9, 147.5, 143.3, 137.7, 136. 6, 128.3, 127.4, 122.4, 120.5, 120.3, 118.5, 110.8, 95.9, 61.6, 13.1, 10.4. υ_{max} (neat): 3250, 2975, 1720, 1574 cm^{-1}. HRMS: exact mass calculated for $[M+H]^+$ ($C_{17}H_{16}ClN_2O_2S$) *m/z* requires 349.0585, *m/z* found 349.0587.

6-((6-Chloro-2-methyl-1*H*-indol-3-yl)thio)picolinic acid (17). Prepared according to General Procedure 3 using ethyl 6-((6-chloro-2-methyl-1*H*-indol-3-yl)thio)picolinate (**16**) (100 mg, 0.289 mmol, 1 equiv.) and 2 M aq. NaOH (1 mL) in THF (1 mL, 0.3 M). Purified using MDAP to afford the desired product as a yellow amorphous solid (79 mg, 86%). ^{1}H NMR (400 MHz, MeOD): δ 7.77 (dd, *J* = 7.6, 0.8 Hz, 1H), 7.58 (app t, *J* = 7.9 Hz, 1H), 7.40 (d, *J* = 1.9 Hz, 1H), 7.33 (d, *J* = 8.4 Hz, 1H), 7.04 (dd, *J* = 8.4, 1.8 Hz, 1H), 6.74 (dd, *J* = 8.1, 0.8 Hz, 1H), 2.49 (s, 3H). CO_2H and NH protons not observed ^{13}C NMR (101 MHz, MeOD): δ 165.9, 163.6, 147.5, 143.3, 137.8, 136.5, 128.3, 127.4, 122.4, 120.5, 120.2, 118.5, 110.8, 95.9, 10.4. υ_{max} (neat): 3302, 1734, 1685 cm^{-1}. HRMS: exact mass calculated for $[M+H]^+$ ($C_{15}H_{12}ClN_2O_2S$) *m/z* requires 319.0303, *m/z* found 319.0307.

6-((4-Chloro-2-methyl-1-(1-methyl-1*H*-pyrazol-4-yl)-1*H*-indol-3-yl)thio)picolinic acid (18). Prepared according to General Procedure 2 using 1,10-phenanthroline (54 mg, 0.300 mmol, 1 equiv.), CuI (28 mg, 0.150 mmol, 0.5 equiv.), Cs_2CO_3 (196 mg, 0.600 mmol, 2 equiv.), 4-iodo-1-methyl-1*H*-pyrazole (125 mg, 0.600 mmol, 2 equiv.), and ethyl 6-((7-chloro-2-methyl-1*H*-indol-

3-yl)thio)picolinate (**83**) (104 mg, 0.300 mmol, 1 equiv.) in DMF (1 mL, 0.3 M). Purified using MDAP to afford the desired product as an off white solid (32 mg, 27%). ^{1}H NMR (600 MHz, $CDCl_3$): δ 7.84 (d, *J* = 7.5 Hz, 1H), 7.65-7.61 (m, 3H), 7.19-7.03 (m, 4H), 4.04 (s, 3H), 2.37 (s, 3H). CO_2H proton not observed. ^{13}C NMR (151 MHz, MeOD): δ 160.1, 159.2, 142.0, 141.8, 136.2, 134.4, 133.2, 123.8, 121.7, 121.2, 120.6, 119.1, 119.0, 115.2, 115.0, 105.5, 93.2, 35.9, 7.7. υ_{max} (neat):1735, 1510, 1500 cm^{-1}. HRMS: exact mass calculated for $[M+H]^+$ ($C_{19}H_{16}ClN_4O_2S$) *m/z* requires 399.0677, *m/z* found 399.0680.

6-((2-Methyl-1*H*-indol-3-yl)thio)picolinic acid (19). Prepared according to General Procedure 3 using ethyl 6-((2-methyl-1*H*-indol-3-yl)thio)picolinate (**36**) (56 mg, 0.179 mmol, 1equiv.) and 2 M aq. NaOH (0.5 mL) in THF (0.5 mL, 0.4 M). Purified using MDAP to afford the title compound as a brown amorphous solid (27 mg, 53%). ^{1}H NMR (400 MHz, MeOD): δ 7.75 (dd, *J* = 7.6, 0.8 Hz, 1H), 7.56 (app t, *J* = 7.9 Hz, 1H), 7.42-7.34 (m, 2H), 7.18-7.10 (m, 1H), 7.10-7.01 (m, 1H), 6.75 (dd, *J* = 8.1, 0.8 Hz, 1H), 2.49 (s, 3H). NH and CO_2H protons not observed. ^{13}C NMR (101 MHz, MeOD): δ 166.2, 164.1, 163.2, 147.6, 142.1, 137.6, 136.2, 129.6, 122.4, 121.6, 120.0, 117.4, 110.9, 95.4, 10.4. υ_{max} (neat): 3281, 1749, 1716, 1575, 1558 cm^{-1}. HRMS: exact mass calculated for $[M+H]^+$ ($C_{15}H_{13}N_2O_2S$) *m/z* requires 285.0692, *m/z* found 285.0693.

6-((5-Chloro-2-methyl-1*H*-indol-3-yl)thio)picolinic acid (20). Prepared according to General Procedure 3 using ethyl 6-((5-chloro-2-methyl-1*H*-indol-3-yl)thio)picolinate (**82**) (46 mg, 0.133 mmol, 1 equiv.) and 2 M aq. NaOH (0.5 mL) in THF (0.5 mL, 0.3 M). Purified using reverse-phase HPLC to afford the title compound as a pale brown amorphous solid (37 mg, 87%). ^{1}H NMR (400 MHz, MeOD): δ 7.79 (dd, *J* = 7.6, 0.8 Hz, 1H), 7.63-7.58 (m, 1H), 7.37 (d, *J* = 8.6 Hz, 1H), 7.35 (d, *J* = 1.9 Hz, 1H), 7.13 (dd, *J* = 8.6, 2.0 Hz, 1H), 6.77 (dd, *J* = 8.2, 0.8 Hz, 1H), 2.51 (s, 3H). NH and CO_2H protons not observed. ^{13}C NMR (151 MHz, MeOD): δ 166.0, 163.6,

147.7, 144.1, 137.8, 134.6, 130.9, 126.0, 122.3, 121.8, 120.2, 116.8, 112.2, 95.4, 10.4. υ_{max} (neat): 3304, 2960, 2975 1751, 1705, 1656, 1577 cm^{-1}. HRMS: exact mass calculated for $[M+H]^+$ ($C_{15}H_{12}ClN_2O_2S$) *m/z* requires 319.0303, *m/z* found 319.0307.

6-((7-Chloro-2-methyl-1*H*-indol-3-yl)thio)picolinic acid (21). Prepared according to General Procedure 5 using ethyl 6-((2-oxopropyl)thio)picolinate (**13**) (1 g, 4.18 mmol, 1 equiv.) and (2-chlorophenyl)hydrazine hydrochloride (748 mg, 4.18 mmol, 1 equiv.) in EtOH (25 mL, 0.2 M). Following aqueous work-up, the reaction mixture was then used in the next step without further purification. The crude material was used according to General Procedure 3 using 2 M aq. NaOH (6 mL) in THF (6 mL, 0.7 M). Purified using MDAP to afford the title compound as a pale yellow amorphous solid (289 mg, 22% over 2 steps). ^{1}H NMR (600 MHz, MeOD): δ 7.63 (dd, *J* = 7.5, 0.7 Hz, 1H), 7.47 (app t, *J* = 7.8 Hz, 1H), 7.38 (dd, *J* = 7.9, 0.7 Hz, 1H), 7.18 (dd, *J* = 7.6, 0.7 Hz, 1H), 7.05 (app t, *J* = 7.8 Hz, 1H), 6.56 (dd, *J* = 8.1, 0.7 Hz, 1H), 2.56 (s, 3H). NH and CO_2H protons not observed. ^{13}C NMR (151 MHz, MeOD): δ 171.4, 162.1, 154.9, 143.4, 137.0, 133.1, 131.6, 121.0, 120.7, 119.6, 119.0, 116.5, 116.2, 97.8, 10.3. υ_{max} (neat): 3130, 1591, 1556 cm^{-1}. HRMS: exact mass calculated for $[M+H]^+$ ($C_{15}H_{12}ClN_2O_2S$) *m/z* requires 319.0303, *m/z* found 319.0306.

6-((4-Fluoro-2-methyl-1*H*-indol-3-yl)thio)picolinic acid (**22**)**.** Prepared according to General Procedure 3 using ethyl 6-((4-fluoro-2-methyl-1*H*-indol-3-yl)thio)picolinate (**85**) (51 mg, 0.154 mmol, 1 equiv.) and 2 M aq. NaOH solution (0.5 mL) in THF (0.5 mL, 0.3 M). Purified using MDAP to afford the title compound as a yellow amorphous solid (46 mg, 99%). ^{1}H NMR (600 MHz, MeOD): δ 7.75 (dd, *J* = 7.5, 0.7 Hz, 1H), 7.58 (app t, *J* = 7.9 Hz, 1H), 7.18 (d, *J* = 8.2 Hz, 1H), 7.07-7.03 (m, 1H), 6.86 (d, *J* = 8.2 Hz, 1H), 6.68 (dd, *J* = 11.1, 7.9 Hz, 1H), 2.46 (s, 3H). NH and CO_2H protons not observed. ^{13}C NMR (151 MHz, MeOD): δ 166.1, 164.7, 155.9 (d, ^1J_C-

$_F$ = 246.5 Hz), 147.3, 142.8, 139.0 (d, $^3J_{C-F}$ = 10.3 Hz), 137.7, 122.5, 121.9 (d, $^3J_{C-F}$ = 7.7 Hz), 120.0, 117.7 (d, $^2J_{C-F}$ = 17.3 Hz), 107.2 (d, J_{C-F} = 3.8 Hz), 105.3 (d, $^2J_{C-F}$ = 19.2 Hz), 93.2 (d, J_{C-F} = 1.6 Hz), 10.1. ^{19}F NMR (376 MHz, MeOD): δ -129.6. υ_{max} (neat): 3300, 2600, 1687, 1573 cm^{-1}. HRMS: exact mass calculated for $[M+H]^+$ ($C_{15}H_{12}FN_2O_2S$) requires *m/z* 303.0598, found *m/z* 303.0596.

6-((6-Fluoro-2-methyl-1*H*-indol-3-yl)thio)picolinic acid (23). Prepared according to General Procedure 3 using ethyl 6-((6-fluoro-2-methyl-1*H*-indol-3-yl)thio)picolinate (**84**) (50 mg, 0.152 mmol, 1 equiv.) and 2 M aq. NaOH (0.5 mL) in THF (0.5 mL, 0.3 M). Purified using MDAP to afford the title compound as a brown amorphous solid (3 mg, 6%). ^{1}H NMR (400 MHz, MeOD): δ 7.62 (d, *J* = 7.5 Hz, 1H), 7.46 (app t, *J* = 7.8 Hz, 1H), 7.33 (dd, *J* = 8.6, 5.3 Hz, 1H), 7.09 (dd, *J* = 9.6, 2.2 Hz, 1H), 6.85-6.79 (m, 1H), 6.57 (d, *J* = 8.0 Hz, 1H), 2.46 (s, 3H). NH and CO_2H protons not observed. ^{13}C NMR (101 MHz, MeOD): δ 169.1, 163.0, 160.0 (d, $^1J_{C-F}$ = 235.9 Hz), 151.6, 142.7 (d, J_{C-F} = 0.4 Hz), 137.3, 136.1 (d, $^3J_{C-F}$ = 12.6 Hz), 126.1, 120.9, 119.5, 118.4 (d, $^3J_{C-F}$ = 10 Hz), 108.1 (d, $^2J_{C-F}$ = 24.7 Hz), 97.2 (d, $^2J_{C-F}$ = 26.4 Hz), 96.1, 10.4. ^{19}F NMR (376 MHz, MeOD): δ -123.86. υ_{max} (neat): 3338, 1732, 1608, 1583, 1556 cm^{-1}. HRMS: exact mass calculated for $[M+H]^+$ ($C_{15}H_{12}FN_2O_2S$) requires *m/z* 303.0598, found *m/z* 303.0596.

6-((2,4-Dimethyl-1*H*-indol-3-yl)thio)picolinic acid (24) and 6-((2,4-dimethyl-1-(1-methyl-1*H*-pyrazol-4-yl)-1*H*-indol-3-yl)thio)picolinic acid (32). Prepared according to General Procedure 2 using 1,10-phenanthroline (49 mg, 0.270 mmol, 1 equiv.), CuI (26 mg, 0.135 mmol, 0.5 equiv.), Cs_2CO_3 (176 mg, 0.540 mmol, 2 equiv.), 4-iodo-1-methyl-1*H*-pyrazole (112 mg, 0.540 mmol, 2 equiv.), and ethyl 6-((2,4-dimethyl-1*H*-indol-3-yl)thio)picolinate (**87**) (88 mg, 0.270 mmol, 1 equiv.) in DMF (1 mL, 0.3 M). Purified using MDAP to afford the desired 6-((2,4-dimethyl-1*H*-indol-3-yl)thio)picolinic acid (**24**) as a an off white amorphous solid (31 mg,

38%) and 6-((2,4-dimethyl-1-(1-methyl-1*H*-pyrazol-4-yl)-*1H*-indol-3-yl)thio)picolinic acid (**32**) as a white solid (24 mg, 24%). 6-((2,4-Dimethyl-1*H*-indol-3-yl)thio)picolinic acid (**24**): ^{1}H NMR (400 MHz, MeOD): δ 7.76 (dd, *J* = 7.6, 0.9 Hz, 1H), 7.63-7.55 (m, 1H), 7.23 (d, *J* = 8.1 Hz, 1H), 7.05-6.97 (m, 1H), 6.84-6.75 (m, 2H), 2.56 (s, 3H), 2.47 (s, 3H). NH and CO_2H protons not observed. ^{13}C NMR (101 MHz, MeOD): δ 166.1, 165.9, 147.4, 142.3, 137.8, 136.4, 129.5, 127.1, 122.5, 121.8, 121.4, 119.9, 108.9, 95.2, 17.5, 10.3. υ_{max} (neat): 3302, 1690, 1580, 1558 cm^{-1}. HRMS: exact mass calculated for $[M+H]^+$ ($C_{16}H_{15}N_2O_2S$) requires *m/z* 299.0849, found *m/z* 299.0849. 6-((2,4-Dimethyl-1-(1-methyl-1*H*-pyrazol-4-yl)-*1H*-indol-3-yl)thio)picolinic acid (**32**): ^{1}H NMR (600 MHz, DMSO-*d*$_6$): δ 7.16 (s, 1H), 6.94 (d, *J* = 7.5 Hz, 1H), 6.88 (s, 1H), 6.80 (app t, *J* = 7.8 Hz, 1H), 6.30-6.18 (m, 2H), 6.13-5.98 (m, 2H), 4.01 (s, 3H), 1.78 (s, 3H), 1.56 (s, 3H). CO_2H proton not observed. ^{13}C NMR (151 MHz, DMSO-*d*$_6$): δ 166.8, 163.9, 148.9, 143.5, 138.3, 137.0, 135.8, 129.2, 127.9, 125.7, 122.1, 121.3, 121.0, 119.0, 118.6, 107.3, 96.8, 37.5, 16.8, 9.2. υ_{max} (neat): 2943, 2921, 1720, 1686, 1619, 1574, 1561 cm^{-1}. HRMS: exact mass calculated for $[M+H]^+$ ($C_{20}H_{19}N_4O_2S$) requires *m/z* 379.1223, found *m/z* 379.1220.

6-((2,6-Dimethyl-1*H*-indol-3-yl)thio)picolinic acid (25). Prepared according to General Procedure 2 using 1,10-phenanthroline (49 mg, 0.270 mmol, 1 equiv.), CuI (26 mg, 0.135 mmol, 0.5 equiv.), Cs_2CO_3 (176 mg, 0.540 mmol, 2 equiv.), 4-iodo-1-methyl-1*H*-pyrazole (112 mg, 0.540 mmol, 2 equiv.), and ethyl 6-((2,6-dimethyl-1*H*-indol-3-yl)thio)picolinate (**86**) (88 mg, 0.270 mmol, 1 equiv.) in DMF (1 mL, 0.3 M). Purified using MDAP to afford 6-((2,6-dimethyl-1*H*-indol-3-yl)thio)picolinic acid (**25**) as a yellow amorphous solid (8 mg, 10%): ^{1}H NMR (400 MHz, MeOD): δ 7.64 (d, *J* = 7.5 Hz, 1H), 7.46 (app t, *J* = 7.8 Hz, 1H), 7.24 (d, *J* = 8.0 Hz, 1H), 7.18 (d, *J* = 0.5 Hz, 1H), 6.88 (dd, *J* = 8.0, 0.9 Hz, 1H), 6.63 (d, *J* = 8.0 Hz, 1H), 2.45 (s, 3H), 2.42 (s, 3H). NH and CO_2H not observed. ^{13}C NMR (101 MHz, MeOD): δ 169.2, 163.5, 151.7,

141.2, 137.1, 136.6, 131.4, 127.5, 121.5, 120.9, 119.2, 117.2, 110.8, 95.6, 20.3, 10.3. υ_{max} (neat): 3280, 3249, 2900, 1722, 1578, 1560, 1441 cm^{-1}. HRMS: exact mass calculated for $[M+H]^+$ ($C_{16}H_{15}N_2O_2S$) requires *m/z* 299.0849, found *m/z* 299.0849.

6-((4-Methoxy-2-methyl-1*H*-indol-3-yl)thio)picolinic acid (26). Prepared according to General Procedure 3 using ethyl 6-((4-methoxy-2-methyl-1*H*-indol-3-yl)thio)picolinate (**89**) (47 mg 0.137 mmol, 1 equiv.) and 2 M aq. NaOH (0.5 mL) in THF (0.5 mL, 0.3 M). Purified using MDAP to afford the title compound as a yellow amorphous solid (42 mg, 98%). ^{1}H NMR (400 MHz, MeOD): δ 7.72 (d, *J* = 7.5 Hz, 1H), 7.55 (app t, *J* = 7.9 Hz, 1H), 7.06-6.93 (m, 2H), 6.89 (d, *J* = 8.2 Hz, 1H), 6.49 (d, *J* = 7.5 Hz, 1H), 3.59 (s, 3H), 2.43 (s, 3H). NH and CO_2H protons not observed. ^{13}C NMR (101 MHz, MeOD): δ 165.9, 165.8, 153.5, 146.7, 140.7, 137.8, 137.5, 123.1, 122.4, 119.7, 118.6, 104.4, 101.0, 94.2, 54.4, 10.2. υ_{max} (neat): 3273, 2950, 1716, 1583, 1539 cm^{-1}. HRMS: exact mass calculated for $[M+H]^+$ ($C_{16}H_{15}N_2O_3S$) requires *m/z* 315.0798, found *m/z* 315.0798.

6-((6-Methoxy-2-methyl-1*H*-indol-3-yl)thio)picolinic acid (27). Prepared according to General Procedure 3 using ethyl 6-((6-methoxy-2-methyl-1*H*-indol-3-yl)thio)picolinate (**88**) (46 mg, 0.134 mmol, 1 equiv.) and 2 M aq. NaOH (0.5 mL) in THF (0.5 mL, 0.3 M). Purified using MDAP to afford the title compound as a brown amorphous solid (36 mg, 86%). ^{1}H NMR (400 MHz, MeOD): δ 7.75 (dd, *J* = 7.6, 0.9 Hz, 1H), 7.58-7.51 (m, 1H), 7.21 (d, *J* = 8.6 Hz, 1H), 6.93 (d, *J* = 2.1 Hz, 1H), 6.78 (dd, *J* = 8.1, 0.9 Hz, 1H), 6.70 (dd, *J* = 8.6, 2.2 Hz, 1H), 3.80 (s, 3H), 2.44 (s, 3H). NH and CO_2H protons not observed. ^{13}C NMR (101 MHz, MeOD): δ 165.8, 164.2, 156.7, 147.1, 140.9, 137.9, 136.9, 123.5, 122.7, 120.1, 118.0, 109.7, 94.8, 94.7, 54.7, 10.4. υ_{max} (neat): 3286, 2995, 1724, 1627, 1581, 1500 cm^{-1}. HRMS: exact mass calculated for $[M-H]^-$ ($C_{16}H_{13}N_2O_3S$) requires *m/z* 315.0798, found *m/z* 315.0798.

6-((2-Methyl-1-(1-methyl-1*H*-pyrazol-4-yl)-1*H*-indol-3-yl)thio)picolinic acid (28). Prepared according General Procedure 4 using ethyl 6-((2-methyl-1*H*-indol-3-yl)thio)picolinate (**36**) (198 mg, 0.635 mmol, 1 equiv.), 4-bromo-1-methyl-1*H*-pyrazole (198 μL, 1.90 mmol, 3 equiv.), K_2CO_3 (114 mg, 0.826 mmol, 1.3 equiv.), and CuO (102 mg, 1.27 mmol, 2 equiv.) in pyridine (2 mL, 0.3 M). Purified using reverse-phase HPLC to afford the title compound as a yellow amorphous solid (15 mg, 6%). ^{1}H NMR (400 MHz, $CO(CD_3)_2$) δ 11.03 (br s, 1H), 8.08 (s, 1H), 7.81 (d, *J* = 7.4 Hz, 1H), 7.76 – 7.61 (m, *J* = 7.8 Hz, 2H), 7.48 (d, *J* = 7.4 Hz, 1H), 7.30 – 7.11 (m, 3H), 6.99 (d, *J* = 7.9 Hz, 1H), 4.05 (s, 3H), 2.43 (s, 3H). ^{13}C NMR (101 MHz, $CO(CD_3)_2$) δ 165.2, 163.3, 148.1, 145.4, 139.7, 139.4, 137.2, 129.9, 129.1, 123.8, 123.5, 122.2, 120.7, 118.8, 111.5, 98.0, 55.3, 39.8, 11.6. υ_{max} (neat): 2924, 2852, 1708, 1693, 1573 cm^{-1}. HRMS: exact mass calculated for $[M+H]^+$ ($C_{19}H_{17}N_4O_2S$) *m/z* requires 365.1067, *m/z* found 365.1070.

6-((5-Chloro-2-methyl-1-(1-methyl-1*H*-pyrazol-4-yl)-1*H*-indol-3-yl)thio) picolinic acid (29). Prepared according to General Procedure 2 using 1,10-phenanthroline (57 mg, 0.318 mmol, 1 equiv.), CuI (30 mg, 0.159 mmol, 0.5 equiv.), Cs_2CO_3 (207 mg, 0.636 mmol, 2 equiv.), 4-iodo-1-methyl-1*H*-pyrazole (132 mg, 0.636 mmol, 2 equiv.), and ethyl 6-((5-chloro-2-methyl-1*H*-indol-3-yl)thio)picolinate (**82**) (110 g, 0.318 mmol, 1 equiv.) in DMF (1 mL, 0.3 M). Purified using MDAP to afford the title compound as a white amorphous solid (28 mg, 21%). ^{1}H NMR (400 MHz, $CDCl_3$): δ 7.88 (d, *J* = 7.5 Hz, 1H), 7.65-7.61 (m, 3H), 7.50 (d, *J* = 1.7 Hz, 1H), 7.19-7.05 (m, 3H), 4.05 (s, 3H), 2.38 (s, 3H). CO_2H proton not observed. ^{13}C NMR (101 MHz, $CDCl_3$): δ 163.6, 161.3, 145.9, 145.6, 138.6, 137.1, 137.0, 130.2, 127.7, 127.5, 124.0, 123.2, 119.4, 118.0, 111.7, 97.2, 39.9, 11.7. One carbon not observed/coincident. υ_{max} (neat): 3025, 1730, 1577, 1558, 1531 cm^{-1}. HRMS: exact mass calculated for $[M+H]^+$ ($C_{19}H_{16}ClN_4O_2S$) *m/z* requires 399.0677, *m/z* found 399.0680.

6-((4-Fluoro-2-methyl-1-(1-methyl-1*H*-pyrazol-3-yl)-1*H*-indol-3-yl)thio)picolinic acid (30). Prepared according to General Procedure 2 using 1,10-phenanthroline (80 mg, 0.442 mmol, 1 equiv.), CuI (42 mg, 0.221 mmol, 0.5 equiv.), Cs_2CO_3 (288 mg, 0.884 mmol, 2 equiv.), 4-iodo-1-methyl-1*H*-pyrazole (184 mg, 0.884 mmol, 2 equiv.), and ethyl 6-((7-chloro-2-methyl-1*H*-indol-3-yl)thio)picolinate (**83**) (146 mg, 0.442 mmol, 1 equiv.) in DMF (1.5 mL, 0.3 M). Purified using MDAP to afford the title compound as a red amorphous solid (6 mg, 3%). ^{1}H NMR (600 MHz, $CDCl_3$): δ 7.87 (d, *J* = 7.3 Hz, 1H), 7.67 (d, *J* = 7.4 Hz, 1H), 7.63 (s, 1H), 7.61 (s, 1H), 7.22 (s, 1H), 7.11 (dd, *J* = 12.8, 8.0 Hz, 1H), 7.00 (d, *J* = 8.2 Hz, 1H), 6.88-6.75 (m, 1H), 4.05 (s, 3H), 2.37 (s, 3H). CO_2H proton not observed. ^{13}C NMR (151 MHz, $CDCl_3$): δ 162.1, 155.9 (d, $^1J_{C\text{-}F}$ = 249.1 Hz), 144.5, 142.2, 141.3 (d, $^3J_{C\text{-}F}$ = 9.4 Hz), 138.5, 137.1, 127.6, 124.2, 123.1 (d, $^3J_{C\text{-}F}$ = 7.5 Hz), 119.2, 117.5 (d, $^2J_{C\text{-}F}$ = 17.9 Hz), 107.3 (d, $^2J_{C\text{-}F}$ = 18.8 Hz), 106.8 (d, $J_{C\text{-}F}$ = 3.3 Hz), 95.1, 39.9, 11.4. Two carbons not observed/coincident. ^{19}F NMR (376 MHz, $CDCl_3$): δ -126.82. υ_{max} (neat): 2800, 2500, 1735, 1577, 1558 cm^{-1}. HRMS: exact mass calculated for $[M+H]^+$ ($C_{19}H_{16}FN_4O_2S$) requires *m/z* 383.0973, found *m/z* 383.0975.

6-((6-Fluoro-2-methyl-1-(1-methyl-1*H*-pyrazol-3-yl)-1*H*-indol-3-yl)thio) picolinic acid (31). Prepared according to General Procedure 2 using 1,10-phenanthroline (55 mg, 0.304 mmol, 1 equiv.), CuI (29 mg, 0.152 mmol 0.5 equiv.), Cs_2CO_3 (198 mg, 0.608 mmol, 2 equiv.), 4-iodo-1-methyl-1*H*-pyrazole (126 mg, 0.608 mmol, 2 equiv.), and ethyl 6-((6-fluoro-2-methyl-1*H*-indol-3-yl)thio)picolinate (**84**) (100 mg, 0.304 mmol, 1 equiv.) in DMF (1 mL, 0.3 M). Purified using MDAP to afford the title compound as a yellow amorphous solid (25 mg, 22%). ^{1}H NMR (600 MHz, MeOD): δ 8.01 (s, 1H), 7.73 (s, 1H), 7.71 (d, *J* = 7.6 Hz, 1H), 7.56 (app t, *J* = 7.8 Hz, 1H), 7.42 (dd, *J* = 8.1, 5.2 Hz, 1H), 6.93 (d, *J* = 9.4 Hz, 1H), 6.90-6.86 (m, 2H), 4.03 (s, 3H), 2.39 (s, 3H). CO_2H proton not observed. ^{13}C NMR (151 MHz, $CDCl_3$): δ 162.1, 155.9 (d, $^1J_{C\text{-}F}$ = 249.1

Hz), 144.5, 142.2, 141.3 (d, $^{3}J_{C\text{-}F}$ = 9.4 Hz), 138.5, 137.1, 127.6, 124.2, 123.1 (d, $^{3}J_{C\text{-}F}$ = 7.5 Hz), 119.2, 117.5 (d, $^{2}J_{C\text{-}F}$ = 17.9 Hz), 107.3 (d, $^{2}J_{C\text{-}F}$ = 18.8 Hz), 106.8 (d, $J_{C\text{-}F}$ = 3.3 Hz), 95.1, 39.9, 11.4. Two carbons not observed/coincident. υ_{max} (neat): 2900, 1725, 1618, 1575, 1558 cm^{-1}. HRMS: exact mass calculated for $[M+H]^{+}$ ($C_{19}H_{16}FN_4O_2S$) requires *m/z* 383.0973, found *m/z* 383.0979.

6-((2,6-Dimethyl-1-(1-methyl-1*H*-pyrazol-4-yl)-1*H*-indol-3-yl)thio)picolinic acid (33). Prepared according to General Procedure 2 using 1,10-phenanthroline (49 mg, 0.270 mmol, 1 equiv.), CuI (26 mg, 0.135 mmol, 0.5 equiv.), Cs_2CO_3 (176 mg, 0.540 mmol, 2 equiv.), 4-iodo-1-methyl-1*H*-pyrazole (112 mg, 0.540 mmol, 2 equiv.), and ethyl 6-((2,6-dimethyl-1*H*-indol-3-yl)thio)picolinate (**86**) (88 mg, 0.270 mmol, 1 equiv.) in DMF (1 mL, 0.3 M). Purified using MDAP to afford 6-((2,6-dimethyl-1-(1-methyl-1*H*-pyrazol-4-yl)-1*H*-indol-3-yl)thio)picolinic acid (**33**) as a yellow amorphous solid (28 mg, 27%): ^{1}H NMR (400 MHz, MeOD): δ 7.99 (s, 1H), 7.72 (d, *J* = 0.6 Hz, 1H), 7.68 (d, *J* = 7.4 Hz, 1H), 7.51 (app t, *J* = 7.8 Hz, 1H), 7.33 (d, *J* = 8.0 Hz, 1H), 7.01 (s, 1H), 6.97 (d, *J* = 8.0 Hz, 1H), 6.72 (d, *J* = 8.0 Hz, 1H), 4.03 (s, 3H), 2.40 (s, 3H), 2.38 (s, 3H). CO_2H proton not observed. ^{13}C NMR (125 MHz, DMSO-*d*$_6$): δ 147.1, 143.1, 141.2, 140.5, 136.4, 132.6, 130.8, 126.5, 125.0, 124.8, 123.4, 121.6, 113.9, 42.2, 24.2, 14.0. Four carbons not observed/coincident. υ_{max} (neat): 2921, 2852, 1680, 1615, 1558, 1573 cm^{-1}. HRMS: exact mass calculated for $[M+H]^{+}$ ($C_{20}H_{19}N_4O_2S$) requires *m/z* 379.1223, found *m/z* 379.1220.

6-((4-Methoxy-2-methyl-1-(1-methyl-1*H*-pyrazol-4-yl)-1*H*-indol-3-yl)thio) picolinic acid (34). Prepared according to General Procedure 2 using 1,10-phenanthroline (53 mg, 0.292 mmol, 1 equiv.), CuI (28 mg, 0.146 mmol, 0.5 equiv.), Cs_2CO_3 (190 mg, 0.584 mmol, 2 equiv.), 4-iodo-1-methyl-1*H*-pyrazole (121 mg, 0.584 mmol, 2 equiv.), and ethyl 6-((4-methoxy-2-methyl-1*H*-indol-3-yl)thio)picolinate (**89**) (100 mg, 0.292 mmol, 1 equiv.) in DMF (2 mL, 0.1 M). Purified

using MDAP to afford the title compound as an off-white amorphous solid (21 mg, 18%). ^{1}H NMR (600 MHz, MeOD): δ 7.96 (s, 1H), 7.68 (s, 1H), 7.60 (d, *J* = 7.3 Hz, 1H), 7.47 (app t, *J* = 7.8 Hz, 1H), 7.07 (app t, *J* = 8.1 Hz, 1H), 6.79 (d, *J* = 8.2 Hz, 1H), 6.75 (d, *J* = 7.8 Hz, 1H), 6.59 (d, *J* = 7.8 Hz, 1H), 4.02 (s, 3H), 3.64 (s, 3H), 2.35 (s, 3H). CO_2H proton not observed. ^{13}C NMR (151 MHz, MeOD): δ 163.9, 153.8, 142.3, 140.4, 136.6, 136.6, 128.7, 123.0, 120.5, 119.6, 118.6, 118.2, 110.0, 103.3, 102.0, 97.5, 54.5, 38.2, 9.9. One carbon not observed/coincident. υ_{max} (neat): 3150, 2900, 2800, 1602, 1556 cm^{-1}. HRMS: exact mass calculated for $[M+H]^+$ ($C_{20}H_{19}N_4O_3S$) requires *m/z* 395.1172, found *m/z* 395.1174.

6-((6-Methoxy-2-methyl-1-(1-methyl-1*H*-pyrazol-4-yl)-1*H*-indol-3-yl)thio) picolinic acid (35). Prepared according to General Procedure 2 using 1,10-phenanthroline (56 mg, 0.311 mmol, 1 equiv.), CuI (30 mg, 0.156 mmol, 0.5 equiv.), Cs_2CO_3 (203 mg, 0.622 mmol, 2 equiv.), 4-iodo-1-methyl-1*H*-pyrazole (129 mg, 0.622 mmol, 2 equiv.), and ethyl 6-((6-methoxy-2-methyl-1*H*-indol-3-yl)thio)picolinate (**88**) (106 mg, 0.311 mmol, 1 equiv.) in DMF (1 mL, 0.3 M). Purified using MDAP to afford the title compound as a pink amorphous solid (32 mg, 26%). ^{1}H NMR (600 MHz, $CDCl_3$): δ 7.85 (d, *J* = 7.4 Hz, 1H), 7.65 (s, 1H), 7.63-7.58 (m, 2H), 7.38 (d, *J* = 8.6 Hz, 1H), 7.09 (d, *J* = 8.1 Hz, 1H), 6.83 (dd, *J* = 8.6, 2.1 Hz, 1H), 6.70 (d, *J* = 2.2 Hz, 1H), 4.05 (s, 3H), 3.79 (s, 3H), 2.35 (s, 3H). CO_2H proton not observed. ^{13}C NMR (151 MHz, $CDCl_3$): δ 163.8, 162.1, 157.3, 145.8, 142.8, 139.5, 138.5, 137.1, 127.6, 124.0, 122.9, 119.5, 119.2, 119.1, 111.0, 97.2, 94.6, 55.8, 39.8, 11.6. υ_{max} (neat): 3300, 1755, 1616, 1583, 1556 cm^{-1}. HRMS: exact mass calculated for $[M+H]^+$ ($C_{20}H_{19}N_4O_3S$) requires *m/z* 395.1172, found *m/z* 395.1173.

Ethyl 6-((2-methyl-1*H*-indol-3-yl)thio)picolinate (36). Prepared according to the General Procedure 1 using ethyl 6-((2-oxopropyl)thio)picolinate (**13**) (1 g, 4.24 mmol, 1 equiv.), and phenylhydrazine hydrochloride (615 mg, 4.24 mmol, 1 equiv.) in *t*BuOH (50 mL, 0.1 M), with

additional 1 M HCl in Et_2O (0.6 mL) and AcOH (0.6 mL). Purified using silica chromatography, eluting with 10-80% EtOAc/petroleum ether, to afford the title compound as a brown amorphous solid (1.23 g, 93%). ^{1}H NMR (400 MHz, $CDCl_3$): δ 8.59 (br s, 1H), 7.74 (dd, *J* = 7.6, 0.8 Hz, 1H), 7.51 (d, *J* = 7.9 Hz, 1H), 7.41 (d, *J* = 8.4 Hz, 1H), 7.37 (d, *J* = 8.7 Hz, 1H), 7.24-7.19 (m, 1H), 7.13 (td, *J* = 7.7, 1.0 Hz, 1H), 6.76 (d, *J* = 8.1 Hz, 1H), 4.47 (q, *J* = 7.1 Hz, 2H), 2.53 (s, 3H), 1.43 (t, *J* = 7.1 Hz, 3H). ^{13}C NMR (101 MHz, $CDCl_3$): δ 165.1, 164.1, 148.0, 141.6, 137.2, 135.7, 129.8, 122.5, 122.4, 120.9, 120.5, 118.8, 110.9, 97.8, 61.9, 14.3, 12.2. υ_{max} (neat): 3281, 1732, 1716, 1573 cm^{-1}. HRMS: exact mass calculated for $[M+H]^+$ ($C_{17}H_{17}N_2O_2S$) *m/z* requires 313.1005, *m/z* found 313.1005.

6-((1,2-Dimethyl-1*H*-indol-3-yl)thio)picolinic acid (37). Prepared according to General Procedure 6 using methyl ethyl 6-((2-methyl-1*H*-indol-3-yl)thio)picolinate (**36**) (301 mg, 0.965 mmol, 1 equiv.), NaH 95% w/w (73 mg, 2.89 mmol, 3 equiv.), and MeI (120 μL, 1.93 mmol, 2 equiv.) in DMF (3 mL, 0.3 M). The crude material was then used in General Procedure C using 2 M aq. NaOH (0.25 mL). Purified by reverse-phase HPLC to afford the title compound as a dark red amorphous solid (35 mg, 12% over 2 steps). ^{1}H NMR (500 MHz, $CDCl_3$): δ 7.83 (d, *J* = 7.5 Hz, 1H), 7.57 (dd, *J* = 9.7, 5.9 Hz, 1H), 7.52 (d, *J* = 7.8 Hz, 1H), 7.39 (d, *J* = 8.1 Hz, 1H), 7.29 (d, *J* = 7.3 Hz, 1H), 7.17 (app t, *J* = 7.4 Hz, 1H), 6.98 (d, *J* = 8.1 Hz, 1H), 3.81 (s, 3H), 2.53 (s, 3H). CO_2H proton not observed. ^{13}C NMR (101 MHz, $CDCl_3$): δ 145.2, 138.0, 137.9, 123.5, 123.4, 122.2, 121.8, 120.7, 120.5, 118.6, 118.5, 118.0, 110.5, 108.9, 29.2, 10.4. υ_{max} (neat): 2992, 2852, 1693, 1571, 1550 cm^{-1}. HRMS: exact mass calculated for $[M+H]^+$ ($C_{16}H_{15}N_2O_2S$) requires *m/z* 299.0854, found *m/z* 299.0853

6-((1-Cyclopentyl-2-methyl-1*H*-indol-3-yl)thio)picolinic acid (38). Prepared according to General Procedure 6 using ethyl 6-((2-methyl-1*H*-indol-3-yl)thio)picolinate (**36**) (300 mg, 0.962

mmol, 1 equiv.), NaH 60% w/w (116 mg, 2.89 mmol, 3 equiv.), and bromocyclopentane (309 μL, 2.89 mmol, 3 equiv.) in DMF (3 mL, 0.3 M). Purified by reverse-phase HPLC to afford the title compound as a yellow amorphous solid (36 mg, 11%). ^{1}H NMR (400 MHz, $CDCl_3$): δ 9.10 (s, 1H), 7.70 (d, *J* = 7.6 Hz, 1H), 7.49 (d, *J* = 7.8 Hz, 1H), 7.41-7.37 (m, 2H), 7.24-7.19 (m, 1H), 7.16-7.11 (m, 1H), 6.79 (d, *J* = 8.7 Hz, 1H), 5.49-5.44 (m, 1H), 2.53 (s, 3H), 2.07-1.96 (m, 2H), 1.93-1.75 (m, 4H), 1.67-1.62 (m, 2H). ^{13}C NMR (101 MHz, $CDCl_3$): δ 164.3, 163.7, 147.7, 141.4, 136.7, 135.3, 129.3, 121.9, 121.8, 120.3, 119.9, 118.1, 110.6, 96.9, 78.3, 32.2, 23.3, 11.7. υ_{max} (neat): 3275, 2918, 1714, 1570 cm^{-1}. HRMS: exact mass calculated for $[M-H]^-$ ($C_{20}H_{19}N_2O_2S$) requires *m/z* 351.1173, found *m/z* 351.1170.

6-((2-Methyl-1-phenyl-1*H*-indol-3-yl)thio)picolinic acid (39). Prepared according to General Procedure 4 using ethyl 6-((2-methyl-1*H*-indol-3-yl)thio)picolinate (**36**) (200 mg, 0.641 mmol, 1 equiv.), bromobenzene (204 μL, 1.92 mmol, 3 equiv.), CuO (102 mg, 1.28 mmol, 2 equiv.), and K_2CO_3 (115 mg, 0.833 mmol, 1.3 equiv.) in pyridine (2 mL, 0.3 M). Purified by reverse-phase HPLC to afford the title compound as a brown amorphous solid (12 mg, 5%). ^{1}H NMR (400 MHz, $CDCl_3$): δ 7.87 (d, *J* = 7.4 Hz, 1H), 7.67-7.49 (m, 5H), 7.41-7.39 (m, 2H), 7.23-7.14 (m, 3H), 7.12 (d, *J* = 8.0 Hz, 1H), 2.39 (s, 3H). CO_2H proton not observed. ^{13}C NMR (101 MHz, $CDCl_3$): δ 163.2, 161.6, 145.3, 142.9, 138.0, 137.7, 136.7, 129.3, 128.2, 127.4, 123.6, 122.3, 121.1, 118.7, 118.0, 110.3, 96.9, 11.2. υ_{max} (neat): 2920, 2850, 1693, 1573, 1550 cm^{-1}. HRMS: exact mass calculated for $[M+H]^+$ ($C_{21}H_{17}N_2O_2S$) requires *m/z* 361.1010, found *m/z* 361.1010.

6-((6-Chloro-1,2-dimethyl-1*H*-indol-3-yl)thio)picolinic acid (40). Prepared according to General Procedure 6 using ethyl 6-((6-chloro-2-methyl-1*H*-indol-3-yl)thio)picolinate (**16**) (138 mg, 0.399 mmol, 1 equiv.), NaH 60% w/w (64 mg, 1.60 mmol, 4 equiv.), and MeI (74 μL, 1.19 mmol, 3 equiv.) in DMF (2 mL, 0.2 M). Purified using reverse-phase HPLC to afford the title

compound as a yellow amorphous solid (28 mg, 21%). ^{1}H NMR (400 MHz, $CDCl_3$): δ 7.84 (d, *J* = 7.3 Hz, 1H), 7.58 (app t, *J* = 7.8 Hz, 1H), 7.43-7.36 (m, 2H), 7.12 (d, *J* = 8.3 Hz, 1H), 6.94 (d, *J* = 7.9 Hz, 1H), 3.76 (s, 3H), 2.51 (s, 3H). CO_2H proton not observed. ^{13}C NMR (101 MHz, $CDCl_3$): δ 161.6, 143.5, 138.0, 137.2, 127.8, 127.7, 127.1, 123.3, 121.1, 118.9, 118.8, 109.2, 95.4, 30.2, 29.2, 10.6. υ_{max} (neat): 2916, 2848, 1703, 1573, 1556 cm^{-1}. HRMS: exact mass calculated for $[M+H]^+$ ($C_{16}H_{14}ClN_2O_2S$) requires *m/z* 333.0462, found *m/z* 333.0463.

6-((6-Chloro-1-cyclopentyl-2-methyl-1*H*-indol-3-yl)thio)picolinic acid (41). Prepared according to General Procedure 6 using ethyl 6-((6-chloro-2-methyl-1*H*-indol-3-yl)thio)picolinate (**16**) (193 mg, 0.558 mmol, 1 equiv.), NaH 60% w/w (178 mg 4.46 mmol, 8 equiv.), and bromocyclopentane (359 μL, 3.35 mmol, 6 equiv.) in DMF (3 mL, 0.2 M). Purified by reverse-phase HPLC to afford the title compound as an off white solid (19 mg, 10%). ^{1}H NMR (400 MHz, $CDCl_3$): δ 7.85 (dd, *J* = 7.5, 0.8 Hz, 1H), 7.65-7.57 (m, 1H), 7.48-7.43 (m, 2H), 7.42 (s, 1H), 7.11 (dd, *J* = 8.4, 1.7 Hz, 1H), 6.96 (dd, *J* = 8.1, 0.8 Hz, 1H), 4.85 (m, 1H), 2.54 (s, 3H), 2.33-2.20 (m, 2H), 2.20-2.04 (m, 4H), 1.90-1.77 (m, 2H). ^{13}C NMR (126 MHz, $CDCl_3$): δ 163.6, 162.1, 145.7, 144.1, 138.5, 135.2, 128.6, 127.7, 123.9, 121.3, 119.7, 119.2, 111.6, 96.1, 57.5, 30.2, 25.2, 11.9. υ_{max} (neat): 2958, 2872, 1699, 1570 cm^{-1}. HRMS: exact mass calculated for $[M-H]^-$ ($C_{20}H_{18}ClN_2O_2S$) requires *m/z* 385.0783, found *m/z* 385.0778.

6-((6-Chloro-2-methyl-1-phenyl-1*H*-indol-3-yl)thio)picolinic acid (42). Prepared according to General Procedure 2 using 1,10-phenanthroline (104 mg, 0.578 mmol, 1 equiv.), CuI (55 mg, 0.289 mmol, 0.5 equiv.), Cs_2CO_3 (377 mg, 1.15 mmol, 2 equiv.), iodobenzene (147 μL, 1.15 mmol, 2 equiv.), and ethyl 6-((6-chloro-2-methyl-1*H*-indol-3-yl)thio)picolinate (**16**) (200 mg, 0.578 mmol, 1 equiv.) in DMF (2 mL, 0.1 M). Purified using MDAP to afford the title compound as a white amorphous solid (9 mg, 4%). ^{1}H NMR (500 MHz, MeOD): δ 7.88 (d, *J* =

7.3 Hz, 1H), 7.66 (app t, *J* = 7.8 Hz, 1H), 7.61 (app t, *J* = 7.4 Hz, 2H), 7.55 (app t, *J* = 7.4, 1H), 7.47 (d, *J* = 8.4 Hz, 1H), 7.40-7.36 (m, 2H), 7.19-7.13 (m, 2H), 7.11 (d, *J* = 8.1 Hz, 1H), 2.37 (s, 3H). CO_2H proton not observed. ^{13}C NMR (151 MHz, MeOD): δ 162.6, 144.6, 138.6, 137.8, 136.8, 129.8, 128.8, 128.3, 127.8, 127.7, 122.1, 121.5, 120.2, 119.1, 110.1, 110.0, 98.3, 10.3. One carbon not observed/coincident. υ_{max} (neat): 3051, 1771, 1598, 1559, 1501 cm^{-1}. HRMS: exact mass calculated for $[M+H]^+$ ($C_{21}H_{16}ClN_2O_2S$) requires *m/z* 395.0616, found *m/z* 395.0617.

1-((3-Bromophenyl)thio)propan-2-one (44). A flask containing 3-bromothiophenol (**43**) (273 μL, 2.65 mmol, 1 equiv.) in THF (15 mL, 0.2 M) was cooled to 0 °C. DIPEA (2.3 mL, 13.2 mmol, 5 equiv.) was added portion wise and allowed to stir for 30 min before the addition of chloroacetone (2.3 mL, 29.0 mmol, 11 equiv.). The reaction mixture was then allowed to warm to room temperature and stirred for 16 h. The reaction mixture was concentrated under vacuum, diluted with EtOAc (30 mL) and washed with H_2O (30 mL). The organic layer was collected, dried (hydrophobic frit), and concentrated under vacuum. Purified using silica chromatography, eluting with 0-40% EtOAc/petroleum ether, to afford the title compound as a colourless oil (540 mg, 83%). ^1H NMR (400 MHz, $CDCl_3$): δ 7.45 (app t, *J* = 1.8 Hz, 1H), 7.33-7.29 (m, 1H), 7.24-7.20 (m, 1H), 7.13 (t, *J* = 7.9 Hz, 1H), 3.68 (s, 2H), 2.26 (s, 3H). ^{13}C NMR (101 MHz, $CDCl_3$): δ 202.8, 137.2, 131.6, 130.4, 129.8, 127.6, 122.9, 44.3, 28.1. υ_{max} (neat): 3050, 1571, 1559 cm^{-1}. HRMS: exact mass calculated for $[M+H]^+$ ($C_9H_{10}BrOS$) requires *m/z* 246.9609, found *m/z* 246.9601.

3-((3-Bromophenyl)thio)-6-chloro-2-methyl-1*H*-indole (45). Prepared according to General Procedure 5 using (3-chlorophenyl)hydrazine hydrochloride (1.5 g, 8.18 mmol, 1 equiv.) and 1-((3-bromophenyl)thio)propan-2-one (**44**) (2 g, 8.18 mmol, 1 equiv.) in EtOH (40 mL, 0.2 M). Purified by silica chromatography, eluting with 0-10% EtOAc/petroleum ether, to afford the title

compound as a cream amorphous solid (639 mg, 22%). ^{1}H NMR (400 MHz, $CO(CD_3)_2$) δ: 10.97 (br s, 1H), 7.48 (d, *J* = 1.9 Hz, 1H), 7.38 (d, *J* = 8.4 Hz, 1H), 7.26-7.23 (m, 1H), 7.15 (app t, *J* = 7.9 Hz, 1H), 7.11 (app t, *J* = 1.8 Hz, 1H), 7.08 (dd, *J* = 8.4 Hz, 1H), 7.03-7.01 (m, 1H), 2.52 (s, 3H). ^{13}C NMR (101 MHz, $CDCl_3$): δ 143.0, 142.8, 136.3, 132.2, 129.5, 127.3, 127.0, 125.4, 123.4, 122.4, 122.2, 121.8, 109.1, 97.8, 11.7. υ_{max} (neat): 3409, 1573, 1557, 1536 cm^{-1}. HRMS: exact mass calculated for $[M+H]^+$ ($C_{15}H_{12}BrClNS$) *m/z* requires 353.9534, *m/z* found 353.9529.

Methyl 3-((6-chloro-2-methyl-1*H*-indol-3-yl)thio)benzoate (46). Prepared according to General Procedure 7 using *trans*-bis(acetato)bis[*o*-(di-*o*-tolylphosphino)benzyl]dipalladium(II) (90 mg, 0.0959 mmol, 5 mol%), 3-((3-bromophenyl)thio)-6-chloro-2-methyl-1*H*-indole (**45**) (639 mg, 1.81 mmol, 1 equiv.), $Mo(CO)_6$ (478 mg, 1.81 mmol, 1 equiv.), [*t*Bu_3PH]BF_4 (112 mg, 0.386 mmol, 20 mol%), and DBU (433 μL, 2.90 mmol, 1.6 equiv.) in MeCN/MeOH (20 mL, 1:4, 0.3 M). Purified by column chromatography, eluting with 0-20% EtOAc/petroleum ether, to afford the title compound as a cream amorphous solid (463 mg, 77%). ^{1}H NMR (400 MHz, $CO(CD_3)_2$) δ: 10.92 (br s, 1H), 7.73-7.66 (m, 2H), 7.47 (d, *J* = 1.8 Hz, 1H), 7.38 (d, *J* = 8.4 Hz, 1H), 7.34-7.30 (m, 1H), 7.25-7.18 (m, 1H), 7.07 (dd, *J* = 8.4, 1.9 Hz, 1H), 3.81 (s, 3H), 2.53 (s, 3H). ^{13}C NMR (101 MHz, $CO(CD_3)_2$) δ: 166.8, 144.4, 141.2, 137.4, 131.9, 130.6, 130.0, 129.7, 128.1, 126.9, 126.6, 121.6, 120.0, 112.1, 98.4, 52.4, 12.0. υ_{max} (neat): 3405, 3321, 2950, 1699, 1621, 1591, 1575, 1539 cm^{-1}. HRMS: exact mass calculated for $[M+H]^+$ ($C_{17}H_{15}ClNO_2S$) *m/z* requires 334.0476, *m/z* found 334.0474.

3-((6-Chloro-1,2-dimethyl-1*H*-indol-3-yl)thio)benzoic acid (47). Prepared according to General Procedure 6 using methyl 3-((6-chloro-2-methyl-1*H*-indol-3-yl)thio)benzoate (**46**) (200 mg, 0.604 mmol, 1 equiv.), NaH 60% w/w (193 mg, 4.82 mmol, 8 equiv.) and MeI (150 μL, 2.41 mmol, 4 equiv.) in DMF (3 mL, 0.2 M). Following aqueous work-up, the reaction mixture was

then used in the next step without further purification. The crude material was used according to General Procedure 3 using 4 M aq. NaOH (5 mL) in THF (3 mL, 0.2 M). Purified by reverse-phase HPLC to afford the title compound as a cream amorphous solid (2 mg, 1% over 2 steps). ^{1}H NMR (400 MHz, $CDCl_3$) δ: 7.82-7.73 (m, 2H), 7.43 (d, *J* = 8.4 Hz, 1H), 7.35 (d, *J* = 1.7 Hz, 1H), 7.23 (app t, *J* = 7.7 Hz, 1H), 7.19-7.13 (m, 1H), 7.09 (dd, *J* = 8.4, 1.8 Hz, 1H), 3.75 (s, 3H), 2.51 (s, 3H). CO_2H proton not observed. ^{13}C NMR (151 MHz, $CDCl_3$) δ: 170.1, 144.0, 140.6, 137.7, 130.6, 129.8, 129.0, 128.2, 128.1, 127.2, 126.6, 121.4, 119.8, 109.5, 98.0, 30.7, 11.1. υ_{max} (neat): 3436, 2900, 2651, 2543, 1679, 1574 cm^{-1}. HRMS: exact mass calculated for $[M-H]^-$ ($C_{17}H_{13}ClNO_2S$) *m/z* requires 332.0330, *m/z* found 332.0324.

3-((4-Chloro-2-methyl-1*H*-indol-3-yl)thio)benzoic acid (48) and 3-((6-chloro-2-methyl-1*H*-indol-3-yl)thio)benzoic acid (49). Prepared according to General Procedure 5 using (3-chlorophenyl)hydrazine hydrochloride (3.3 g, 18.6 mmol, 1 equiv.) and 1-((3-bromophenyl)thio)propan-2-one (**44**) (4.6 g, 18.6 mmol, 1 equiv.) in EtOH (90 mL, 0.2 M). Following aqueous work-up, the reaction mixture was then used in the next step without further purification. The crude material was used according to General Procedure 7 using t*rans*-bis(acetato)bis[*o*-(di-*o*-tolylphosphino)benzyl]dipalladium(II) (200 mg, 0.213 mmol, 1 mol%), $Mo(CO)_6$ (4.9 g, 18.6 mmol, 1 equiv.), [*t*Bu_3PH]BF_4 (1.08 g, 3.72 mmol, 20 mol%), and DBU (4.2 mL, 27.9 mmol, 1.5 equiv.) in MeCN/4 M aq. NaOH (60 mL, 1:4, 0.3 M). 1 g of crude material was purified by MDAP to afford 3-((4-chloro-2-methyl-1*H*-indol-3-yl)thio)benzoic acid (**48**) as a cream amorphous solid (100 mg, 2% over 2 steps) and 3-((6-chloro-2-methyl-1*H*-indol-3-yl)thio)benzoic acid (**49**) as a cream amorphous solid (70 mg, 1% over 2 steps). 3-((4-Chloro-2-methyl-1*H*-indol-3-yl)thio)benzoic acid (**48**): ^{1}H NMR (400 MHz, $CO(CD_3)_2$) δ: 11.04 (br s, 1H), 7.80-7.69 (m, 2H), 7.40 (dd, *J* = 7.8, 1.0 Hz, 1H), 7.35-7.27 (m, 1H), 7.23 (d, *J* = 8.2 Hz,

1H), 7.13-6.98 (m, 2H), 2.53 (s, 3H). CO_2H proton not observed. ^{13}C NMR (101 MHz, $CO(CD_3)_2$) δ: 167.9, 145.3, 143.0, 138.5, 132.3, 130.2, 129.6, 126.9, 126.7, 126.5, 125.8, 123.1, 122.3, 111.2, 97.7, 12.0. υ_{max} (neat): 3410, 2869, 2658, 2543, 1681, 1569, 1537 cm^{-1}. HRMS: exact mass calculated for $[M+H]^+$ ($C_{16}H_{13}ClNO_2S$) *m/z* requires 318.0174, *m/z* found 318.0167.

3-((6-Chloro-2-methyl-1*H*-indol-3-yl)thio)benzoic acid (**49**): ^1H NMR (400 MHz, $CO(CD_3)_2$) δ: 10.84 (br s, 1H), 7.76-7.72 (m, 2H), 7.47 (d, *J* = 1.8 Hz, 1H), 7.40 (d, *J* = 8.4 Hz, 1H), 7.32 (app t, *J* = 7.5 Hz, 1H), 7.26-7.23 (m, 1H), 7.07 (dd, *J* = 8.4, 1.9 Hz, 1H), 2.53 (s, 3H). CO_2H proton not observed. ^{13}C NMR (101 MHz, $CO(CD_3)_2$) δ: 167.3, 144.3, 141.0, 137.4, 132.1, 130.5, 129.8, 129.7, 128.0, 127.2, 126.9, 121.5, 120.0, 112.1, 98.5, 12.0. υ_{max} (neat): 3385, 2850, 2665, 2549, 1667, 1591, 1570, 1539 cm^{-1}. HRMS: exact mass calculated for $[M+H]^+$ ($C_{16}H_{13}ClNO_2S$) *m/z* requires 318.0174, *m/z* found 318.0163.

3-((6-Chloro-1-cyclopentyl-2-methyl-1*H*-indol-3-yl)thio)benzoic acid (50). Prepared according to General Procedure 6 using methyl 3-((6-chloro-2-methyl-1*H*-indol-3-yl)thio)benzoate (**46**) (25 mg, 0.0755 mmol, 1 equiv.), NaH 60% w/w (24 mg, 0.602 mmol, 8 equiv.) and bromocyclopentane (32 μL, 0.301 mmol, 4 equiv.) in DMF (1 mL, 0.1 M). Following aqueous work-up, the reaction mixture was then used in the next step without further purification. The crude material was used according to General Procedure 3 using 4 M aq. NaOH (1 mL) in THF (1 mL, 0.1 M). Purified using silica chromatography, eluting with 0-20% EtOAc/petroleum ether, to afford the title compound as a pale yellow gum (2 mg, 7% over 2 steps). ^1H NMR (400 MHz, $CO(CD_3)_2$) δ: 7.78-7.69 (m, 2H), 7.59 (d, *J* = 1.7 Hz, 1H), 7.46 (d, *J* = 8.4 Hz, 1H), 7.32 (app t, *J* = 7.8 Hz, 1H), 7.21-7.18 (m, 1H), 7.09 (dd, *J* = 8.4, 1.8 Hz, 1H), 5.20-5.04 (m, 1H), 2.62 (s, 3H), 2.28-2.19 (m, 4H), 2.16-2.06 (m, 2H), 1.91-1.78 (m, 2H). CO_2H proton not observed. ^{13}C NMR (151 MHz, $CO(CD_3)_2$) δ: 145.9, 141.1, 136.4, 130.6, 130.2,

130.0, 127.9, 127.4, 127.1, 121.6, 120.7, 112.4, 98.8, 58.4, 30.8, 25.8, 12.1. Two carbons not observed/coincident. υ_{max} (neat): 3406, 2924, 2872, 1716, 1608, 1593, 1577, 1534 cm^{-1}. HRMS: exact mass calculated for $[M+H]^+$ ($C_{21}H_{21}ClNO_2S$) *m/z* requires 388.0945, *m/z* found 388.0948.

3-((6-Chloro-2-methyl-1-phenyl-1*H*-indol-3-yl)thio)benzoic acid (51). Prepared according to General Procedure 2 using 3-((6-chloro-2-methyl-1*H*-indol-3-yl)thio)benzoic acid (**49**) (65 mg, 0.205 mmol, 1 equiv.), iodobenzene (46 μL, 0.409 mmol, 2 equiv.), CuI (19 mg, 0.102 mmol, 0.5 equiv.), Cs_2CO_3 (133 mg, 0.409 mmol, 2 equiv.), and 1,10-phenanthroline (37 mg, 0.205 mmol, 1 equiv.) in DMF (1 mL, 0.2 M). Purified by reverse-phase HPLC to afford the title compound as a white amorphous solid (11 mg, 14%). ^{1}H NMR (400 MHz, $CO(CD_3)_2$) δ: 7.81 (dd, *J* = 2.4, 1.1 Hz, 1H), 7.77 (dt, *J* = 7.3, 1.5 Hz, 1H), 7.73-7.66 (m, 2H), 7.66-7.59 (m, 1H), 7.59-7.54 (m, 2H), 7.51(d, *J* = 8.4 Hz, 1H), 7.40-7.27 (m, 2H), 7.16 (dd, *J* = 8.4, 1.8 Hz, 1H), 7.13-7.08 (m, 1H), 2.41 (s, 3H). CO_2H proton not observed. ^{13}C NMR (101 MHz, $CO(CD_3)_2$) δ: 165.7, 144.1, 139.0, 138.0, 136.3, 130.9, 129.5, 129.3, 128.6, 128.5, 127.4, 126.0, 125.7, 121.0, 119.0, 109.8, 99.0, 10.4. Two carbons not observed/coincident. υ_{max} (neat): 3058, 2978, 2924, 2658, 1690, 1593, 1577, 1536, 1502 cm^{-1}. HRMS: exact mass calculated for $[M-H]^-$ ($C_{22}H_{15}ClNO_2S$) *m/z* requires 394.0487, *m/z* found 394.0480.

3-((6-Chloro-2-methyl-1-(1-methyl-1*H*-pyrazol-4-yl)-1*H*-indol-3-yl)thio)benzoic acid (52). Prepared according to General Procedure 3 using methyl 3-((6-chloro-2-methyl-1-(1-methyl-1*H*-pyrazol-4-yl)-1*H*-indol-3-yl)thio)benzoate (**90**) (68 mg, 0.165 mmol, 1 equiv.) and 4 M aq. NaOH (1 mL) in THF (1 mL, 0.2 M). Purified using silica chromatography, eluting with 10% MeOH/DCM, to afford the title compound as a cream amorphous solid (16 mg, 24%). ^{1}H NMR (500 MHz, $CO(CD_3)_2$): δ 11.29 (br s, 1H), 8.09 (s, 1H), 7.80 (s, 1H), 7.76 (d, *J* = 7.6 Hz, 1H), 7.72 (s, 1H), 7.46 (d, *J* = 8.4 Hz, 1H), 7.35 (app t, *J* = 7.7 Hz, 1H), 7.29 (d, *J* = 7.9 Hz, 1H), 7.22

(s, 1H), 7.14 (dd, *J* = 8.4, 1.7 Hz, 1H), 4.04 (s, 3H), 2.42 (s, 3H). ^{13}C NMR (126 MHz, $CO(CD_3)_2$): δ 146.4, 140.4, 140.0, 137.2, 132.3, 130.8, 130.0, 129.2, 129.0, 128.8, 127.5, 127.2, 122.4, 120.3, 119.3, 111.4, 100.0, 39.9, 11.7. One carbon not observed/coincident. υ_{max} (neat): 2920, 2848, 1718, 1571, 1537 cm^{-1}. HRMS: exact mass calculated for $[M-H]^-$ ($C_{20}H_{15}ClN_3O_2S$) *m/z* requires 398.0548, *m/z* found 398.0539.

3-((2-Methyl-1*H*-indol-3-yl)thio)benzoic acid (53). Prepared according to General Procedure 3 using methyl 3-((2-methyl-1*H*-indol-3-yl)thio)benzoate (**92**) (100 mg, 0.337 mmol, 1 equiv.) and 2 M aq. NaOH (1 mL) in THF (1 mL, 0.3 M). Purified by reverse-phase HPLC to afford the title compound as a cream amorphous solid (71 mg, 74%). ^{1}H NMR (400 MHz, $CO(CD_3)_2$): δ 10.71 (br s, 1H), 7.76 (app t, *J* = 1.5 Hz, 1H), 7.74-7.72 (m, 1H), 7.48-7.39 (m, 2H), 7.30 (app t, *J* = 7.7 Hz, 1H), 7.25-7.22 (m, 1H), 7.15-7.11 (m, 1H), 7.07-7.04 (m, 1H), 2.53 (s, 3H). One exchangeable proton not observed. ^{13}C NMR (101 MHz, $CO(CD_3)_2$): δ 167.4, 143.1, 141.6, 137.0, 132.1, 131.0, 130.4, 129.7, 127.1, 126.7, 122.7, 121.1, 118.8, 112.1, 97.9, 12.0. υ_{max} (neat): 3390, 3057, 2885, 2654, 2546, 1686, 1570, 1543 cm^{-1}. HRMS: exact mass calculated for $[M+H]^+$ ($C_{16}H_{14}NO_2S$) *m/z* requires 284.0740, *m/z* found 284.0740.

3-((1,2-Dimethyl-1*H*-indol-3-yl)thio)benzoic acid (54). Prepared according to General Procedure 3 using methyl 3-((1,2-dimethyl-1*H*-indol-3-yl)thio)benzoate (**93**) (54 mg, 0.174 mmol, 1 equiv.) and 2 M aq. NaOH (1 mL) in THF (1 mL, 0.2 M). Purified by reverse-phase HPLC to afford the title compound as a cream amorphous solid (31 mg, 60%). ^{1}H NMR (400 MHz, $CDCl_3$): δ 7.84 (app t, *J* = 1.5Hz, 1H), 7.76-7.74 (m, 1H), 7.55 (d, *J* = 7.8 Hz, 1H), 7.36 (d, *J* = 8.2 Hz, 1H), 7.25-7.11 (m, 4H), 3.79 (s, 3H), 2.53 (s, 3H). CO_2H proton not observed. ^{13}C NMR (101 MHz, $CDCl_3$): δ 171.1, 143.2, 141.1, 137.3, 130.7, 129.8, 129.7, 128.9, 127.2, 126.4, 122.1, 120.8, 118.9, 109.3, 97.4, 30.6, 11.0. υ_{max} (neat): 2922, 2546, 1680, 1572, 1521 cm^{-1}.

HRMS: exact mass calculated for $[M+H]^+$ ($C_{17}H_{16}NO_2S$) *m/z* requires 298.0896, *m/z* found 298.0893.

3-((1-Cyclopentyl-2-methyl-1*H*-indol-3-yl)thio)benzoic acid (55). Prepared according to General Procedure 6 using methyl 3-((2-methyl-1*H*-indol-3-yl)thio)benzoate (**92**) (200 mg, 0.673 mmol, 1 equiv.), NaH 60% w/w (216 mg, 5.39 mmol, 8 equiv.), and bromocyclopentane (288 μL, 2.69 mmol, 4 equiv.) in DMF (3 mL, 0.2 M). Following aqueous work-up, the reaction mixture was then used in the next step without further purification. The crude material was used according to General Procedure 3 using 4 M aq. NaOH (5 mL) in THF (3 mL, 0.2 M). Purified by reverse-phase HPLC to afford the title compound as a white amorphous solid (15 mg, 6% over 2 steps). ^{1}H NMR (400 MHz, $CO(CD_3)_2$): δ 7.78-7.70 (m, 2H), 7.57 (d, *J* = 8.3 Hz, 1H), 7.49 (d, *J* = 7.5 Hz, 1H), 7.30 (app t, *J* = 7.7 Hz, 1H), 7.22-7.17 (m, 1H), 7.17-7.12 (m, 1H), 7.09-7.07 (m, 1H), 5.14-5.05 (m, 1H), 2.61 (s, 3H), 2.37-2.23 (m, 2H), 2.23-2.07 (m, 4H), 1.92-1.73 (m, 2H). CO_2H proton not observed. ^{13}C NMR (101 MHz, $CO(CD_3)_2$): δ 167.2, 144.5, 141.6, 135.9, 132.1, 131.4, 130.4, 129.8, 127.2, 126.8, 122.3, 121.0, 119.5, 112.5, 97.9, 58.2, 30.6, 25.8, 11.7. υ_{max} (neat): 3388, 2976, 2954, 2870, 2660, 2539, 1668, 1591, 1571, 1530 cm^{-1}. HRMS: exact mass calculated for $[M-H]^-$ ($C_{21}H_{20}NO_2S$) *m/z* requires 350.1220, *m/z* found 350.1216.

3-((2-Methyl-1-phenyl-1*H*-indol-3-yl)thio)benzoic acid (56). Prepared according to General Procedure 2 using methyl 3-((2-methyl-1*H*-indol-3-yl)thio)benzoate (**92**) (127 mg, 0.428 mmol, 1 equiv.), iodobenzene (95 μL, 0.856 mmol, 2 equiv.), CuI (41 mg, 0.214 mmol, 0.5 equiv.), Cs_2CO_3 (279 mg, 0.856 mmol, 2 equiv.), and 1,10-phenanthroline (77 mg, 0.428 mmol, 1 equiv.) in DMF (1 mL, 0.4 M). Following aqueous work-up, the reaction mixture was then used in the next step without further purification. The crude material was used according to General

Procedure 3 using 4 M aq. NaOH (1 mL) in THF (2 mL, 0.2 M). Purified by reverse-phase HPLC to afford the title compound as a cream amorphous solid (14 mg, 9% over 2 steps). ^{1}H NMR (400 MHz, $CDCl_3$): δ 7.95-7.89 (m, 1H), 7.82-7.76 (m, 1H), 7.63-7.55 (m, 3H), 7.54-7.48 (m, 1H), 7.41 (dd, *J* = 8.3, 1.3 Hz, 2H), 7.29-7.26 (m, 2H), 7.20-7.12 (m, 3H), 2.40 (s, 3H). CO_2H proton not observed. ^{13}C NMR (101 MHz, $CDCl_3$): δ 143.4, 140.6, 138.2, 137.6, 130.8, 129.8, 129.6, 129.0, 128.6, 128.1, 127.4, 126.6, 122.6, 121.4, 118.8, 110.6, 99.5, 11.9. Two carbons not observed/coincident. υ_{max} (neat): 2917, 2852, 2651, 2536, 1679, 1597, 1571, 1530, 1501 cm^{-1}. HRMS: exact mass calculated for $[M-H]^-$ ($C_{22}H_{16}NO_2S$) *m/z* requires 358.0907, *m/z* found 358.0900.

3-((2-Methyl-1-(1-methyl-1*H*-pyrazol-4-yl)-1*H*-indol-3-yl)thio)benzoic acid (57). Prepared according to General Procedure 4 using methyl 3-((2-methyl-1*H*-indol-3-yl)thio)benzoate (**92**) (202 mg, 0.680 mmol, 1 equiv.), 4-bromo-1-methyl-1*H*-pyrazole (209 μL, 2.02 mmol, 3 equiv.), CuO (108 mg, 1.35 mmol, 2 equiv.), and K_2CO_3 (122 mg, 0.884 mmol, 1.3 equiv.) in pyridine (2 mL, 0.3 M). Purified using reverse-phase HPLC to afford the title compound as a dark red amorphous solid (22 mg, 9%). ^{1}H NMR (400 MHz, $CDCl_3$): δ 8.33 (s, 1H), 7.81 (app t, *J* = 1.7 Hz, 1H), 7.72-7.69 (m, 1H), 7.52 (d, *J* = 7.8 Hz, 1H), 7.33 (dd, *J* = 4.8, 3.9 Hz, 1H), 7.21-7.19 (m, 2H), 7.16-7.12 (m, 2H), 3.86 (s, 3H), 2.51 (s, 3H). ^{13}C NMR (126 MHz, $CDCl_3$): δ 166.9, 141.3, 140.3, 135.5, 130.6, 130.1, 129.8, 128.7, 126.6, 125.8, 122.3, 120.8, 118.8, 110.8, 98.7, 52.2, 12.1. Three carbons not observed/coincident. υ_{max} (neat): 3381, 3375, 1695, 1572, 1539 cm^{-1}. HRMS: exact mass calculated for $[M-H]^-$ ($C_{20}H_{16}N_3O_2S$) *m/z* requires 362.0969, *m/z* found 362.0967.

Ethyl 3-(2-oxopropoxy)benzoate (59). Chloroacetone (2.4 mL, 30.1 mmol, 1 equiv.) was added to a stirred suspension of ethyl 3-hydroxybenzoate (**58**) (5 g, 30.1 mmol, 1 equiv.) and K_2CO_3

(8.3 g, 60.2 mmol, 2 equiv.) in acetone (150 mL, 0.2 M). The reaction mixture was heated to 60 °C for 16 h then allowed to return to room temperature and concentrated under vacuum. The residue was then dissolved in EtOAc (100 mL) and washed with water (100 mL), followed by 4 M aq. NaOH (100 mL). The organic layer was collected, dried (hydrophobic frit), and concentrated under vacuum. Purified using silica chromatography, eluting with 10% EtOAc/petroleum ether, to afford the title compound as a yellow liquid (3.7 g, 55%). ^{1}H NMR (500 MHz, $CDCl_3$): δ 7.70-7.68 (m, 1H), 7.53 (dd, *J* = 2.6, 1.4 Hz, 1H), 7.37 (app t, *J* = 8.0 Hz, 1H), 7.10 (dd, *J* = 8.2, 2.7, 1H), 4.60 (s, 2H), 4.37 (q, *J* = 7.1 Hz, 2H), 2.29 (s, 3H), 1.39 (t, *J* = 7.1 Hz, 3H). ^{13}C NMR (126 MHz, $CDCl_3$): δ 205.0, 166.3, 157.8, 132.3, 129.8, 123.1, 119.8, 115.0, 73.2, 61.3, 26.8, 14.4. υ_{max} (neat): 2980, 2906, 1714, 1585 cm^{-1}. HRMS: exact mass calculated for $[M+H]^+$ ($C_{12}H_{15}O_4$) *m/z* requires 223.0965, *m/z* found 223.0966.

Ethyl 3-((2-methyl-1*H*-indol-3-yl)oxy)benzoate (60). Prepared according to General Procedure 1 using phenylhydrazine hydrochloride (653 mg, 4.50 mmol, 1 equiv.) and ethyl 3-(2-oxopropoxy)benzoate (**59**) (1 g, 4.50 mmo, 1 equiv.) in *t*BuOH (45 mL, 0.1 M) with additional 1 M HCl in Et_2O (14 mL) and AcOH (14 mL). Purified by reverse-phase HPLC to afford the title compound as a pale brown amorphous solid (167 mg, 12%). ^{1}H NMR (500 MHz, $CDCl_3$): δ 7.91 (s, 1H), 7.79-7.71 (m, 2H), 7.34 (app t, *J* = 8.2 Hz, 1H), 7.28 (app t, *J* = 7.6 Hz, 2H), 7.20-7.12 (m, 2H), 7.06 (app t, *J* = 7.5 Hz, 1H), 4.39 (q, *J* = 7.1 Hz, 2H), 2.29 (s, 3H), 1.40 (t, *J* = 7.1 Hz, 3H). ^{13}C NMR (126 MHz, $CDCl_3$): δ 166.6, 159.4, 133.2, 132.0, 130.0, 129.5, 124.4, 122.9, 121.7, 121.5, 119.8, 119.7, 117.1, 116.6, 111.0, 61.2, 14.4, 10.1. υ_{max} (neat): 3370, 2980, 1715, 1697, 1620, 1584 cm^{-1}. HRMS: exact mass calculated for $[M+H]^+$ ($C_{18}H_{18}NO_3$) *m/z* requires 296.1281, *m/z* found 296.1284.

3-((2-Methyl-1*H*-indol-3-yl)oxy)benzoic acid (61). Prepared according to General Procedure 3 using ethyl 3-((2-methyl-1*H*-indol-3-yl)oxy)benzoate (**60**) (50 mg, 0.169 mmol, 1 equiv.) and 1 M aq. NaOH (1 mL) in THF (2 mL, 0.1 M). Purified by reverse-phase HPLC to afford the title compound as a brown oil (8 mg, 18%). ^{1}H NMR (400 MHz, $CDCl_3$): δ 7.74-7.71 (m, 1H), 7.70-7.64 (m, 2H), 7.35 (app t, *J* = 7.9 Hz, 1H), 7.32-7.28 (m, 1H), 7.24-7.18 (m, 1H), 7.16-7.12 (m, 1H), 7.07-6.99 (m, 1H), 2.34 (s, 3H). NH and CO_2H protons not observed. ^{13}C NMR (101 MHz, $CDCl_3$): δ 170.9, 159.5, 133.3, 130.7, 130.1, 129.7, 124.3, 123.6, 122.0, 121.5, 120.9, 119.9, 117.2, 116.9, 111.0, 10.4. υ_{max} (neat): 3404, 2920, 2558, 1690, 1584, 1572 cm^{-1}. HRMS: exact mass calculated for $[M+H]^+$ ($C_{16}H_{14}NO_3$) *m/z* requires 268.0968, *m/z* found 268.0971.

3-((2-Methyl-1-(1-methyl-1*H*-pyrazol-4-yl)-1*H*-indol-3-yl)oxy)benzoic acid (62). Prepared according to General Procedure 4 using ethyl 3-((2-methyl-1*H*-indol-3-yl)oxy)benzoate (**60**) (94 mg, 0.319 mmol, 1 equiv.), 4-bromo-1-methyl-1*H*-pyrazole (99 μL, 0.956 mmol, 3 equiv.), CuO (51 mg, 0.638 mmol, 2 equiv.), and K_2CO_3 (57 mg, 0.415 mmol, 1.3 equiv.) in pyridine (1 mL, 0.3 M). Following aqueous work-up, the reaction mixture was then used in the next step without further purification. The crude material was used according to General Procedure 3 using 2 M aq. NaOH (1 mL) in THF (1 mL, 0.3 M). Purified by reverse-phase HPLC to afford the title compound as a brown oil (4 mg, 4% over 2 steps). ^{1}H NMR (400 MHz, $CDCl_3$): δ 7.75-7.71 (m, 1H), 7.72-7.69 (m, 1H), 7.64 (s, 1H), 7.59 (s, 1H), 7.37 (app t, *J* = 7.9 Hz, 1H), 7.30-7.23 (m, 2H), 7.22-7.17 (m, 1H), 7.15-7.11 (m, 1H), 7.08-7.02 (m, 1H), 4.04 (s, 3H), 2.12 (s, 3H). CO_2H proton not observed. ^{13}C NMR (101 MHz, $CDCl_3$): δ 170.8, 159.4, 137.4, 136.0, 130.9, 130.8, 129.8, 127.7, 127.2, 123.7, 122.1, 121.0, 120.9, 120.3, 119.8, 117.2, 117.0, 110.3, 39.9, 9.6. υ_{max} (neat): 3121, 3053, 2947, 1697, 1583 cm^{-1}. HRMS: exact mass calculated for $[M+H]^+$ ($C_{20}H_{18}N_3O_3$) *m/z* requires 348.1343, *m/z* found 348.1344.

3-((6-Chloro-2-methyl-1*H*-indol-3-yl)oxy)benzoic acid (63). Prepared according to General Procedure 3 using ethyl 3-((6-chloro-2-methyl-1*H*-indol-3-yl)oxy)benzoate (**94**) (150 mg, 0.454 mmol, 1 equiv.) and 2 M aq. NaOH (1 mL) in THF (1 mL, 0.4 M). Purified by reverse-phase HPLC to afford the title compound as an orange amorphous solid (30 mg, 22%). ^{1}H NMR (400 MHz, $CO(CD_3)_2$): δ 9.95 (br s, 1H), 7.44-7.41 (m, 1H), 7.28 (dd, *J* = 2.5, 1.5 Hz, 1H), 7.16 (app t, *J* = 7.9 Hz, 1H), 7.13 (d, *J* = 1.7 Hz, 1H), 6.94 (dd, *J* = 8.2, 2.6 Hz, 1H), 6.87 (d, *J* = 8.4 Hz, 1H), 6.69 (dd, *J* = 8.4, 1.8 Hz, 1H), 2.05 (s, 3H). One exchangeable proton not observed. ^{13}C NMR (101 MHz, $CO(CD_3)_2$): δ 167.3, 160.4, 134.7, 133.2, 130.6, 130.4, 127.5, 126.9, 123.9, 120.7, 120.5, 118.4, 116.7, 112.0, 111.9, 10.1. υ_{max} (neat): 3327, 3071, 1690, 1601, 1585, 1520 cm^{-1}. HRMS: exact mass calculated for $[M+H]^+$ ($C_{16}H_{13}ClNO_3$) *m/z* requires 304.0549, *m/z* found 304.0544.

3-((6-Chloro-2-methyl-1-(1-methyl-1*H*-pyrazol-4-yl)-1*H*-indol-3-yl)oxy) benzoic acid (64). Prepared according to General Procedure 5 using (3-chlorophenyl)hydrazine hydrochloride (1.9 g, 10.8 mmol, 1 equiv.) and ethyl 3-(2-oxopropoxy)benzoate (**59**) (2.4 g, 10.8 mmol, 1 equiv.) in EtOH (50 mL, 0.2 M). 1 g of the crude material was then used according to General Procedure 4 using 4-bromo-1-methyl-1*H*-pyrazole (940 µL, 9.10 mmol, 3 equiv.), CuO (1.4 g, 18.2 mmol, 6 equiv.), and K_2CO_3 (1.6 g, 11.8 mmol, 4 equiv.) in pyridine (15 mL, 0.7 M). Following aqueous work-up, the reaction mixture was then used in the next step without further purification. The crude material was used according to General Procedure 3 using 2 M aq. NaOH (30 mL) in THF (15 mL, 0.7 M). Purified by reverse-phase HPLC to afford the title compound as a cream amorphous solid (36 mg, 1% over 3 steps). ^{1}H NMR (400 MHz, $CO(CD_3)_2$): δ 8.05 (s, 1H), 7.77-7.67 (m, 2H), 7.62 (dd, *J* = 2.6, 1.5 Hz, 1H), 7.45 (app t, *J* = 7.9 Hz, 1H), 7.26 (dd, *J* = 8.3, 2.7 Hz, 1H), 7.24-7.16 (m, 2H), 7.03 (dd, *J*= 8.4, 1.9 Hz, 1H), 4.03 (s, 3H), 2.21 (s, 3H). CO_2H

proton not observed. ^{13}C NMR (101 MHz, $CO(CD_3)_2$): δ 167.3, 160.0, 137.2, 137.0, 133.1, 131.1, 130.7, 129.4, 129.1, 128.3, 124.1, 121.3, 120.8, 120.4, 119.2, 118.6, 116.8, 111.0, 39.8, 9.5. υ_{max} (neat): 3122, 2949, 2921, 1696, 1606, 1584 cm^{-1}. HRMS: exact mass calculated for $[M+H]^+$ ($C_{20}H_{17}ClN_3O_3$) *m/z* requires 384.0924, *m/z* found 384.0926.

6-Chloro-2-methyl-1-(1-methyl-1*H*-pyrazol-4-yl)-1*H*-indole (66). Prepared according to General Procedure 4 using 6-chloro-2-methyl-1*H*-indole (**65**) (300 mg, 1.81 mmol, 1 equiv.), 4-bromo-1-methyl-1*H*-pyrazole (224 μL, 2.17 mmol, 1.2 equiv.), CuO (290 mg, 3.62 mmol, 2 equiv.), and K_2CO_3 (325 mg, 2.36 mmol, 1.3 equiv.) in pyridine (3.5 mL, 0.5 M). Purified using silica chromatography, eluting with 0-30% EtOAc/petroleum ether, to afford the title compound as a brown amorphous solid (351 mg, 79%). ^{1}H NMR (400 MHz, $CDCl_3$): δ 7.56 (s, 1H), 7.50 (s, 1H), 7.42 (d, *J* = 8.3 Hz, 1H), 7.13-7.08 (m, 1H), 7.06 (dd, *J* = 8.3, 1.9 Hz, 1H), 6.33 (s, 1H), 4.01 (s, 3H), 2.27 (s, 3H). ^{13}C NMR (101 MHz, $CDCl_3$): δ 139.4, 138.6, 137.3, 127.5, 127.2, 126.8, 120.8, 120.5, 119.7, 110.1, 101.2, 39.8, 13.2. υ_{max} (neat): 3119, 2943, 1715, 1676, 1607, 1580 cm^{-1}. HRMS: exact mass calculated for $[M+H]^+$ ($C_{13}H_{13}ClN_3$) *m/z* requires 248.0763, *m/z* found 248.0766.

Methyl 6-((6-chloro-2-methyl-1-(1-methyl-1*H*-pyrazol-4-yl)-1*H*-indol-3-yl)methyl)picolinate (67). Prepared according to General Procedure 7 using *trans*-bis(acetato)bis[*o*-(di-*o*-tolylphosphino)benzyl]dipalladium(II) (9 mg, 0.00959 mmol, 5 mol%), 3-((6-bromopyridin-2-yl)methyl)-6-chloro-2-methyl-1-(1-methyl-1*H*-pyrazol-4-yl)-1*H*-indole (**97**) (84 mg, 0.202 mmol, 1 equiv.), $Mo(CO)_6$ (53 mg, 0.202 mmol, 1 equiv.), [*t*Bu_3PH]BF_4 (12 mg, 0.0414 mmol, 20 mol%), and DBU (45 μL, 0.303 mmol, 1.5 equiv.) in MeCN/MeOH (2.5 mL, 1:4, 0.1 M). Purified using silica chromatography, eluting with 50-70% EtOAc/petroleum ether, to afford the title compound as a cream amorphous solid (61 mg, 76%). ^{1}H NMR (400 MHz,

$CO(CD_3)_2$): δ 7.96 (s, 1H), 7.88 (dd, *J* = 7.7, 1.0 Hz, 1H), 7.80 (app t, *J* = 7.7 Hz, 1H), 7.60 (s, 1H), 7.56 (d, *J* = 8.4 Hz, 1H), 7.40 (dd, *J* = 7.8, 1.0 Hz, 1H), 7.07 (d, *J* = 1.7 Hz, 1H), 7.00 (dd, *J* = 8.4, 1.9 Hz, 1H), 4.32 (s, 2H), 4.01 (s, 3H), 3.93 (s, 3H), 2.36 (s, 3H). ^{13}C NMR (151 MHz, $CO(CD_3)_2$): δ 166.5, 162.6, 148.6, 139.5, 138.4, 137.3, 137.0, 128.9, 127.7, 127.6, 126.5, 123.2, 120.8, 120.4, 119.9, 110.7, 110.4, 52.6, 39.8, 34.0, 11.1. υ_{max} (neat): 3086, 3057, 2950, 2917, 2855, 1712, 1610, 1593, 1584 cm^{-1}. HRMS: exact mass calculated for $[M+H]^+$ ($C_{21}H_{20}ClN_4O_2$) *m/z* requires 397.1240, *m/z* found 397.1236.

6-((6-Chloro-2-methyl-1-(1-methyl-1*H*-pyrazol-4-yl)-1*H*-indol-3-yl)methyl) picolinic acid (68). Prepared according to General Procedure 3 using methyl 6-((6-chloro-2-methyl-1-(1-methyl-1*H*-pyrazol-4-yl)-1*H*-indol-3-yl)methyl)picolinate (**67**) (50 mg, 0.126 mmol, 1 equiv.) and 2 M aq. NaOH (2 mL) in THF (2 mL, 0.1 M). Purified by reverse-phase HPLC to afford the title compound as a yellow oil (23 mg, 48%). ^{1}H NMR (400 MHz, $CO(CD_3)_2$): δ 8.10-7.82 (m, 3H), 7.61 (s, 1H), 7.56 (d, *J* = 8.4 Hz, 1H), 7.52 (dd, *J* = 7.6, 1.0 Hz, 1H), 7.08 (d, *J* = 1.8 Hz, 1H), 7.01 (dd, *J*= 8.4, 1.9 Hz, 1H), 4.37 (s, 2H), 4.01 (s, 3H), 2.36 (s, 3H). CO_2H proton not observed. ^{13}C NMR (101 MHz, $CO(CD_3)_2$): δ 165.3, 161.9, 147.1, 139.7, 139.6, 137.3, 137.1, 128.9, 127.7, 127.7, 127.5, 122.2, 120.9, 120.2, 119.9, 110.5, 110.4, 39.8, 33.4, 11.1. υ_{max} (neat): 3097, 2922, 1716, 1684, 1670, 1610, 1588 cm^{-1}. HRMS: exact mass calculated for $[M+H]^+$ ($C_{20}H_{18}ClN_4O_2$) *m/z* requires 383.1084, *m/z* found 383.1084.

3-((6-Chloro-2-methyl-1-(1-methyl-1*H*-pyrazol-4-yl)-1*H*-indol-3-yl)methyl) benzoic acid (69). Prepared according to General Procedure 4 using methyl 3-((6-chloro-2-methyl-1*H*-indol-3-yl)methyl)benzoate (**96**) (345 mg, 1.10 mmol, 1 equiv.), 4-bromo-1-methyl-1*H*-pyrazole (227 µL, 2.20 mmol, 2 equiv.), CuO (176 mg, 2.20 mmol, 2 equiv.), and K_2CO_3 (197 mg, 1.43 mmol, 1.3 equiv.) in pyridine (3 mL, 0.4 M). Following aqueous work-up, the reaction mixture was then

used in the next step without further purification. The crude material was used according to General Procedure 3 using 2 M aq. NaOH (2 mL) in THF (2 mL, 0.5 M). Purified by reverse-phase HPLC to afford the title compound as a white amorphous solid (5 mg, 1% over 2 steps). ^{1}H NMR (400 MHz, $CO(CD_3)_2$): δ 8.00-7.94 (m, 2H), 7.85 (d, *J*= 7.6 Hz, 1H), 7.62 (s, 1H), 7.52 (dd, *J* = 7.7, 0.6 Hz, 1H), 7.45-7.36 (m, 2H), 7.08 (d, *J* = 1.7 Hz, 1H), 7.00 (dd, *J* = 8.4, 1.9 Hz, 1H), 4.21 (s, 2H), 4.01 (s, 3H), 2.32 (s, 3H). CO_2H proton not observed. ^{13}C NMR (151 MHz, $CO(CD_3)_2$): δ 167.7, 143.0, 139.6, 137.3, 136.6, 133.7, 131.6, 130.3, 129.4, 128.9, 128.1, 127.7, 127.6, 120.8, 120.1, 119.9, 111.7, 110.5, 39.8, 30.6, 11.1. υ_{max} (neat): 2922, 2554, 2361, 2153, 1693, 1606, 1585 cm^{-1}. HRMS: exact mass calculated for $[M+H]^+$ ($C_{21}H_{19}ClN_3O_2$) *m/z* requires 382.1131, *m/z* found 382.1134.

3-((2-Methyl-1-(1-methyl-1*H*-pyrazol-4-yl)-1*H*-indol-3-yl)methyl)benzoic acid (70). Prepared according to General Procedure 3 using methyl 3-((2-methyl-1-(1-methyl-1*H*-pyrazol-4-yl)-1*H*-indol-3-yl)methyl)benzoate (**100**) (100 mg, 0.278 mmol, 1 equiv.) and 2 M aq. NaOH (2 mL) in THF (2 mL, 0.1 M). Purified by reverse-phase HPLC to afford the title compound as cream amorphous solid (10 mg, 10%). ^{1}H NMR (400 MHz, $CO(CD_3)_2$): δ 7.99 (s, 1H), 7.92 (s, 1H), 7.84 (d, *J* = 7.7 Hz, 1H), 7.59 (d, *J* = 0.6 Hz, 1H), 7.53 (d, *J* = 7.6 Hz, 1H), 7.44 (d, *J* = 7.2 Hz, 1H), 7.38 (app t, *J* = 7.7 Hz, 1H), 7.14-6.95 (m, 3H), 4.21 (s, 2H), 4.01 (s, 3H), 2.33 (s, 3H). CO_2H proton not observed. ^{13}C NMR (151 MHz, $CO(CD_3)_2$): δ 143.4, 139.1, 137.3, 135.2, 133.8, 131.5, 130.3, 129.3, 129.0, 128.6, 128.0, 122.0, 120.7, 120.5, 118.8, 111.5, 110.6, 39.7, 30.8, 11.0. One carbon not observed/coincident. υ_{max} (neat): 3113, 3051, 2918, 2467, 1699, 1605, 1584 cm^{-1}. HRMS: exact mass calculated for $[M-H]^-$ ($C_{21}H_{18}N_3O_2$) *m/z* requires 344.1405, *m/z* found 344.1403.

6-((2-Methyl-1-(1-methyl-1*H*-pyrazol-4-yl)-1*H*-indol-3-yl)methyl)picolinic acid (71). Prepared according to General Procedure 3 using methyl 6-((2-methyl-1-(1-methyl-1*H*-pyrazol-4-yl)-1*H*-indol-3-yl)methyl)picolinate (**102**) (50 mg, 0.139 mmol, 1 equiv.) and 2 M aq. NaOH (1 mL) in THF (1 mL, 0.1 M). Purified by reverse-phase HPLC to afford the title compound as a green gum (21 mg, 44%). ^{1}H NMR (400 MHz, $CDCl_3$): δ 10.50 (br s, 1H), 8.15 (d, *J* = 7.6 Hz, 1H), 7.97 (app t, *J* = 7.8 Hz, 1H), 7.66 (s, 1H), 7.59 (s, 1H), 7.50 (d, *J* = 7.9 Hz, 1H), 7.39 (d, *J* = 7.5 Hz, 1H), 7.15 (d, *J* = 3.6 Hz, 2H), 7.11 (dd, *J* = 7.7, 4.1 Hz, 1H), 4.53 (s, 2H), 4.06 (s, 3H), 2.28 (s, 3H). ^{13}C NMR (101 MHz, $CDCl_3$): δ 163.4, 159.8, 144.8, 142.1, 138.4, 137.0, 135.6, 128.3, 127.8, 127.7, 122.9, 122.3, 120.8, 120.2, 117.8, 110.2, 107.4, 39.7, 31.1, 11.0. υ_{max} (neat): 3103, 2950, 1725, 1716, 1696, 1670, 1616, 1588 cm^{-1}. HRMS: exact mass calculated for $[M-H]^-$ ($C_{20}H_{17}N_4O_2$) *m/z* requires 345.1357, *m/z* found 345.1355.

Methyl 6-bromopicolinate (73). Conc. H_2SO_4 (0.35 mL) was added to a round bottomed flask containing 6-bromopicoline (**72**) (1 g, 4.95 mmol, 1 equiv.) in MeOH (30 mL, 0.2 M). The reaction mixture was heated to reflux under N_2 for 16 h, then cooled to 0 °C and 35% aq. NH_4OH (1.6 mL) was added. The resulting solution was then concentrated under vacuum, dissolved in CH_2Cl_2 (50 mL), and washed with brine (50 mL). The organic layer was collected, dried (hydrophobic frit), and concentrated under vacuum to afford the title compound as a white amorphous solid (900 mg, 84%). ^{1}H NMR (500 MHz, $CDCl_3$): δ 8.09 (dd, *J* = 7.0, 1.5 Hz, 1H), 7.73-7.66 (m, 2H), 4.00 (s, 3H). ^{13}C NMR (101 MHz, $CDCl_3$): δ 164.4, 148.7, 142.1, 139.2, 131.8, 124.0, 53.1. υ_{max} (neat): 3000, 1719, 1678, 1562 cm^{-1}. HRMS: exact mass calculated for $[M-H]^-$ ($C_7H_5BrNO_2$) *m/z* requires 217.9634, found 217.9632.

Methyl 6-((3-bromophenyl)thio)picolinate (74). Methyl 6-bromopicolinate (**73**) (499 mg, 2.31 mmol, 1.1 equiv.), Cs_2CO_3 (1.4 g, 4.36 mmol, 2 equiv.), and 3-bromothiophenol (218 μL, 2.12

mmol, 1 equiv.) were dissolved in DMF (10 mL, 0.2 M) and stirred at 45 °C under N_2 for 16 h. The reaction mixture was diluted with H_2O (30 mL) and extracted using EtOAc (3 x 30 mL). The organic layers were combined, dried (hydrophobic frit), and concentrated under vacuum. Purified using silica chromatography, eluting with 10-40% EtOAc/petroleum ether, to afford the title compound as a white amorphous solid (260 mg, 38%). ^{1}H NMR (400 MHz, $CDCl_3$): δ 7.86 (d, *J* = 7.6 Hz, 1H), 7.83-7.79 (m, 1H), 7.63 (app t, *J* = 7.9 Hz, 1H), 7.57-7.53 (m, 2H), 7.32 (d, *J* = 7.9 Hz, 1H), 7.06 (d, *J* = 8.1 Hz, 1H), 3.98 (s, 3H). ^{13}C NMR (101 MHz, $CDCl_3$): δ 165.0, 151.4, 143.9, 142.3, 140.7, 137.0, 136.2, 135.1, 128.8, 127.9, 126.7, 125.5, 55.9 υ_{max} (neat): 2960, 1724, 1560 cm^{-1}. HRMS: exact mass calculated for $[M-H]^-$ ($C_{13}H_9BrNO_2S$) *m/z* requires 325.9666, *m/z* found 325.9666.

6-((3-(1-Methyl-1*H*-pyrazol-4-yl)phenyl)thio)picolinic acid (75). $Pd(OAc)_2$ (2 mg, 0.00893 mmol, 1 mol%) was added to a solution of methyl 6-((3-bromophenyl)thio)picolinate (**74**) (280 mg, 0.864 mmol, 1 equiv.), 1-methylpyrazole-4-boronic acid pinacol ester (269 mg, 1.29 mmol, 1.5 equiv.), and S-Phos (707 mg, 1.72 mmol, 2 equiv.) in THF:H_2O (0.8 mL, 7:1, 1 M) then heated to 50 °C for 16 h under N_2. Following aqueous work-up, the reaction mixture was then used in the next step without further purification. The crude material was used according to General Procedure 3 using 2 M aq. NaOH (0.3 mL). Purified by reverse-phase HPLC to afford the title compound as a cream amorphous solid (37 mg, 14% over two steps). ^{1}H NMR (400 MHz, $CDCl_3$): δ 7.90 (d, *J* = 7.3 Hz, 1H), 7.77 (s, 1H), 7.75-7.67 (m, 2H), 7.64 (s, 1H), 7.62-7.55 (m, 1H), 7.51-7.42 (m, 2H), 7.24 (s, 1H), 3.95 (s, 3H). CO_2H proton not observed. ^{13}C NMR (101 MHz, $CDCl_3$): δ 138.6, 138.2, 136.3, 134.3, 132.7, 131.7, 130.6, 129.9, 128.9, 126.7, 126.5, 121.6, 93.7, 42.4, 38.7. One carbon not observed/coincident. υ_{max} (neat): 3140, 1682,

1634, 1600, 1537, 1403 cm^{-1}. HRMS: exact mass calculated for $[M+H]^+$ ($C_{17}H_{14}N_3O_2S$) *m/z* requires 312.0801, *m/z* found 312.0801.

4-Mercaptobutanoic acid (77). Prepared according to the literature procedure.[39] A solution of 4-bromobutyric acid (**76**) (3 g, 18.0 mmol, 1 equiv.) and thiourea (2 g, 29.8 mmol, 1.6 equiv.) in EtOH (26 mL, 0.7 M) was heated at reflux for 3 h, then allowed to return to room temperature and concentrated under vacuum. The residue was then dissolved in 7.5 M aq. NaOH (20 mL) and refluxed for 16 h. The reaction mixture was then cooled to 0 °C, acidified using 2 M aq. H_2SO_4, and extracted using CH_2Cl_2 (3 x 20 mL). The organics were combined, dried (hydrophobic frit) and concentrated under vacuum to afford the title compound as a colourless oil (1.7 g, 80%). ^{1}H NMR (400 MHz, $CDCl_3$): δ 10.07 (br s, 1H), 2.62-2.53 (m, 2H), 2.49 (t, *J* = 7.3 Hz, 2H), 1.95-1.89 (m, 2H), 1.35 (t, *J* = 8.1 Hz, 1H). ^{13}C NMR (101 MHz, $CDCl_3$): δ 179.5, 32.4, 28.6, 23.8. υ_{max} (neat): 2960, 2550, 1703 cm^{-1}. HRMS: exact mass calculated for $[M+H]^+$ ($C_4H_9O_2S$) *m/z* requires 121.0318, *m/z* found 121.0315.

4-((2-Oxopropyl)thio)butanoic acid (78). A solution of 4-mercaptobutanoic acid (**77**) (1.2 g, 10.0 mmol, 1 equiv.) and DIPEA (4.4 mL, 25.0 mmol, 2.5 equiv.) in THF (30 mL, 0.3 M) was cooled to 0 °C, followed by the addition of chloroacetone (813 μL, 10.5 mmol, 1.05 equiv.) portionwise. The reaction mixture was then allowed to return to room temperature and stirred for 16 h. The reaction was then diluted with EtOAc (50 mL) and washed with water (3 x 30 mL) and brine (1 x 30 mL). The organic layer was then collected, dried (hydrophobic frit), and concentrated under vacuum. Purified using silica chromatography, eluting with CH_2Cl_2, to afford the title compound as a clear oil (266 mg, 15%). ^{1}H NMR (400 MHz, $CDCl_3$): δ 8.14 (br s, 1H), 3.20 (s, 2H), 2.52 (t, *J* = 7.2 Hz, 2H), 2.44 (t, *J* = 7.3 Hz, 2H), 2.27 (s, 3H), 1.96-1.89 (m, 2H). ^{13}C NMR (101 MHz, $CDCl_3$): δ 203.7, 178.2, 41.0, 32.1, 30.6, 27.3, 23.2. υ_{max} (neat): 2924,

2529, 1701 cm^{-1}. HRMS: exact mass calculated for $[M+H]^+$ ($C_7H_{13}O_3S$) *m/z* requires 177.0580, *m/z* found 177.0575.

4-(2-Methyl-1*H*-indol-3-yl)butanoic acid (79). Prepared according to General Procedure 1 using 4-((2-oxopropyl)thio)butanoic acid (**78**) (400 mg, 2.27 mmol, 1 equiv.) and phenylhydrazine hydrochloride (329 mg, 2.27 mmol, 1 equiv.) in *t*BuOH (15 mL, 0.2 M) with additional 1 M HCl in Et_2O (0.4 mL) and AcOH (1 mL). Purified using reverse-phase HPLC to afford the title compound as a yellow oil (308 mg, 54%). ^1H NMR (400 MHz, $CDCl_3$): δ 8.09 (s, 1H), 7.70-7.63 (m, 1H), 7.31-7.27 (m, 1H), 7.19-7.13 (m, 2H), 2.69 (t, *J* = 7.0 Hz, 2H), 2.53 (s, 3H), 2.50 (t, *J* = 7.4 Hz, 2H) 1.85-1.78 (m, 2H). CO_2H proton not observed. ^{13}C NMR (126 MHz, $CDCl_3$): δ 178.7, 140.0, 135.3, 130.5, 121.9, 120.3, 118.6, 110.6, 101.8, 35.1, 32.5, 24.7, 12.2. υ_{max} (neat): 3323, 2926, 2851, 1622, 1566 cm^{-1}. HRMS: exact mass calculated for $[M-H]^-$ ($C_{13}H_{14}NO_2S$) *m/z* requires 248.0751, *m/z* found 248.0752.

4-(2-Methyl-1-(1-methyl-1*H*-pyrazol-4-yl)-1*H*-indol-3-yl)butanoic acid (80). Prepared according to General Procedure 4 using 4-(2-methyl-1*H*-indol-3-yl)butanoic acid (**79**) (200 mg, 0.803 mmol, 1 equiv.), CuO (128 mg, 1.60 mmol, 2 equiv.), K_2CO_3 (144 mg, 1.04 mmol, 1.3 equiv.), and 1-methyl-4-bromopyrazole (248 μL, 2.40 mmol, 3 equiv.) in pyridine (2 mL, 0.4 M) to afford the title compound as a brown oil (4 mg, 2%). ^1H NMR (400 MHz, $CDCl_3$): δ 7.71 (dd, *J* = 6.5, 1.4 Hz, 1H), 7.60 (s, 1H), 7.54 (s, 1H), 7.22-7.13 (m, 3H), 4.03 (s, 3H), 2.73 (t, *J* = 7.1 Hz, 2H), 2.52 (t, *J* = 7.4 Hz, 2H), 2.40 (s, 3H), 1.88-1.80 (m, 2H). CO_2H proton not observed. ^{13}C NMR (101 MHz, $CDCl_3$): δ 102.5, 93.6, 92.6, 92.5, 92.3, 90.5, 89.9, 88.5, 88.2, 87.6, 85.5, 83.6, 67.8, 66.6, 65.9, 64.0, 60.7. υ_{max} (neat): 2910, 2600, 1719, 1580 cm^{-1}. HRMS: exact mass calculated for $[M+H]^+$ ($C_{17}H_{20}N_3O_2S$) *m/z* requires 330.1271, *m/z* found 333.1267.

4-((6-Chloro-2-methyl-1-(1-methyl-1*H*-pyrazol-4-yl)-1*H*-indol-3-yl)thio)butanoic acid (81). Prepared according to General Procedure 1 using 4-((2-oxopropyl)thio)butanoic acid (**78**) (400 mg, 2.27 mmol, 1 equiv.) and 3-chlorophenylhydrazine hydrochloride (406 mg, 2.27 mmol, 1 equiv.) in *t*BuOH (15 mL, 0.2 M), with additional 1 M HCl in Et_2O (1 mL) and AcOH (1 mL). The crude material was then used according to General Procedure 4 using CuO (225 mg, 2.81 mmol, 1.2 equiv.), K_2CO_3 (252 mg, 1.83 mmol, 0.8 equiv.), and 1-methyl-4-bromopyrazole (437 μL, 4.23 mmol, 1.9 equiv.) in pyridine (4 mL, 0.6 M). Purified by reverse-phase HPLC to afford the title compound as a brown oil (7 mg, 1% over 2 steps). ^{1}H NMR (400 MHz, $CDCl_3$): δ 7.60-7.58 (m, 2H), 7.55 (s, 1H), 7.14 (dd, *J* = 8.3, 1.8 Hz, 1H), 7.11 (d, *J* = 1.6 Hz, 1H), 4.03 (s, 3H), 2.71 (t, *J* = 7.1 Hz, 2H), 2.51 (t, *J* = 7.4 Hz, 2H), 2.38 (s, 3H), 1.87-1.80 (m, 2H). CO_2H proton not observed.^{13}C NMR (101 MHz, $CDCl_3$): δ 176.6, 142.8, 138.2, 136.6, 136.6, 128.0, 127.6, 121.0, 119.0, 110.0, 109.7, 102.5, 39.3, 34.8, 31.7, 24.3, 11.1. υ_{max} (neat): 3409, 3000, 2900, 1660 cm^{-1}. HRMS: exact mass calculated for $[M+H]^+$ ($C_{17}H_{19}ClN_3O_2S$) requires *m/z* 364.0881, found *m/z* 364.0878.

Ethyl 6-((5-chloro-2-methyl-1*H*-indol-3-yl)thio)picolinate (82). Prepared according to General Procedure 5 using ethyl 6-((2-oxopropyl)thio)picolinate (**13**) (1 g, 4.18 mmol, 1 equiv.) and (4-chlorophenyl)hydrazine hydrochloride (749 mg, 4.18 mmol, 1 equiv.) in EtOH (25 mL, 0.2 M). Purified using silica chromatography, eluting with 0-50% EtOAc/cyclohexane, to afford the title compound as a brown amorphous solid (460 mg, 32%). ^{1}H NMR (400 MHz, MeOD): δ 7.75 (dd, *J* = 7.6, 0.8 Hz, 1H), 7.59 (app t, *J* = 7.9 Hz, 1H), 7.36-7.32 (m, 2H), 7.11 (dd, *J* = 8.6, 2.0 Hz, 1H), 6.75 (dd, *J* = 8.1, 0.8 Hz, 1H), 4.43 (q, *J* = 7.1 Hz, 2H), 2.49 (s, 3H), 1.42 (t, *J* = 7.1 Hz, 3H). NH proton not observed. ^{13}C NMR (101 MHz, MeOD): δ 164.7, 163.8, 147.5, 144.1, 137.7, 134.6, 130.9, 126.0, 122.3, 121.7, 120.4, 116.8, 112.1, 95.4, 61.6, 13.1, 10.4. υ_{max} (neat): 3263,

1720, 1570, 1500 cm^{-1}. HRMS: exact mass calculated for $[M+H]^+$ ($C_{17}H_{16}ClN_2O_2S$) *m/z* requires 347.0616, *m/z* found 347.0626.

Ethyl 6-((7-chloro-2-methyl-1*H*-indol-3-yl)thio)picolinate (83). Prepared according to General Procedure 5 using ethyl 6-((2-oxopropyl)thio)picolinate (**13**) (550 mg, 2.30 mmol, 1 equiv.) and (2-chlorophenyl)hydrazine hydrochloride (412 mg, 2.30 mmol, 1 equiv.) in EtOH (12 mL, 0.2 M). Purified using silica chromatography, eluting with 0-50% EtOAc/cyclohexane, to afford the title compound as a yellow amorphous solid (386 mg, 48%). ^{1}H NMR (400 MHz, MeOD): δ 7.74 (d, *J* = 7.2 Hz, 1H), 7.57 (app t, *J* = 7.9 Hz, 1H), 7.32 (d, *J* = 7.9 Hz, 1H), 7.15 (d, *J* = 7.6 Hz, 1H), 7.02 (app t, *J* = 7.8 Hz, 1H), 6.74 (d, *J* = 8.1 Hz, 1H), 4.43 (q, *J* = 7.1 Hz, 2H), 2.52 (s, 3H), 1.42 (t, *J* = 7.1 Hz, 3H). NH proton not observed. ^{13}C NMR (101 MHz, MeOD): δ 164.6, 163.8, 147.5, 143.8, 137.7, 133.2, 131.4, 122.4, 121.1, 120.9, 120.3, 116.3, 116.3, 96.9, 61.6, 13.1, 10.3. υ_{max} (neat): 3300, 3000, 1722, 1571 cm^{-1}. HRMS: exact mass calculated for $[M+H]^+$ ($C_{17}H_{16}ClN_2O_2S$) *m/z* requires 347.0616, *m/z* found 347.0616.

Ethyl 6-((6-fluoro-2-methyl-1*H*-indol-3-yl)thio)picolinate (84) and ethyl 6-((4-fluoro-2-methyl-1*H*-indol-3-yl)thio)picolinate (85). Prepared according to General Procedure 5 using ethyl 6-((2-oxopropyl)thio)picolinate (**13**) (1 g, 4.18 mmol, 1 equiv.) and (3-fluorophenyl)hydrazine hydrochloride (677 mg, 4.18 mmol, 1 equiv.) in EtOH (25 mL, 0.2 M). Purified using reverse-phase UPLC to afford ethyl 6-((6-fluoro-2-methyl-1*H*-indol-3-yl)thio)picolinate (**84**) as a yellow amorphous solid (563 mg, 41%) and ethyl 6-((4-fluoro-2-methyl-1*H*-indol-3-yl)thio)picolinate (**85**) as a yellow amorphous solid (332 mg, 24%). Ethyl 6-((6-fluoro-2-methyl-1*H*-indol-3-yl)thio)picolinate (**84**): ^{1}H NMR (400 MHz, MeOD): δ 7.72 (dd, *J* = 7.6, 0.9 Hz, 1H), 7.58-7.51 (m, 1H), 7.30 (dd, *J* = 8.6, 5.2 Hz, 1H), 7.09 (dd, *J* = 9.6, 2.2 Hz, 1H), 6.84-6.79 (m, 1H), 6.74 (dd, *J* = 8.2, 0.9 Hz, 1H), 4.42 (q, *J* = 7.1 Hz, 2H), 2.46 (s, 3H),

1.41 (t, J = 7.1 Hz, 3H). NH proton not observed. ^{13}C NMR (101 MHz, MeOD): δ 164.6, 164.1, 159.9 (d, $^{1}J_{C\text{-}F}$ = 236.1 Hz), 147.4, 142.8,(d, $J_{C\text{-}F}$ = 2.9 Hz), 137.7, 136.1 ($^{3}J_{C\text{-}F}$ = 12.5 Hz), 126.0, 122.4, 120.3, 118.3 (d, $^{3}J_{C\text{-}F}$ = 10.1 Hz), 108.2 (d, $^{2}J_{C\text{-}F}$ = 24.7 Hz), 97.2 (d, $^{2}J_{C\text{-}F}$ = 26.5 Hz), 95.6, 61.6, 13.1, 10.4. ^{19}F NMR (376 MHz, MeOD): δ -123.5. υ_{max} (neat): 3296, 3000, 1722, 1627, 1573, 1560 cm^{-1}. HRMS: exact mass calculated for $[M+H]^+$ ($C_{17}H_{16}FN_2O_2S$) *m/z* requires 331.0911, *m/z* found 331.0917. Ethyl 6-((4-fluoro-2-methyl-1*H*-indol-3-yl)thio)picolinate (**85**): ^{1}H NMR (400 MHz, MeOD): δ 7.74 (dd, J = 7.6, 0.9 Hz, 1H), 7.62-7.57 (m, 1H), 7.19 (d, J = 8.0 Hz, 1H), 7.09-7.04 (m, 1H), 6.86 (dd, J = 8.1, 0.7 Hz, 1H), 6.71-6.66 (m, 1H), 4.42 (q, J = 7.1 Hz, 2H), 2.47 (s, 3H), 1.41 (t, J = 7.1 Hz, 3H). NH proton not observed. ^{13}C NMR (101 MHz, MeOD): δ 165.0, 164.7, 155.9 (d, $^{1}J_{C\text{-}F}$ = 246.5 Hz), 147.2, 142.8, 139.0 (d, $^{3}J_{C\text{-}F}$ = 10.3 Hz), 137.6, 122.4, 122.0 (d, $^{3}J_{C\text{-}F}$ = 7.6 Hz), 120.1, 117.7 (d, $^{2}J_{C\text{-}F}$ = 17.2 Hz), 107.2 (d, $J_{C\text{-}F}$ = 3.7 Hz), 105.2 (d, $^{2}J_{C\text{-}F}$ = 19.2 Hz), 93.2, 61.6, 13.1, 10.1. ^{19}F NMR (376 MHz, DMSO-d_6): δ -130.41. υ_{max} (neat): 3300, 3000, 1718, 1573 cm^{-1}. HRMS: exact mass calculated for $[M+H]^+$ ($C_{17}H_{16}FN_2O_2S$) *m/z* requires 331.0911, *m/z* found 331.0918.

Ethyl 6-((2,6-dimethyl-1*H*-indol-3-yl)thio)picolinate (86) and ethyl 6-((2,4-dimethyl-1*H*-indol-3-yl)thio)picolinate (87). Prepared according to General Procedure 5 using ethyl 6-((2-oxopropyl)thio)picolinate (**13**) (1 g, 4.43 mmol, 1 equiv.) and *m*-tolylhydrazine hydrochloride (704 mg, 4.43 mmol, 1 equiv.) in EtOH (25 mL, 0.2 M). Purified using reverse-phase UPLC to afford ethyl 6-((2,6-dimethyl-1*H*-indol-3-yl)thio)picolinate (**86**) as a yellow amorphous solid (189 mg, 13%) and ethyl 6-((2,4-dimethyl-1*H*-indol-3-yl)thio)picolinate (**87**) as a yellow amorphous solid (156 mg, 11%). Ethyl 6-((2,6-dimethyl-1*H*-indol-3-yl)thio)picolinate (**86**): ^{1}H NMR (400 MHz, MeOD): δ 7.70 (dd, J = 7.6, 0.9 Hz, 1H), 7.53-7.46 (m, 1H), 7.22 (d, J = 8.1 Hz, 1H), 7.17 (s, 1H), 6.86 (dd, J = 8.0, 0.9 Hz, 1H), 6.72 (dd, J = 8.2, 0.9 Hz, 1H), 4.41 (q, J =

7.1 Hz, 2H), 2.45 (s, 3H), 2.40 (s, 3H), 1.41 (t, *J* = 7.1 Hz, 3H). NH proton not observed. ^{13}C NMR (101 MHz, MeOD): δ 164.7, 147.3, 141.4, 137.5, 136.6, 131.4, 127.3, 122.5, 121.6, 120.1, 117.1, 110.8, 95.0, 61.6, 20.3, 13.1, 10.3. One carbon not observed/coincident. υ_{max} (neat): 3296, 2950, 1720, 1574 cm^{-1}. HRMS: exact mass calculated for $[M+H]^+$ ($C_{18}H_{19}N_2O_2S$) requires *m/z* 327.1162, found *m/z* 327.1161. Ethyl 6-((2,4-dimethyl-1*H*-indol-3-yl)thio)picolinate (**87**): ^{1}H NMR (400 MHz, MeOD): δ 7.72 (dd, *J* = 7.6, 0.9 Hz, 1H), 7.60-7.54 (m, 1H), 7.21 (d, *J* = 8.1 Hz, 1H), 7.02-6.96 (m, 1H), 6.82-6.73 (m, 2H), 4.42 (q, *J* = 7.1 Hz, 2H), 2.54 (s, 3H), 2.45 (s, 3H), 1.41 (t, *J* = 7.1 Hz, 3H). NH proton not observed. ^{13}C NMR (101 MHz, MeOD): δ 166.2, 164.7, 147.3, 142.3, 137.7, 136.4, 129.5, 127.1, 122.5, 121.8, 121.4, 120.0, 108.9, 95.1, 61.6, 17.5, 13.1, 10.3. υ_{max} (neat): 3153, 2980, 1720, 1674, 1574 cm^{-1}. HRMS: exact mass calculated for $[M+H]^+$ ($C_{18}H_{19}N_2O_2S$) requires *m/z* 327.1162, found *m/z* 327.1161.

Ethyl 6-((6-methoxy-2-methyl-1*H*-indol-3-yl)thio)picolinate (88) and ethyl 6-((4-methoxy-2-methyl-1*H*-indol-3-yl)thio)picolinate (89). Prepared according to General Procedure 5 using ethyl 6-((2-oxopropyl)thio)picolinate (**13**) (1 g, 4.18 mmol, 1 equiv.) and (3-methoxyphenyl)hydrazine hydrochloride (732 mg, 4.18 mmol, 1 equiv.) in EtOH (25 mL, 0.2 M). Purified using reverse-phase UPLC to afford ethyl 6-((6-methoxy-2-methyl-1*H*-indol-3-yl)thio)picolinate (**88**) as a brown amorphous solid (521 mg, 36%) and ethyl 6-((4-methoxy-2-methyl-1*H*-indol-3-yl)thio)picolinate (**89**) as a yellow amorphous solid (282 mg, 20%). Ethyl 6-((6-methoxy-2-methyl-1*H*-indol-3-yl)thio)picolinate (**88**): ^{1}H NMR (600 MHz, MeOD): δ 7.73 (dd, *J* = 7.6, 0.8 Hz, 1H), 7.61-7.51 (m, 1H), 7.22 (d, *J* = 8.6 Hz, 1H), 6.93 (d, *J* = 2.2 Hz, 1H), 6.77 (dd, *J* = 8.2, 0.8 Hz, 1H), 6.71 (dd, *J* = 8.6, 2.2 Hz, 1H), 4.43 (q, *J* = 7.1 Hz, 2H), 3.81 (s, 3H), 2.44 (s, 3H), 1.42 (t, *J* = 7.1 Hz, 3H). NH proton not observed. ^{13}C NMR (151 MHz, MeOD): δ 164.6, 164.5, 156.7, 147.1, 140.9, 137.7, 136.9, 123.6, 122.6, 120.2, 118.0, 109.7,

94.9, 94.7, 61.6, 54.7, 13.1, 10.3. υ_{max} (neat): 3000, 1726, 1627 cm^{-1}. HRMS: exact mass calculated for $[M+H]^+$ ($C_{18}H_{19}N_2O_3S$) requires *m/z* 343.1111, found *m/z* 343.1113. Ethyl 6-((4-methoxy-2-methyl-1*H*-indol-3-yl)thio)picolinate (**89**): ^1H NMR (600 MHz, MeOD): δ 7.72 (dd, *J* = 7.5, 0.8 Hz, 1H), 7.57 (app t, *J* = 7.9 Hz, 1H), 7.04 (app t, *J* = 7.9 Hz, 1H), 6.99 (dd, *J* = 8.1, 0.6 Hz, 1H), 6.88 (dd, *J* = 8.2, 0.8 Hz, 1H), 6.51 (d, *J* = 7.7 Hz, 1H), 4.43 (q, *J* = 7.1 Hz, 2H), 3.62 (s, 3H), 2.44 (s, 3H), 1.42 (t, *J* = 7.1 Hz, 3H). NH proton not observed. ^{13}C NMR (151 MHz, MeOD): δ 166.4, 164.7, 153.5, 146.7, 140.6, 137.8, 137.3, 123.1, 122.4, 119.8, 118.6, 104.4, 101.0, 94.3, 61.6, 54.4, 13.1, 10.2. υ_{max} (neat): 3288, 2800, 1714, 1575, 1543, 1506 cm^{-1}. HRMS: exact mass calculated for $[M+H]^+$ ($C_{18}H_{19}N_2O_3S$) requires *m/z* 343.1111, found *m/z* 343.1112.

Methyl 3-((6-chloro-2-methyl-1-(1-methyl-1*H*-pyrazol-4-yl)-1*H*-indol-3-yl)thio)benzoate (90). Prepared according to General Procedure 4 using methyl 3-((6-chloro-2-methyl-1*H*-indol-3-yl)thio)benzoate (**46**) (100 mg, 0.302 mmol, 1 equiv.), CuO (48 mg, 0.604 mmol, 2 equiv.), K_2CO_3 (54 mg, 0.393 mmol, 1.3 equiv.), and 1-methyl-4-bromopyrazole (94 μL, 0.906 mmol, 3 equiv.) in pyridine (1 mL, 0.3 M). Purified using silica chromatography, eluting with 50% EtOAc/petroleum ether, to afford the title compound as a cream amorphous solid (74 mg, 59%). ^1H NMR (400 MHz, $CDCl_3$): δ 7.83-7.82 (m, 1H), 7.74-7.72 (m, 1H), 7.63 (s, 1H), 7.61 (s, 1H), 7.44 (d, *J* = 8.3 Hz, 1H), 7.23 (app t, *J* = 7.7 Hz, 1H), 7.19-7.15 (m, 2H), 7.11 (dd, *J* = 8.4, 1.8 Hz, 1H), 4.05 (s, 3H), 3.87 (s, 3H), 2.38 (s, 3H). ^{13}C NMR (101 MHz, $CDCl_3$): δ 166.9, 144.7, 139.7, 139.2, 137.2, 130.9, 130.1, 129.0, 128.7, 128.1, 127.7, 127.0, 126.2, 122.1, 119.8, 119.3, 110.6, 100.1, 52.4, 40.0, 11.8. υ_{max} (neat): 3057, 2985, 2945, 2920, 2883, 2848, 1710, 1606, 1570, 1539 cm^{-1}. HRMS: exact mass calculated for $[M+H]^+$ ($C_{21}H_{19}ClN_3O_2S$) *m/z* requires 414.0850, *m/z* found 414.0851.

3-((3-Bromophenyl)thio)-2-methyl-1*H*-indole (91). Prepared according to General Procedure 5 using phenylhydrazine hydrochloride (592 mg, 4.08 mmol, 1 equiv.) and 1-((3-bromophenyl)thio)propan-2-one (**44**) (1 g, 4.08 mmol, 1 equiv.) in EtOH (20 mL, 0.2 M). Purified using silica chromatography, eluting with 0-10% EtOAc/petroleum ether, to afford the title compound as a brown oil (1.2 g, 92%). ^{1}H NMR (400 MHz, $CDCl_3$): δ 8.30 (br s, 1H), 7.52 (d, *J* = 7.8 Hz, 1H), 7.36 (d, *J* = 8.0 Hz, 1H), 7.23-7.19 (m, 1H), 7.18-7.11 (m, 3H), 7.00 (app t, *J* = 8.1 Hz, 1H), 6.98-6.92 (m, 1H), 2.52 (s, 3H). ^{13}C NMR (101 MHz, $CDCl_3$): δ 142.1, 141.5, 135.6, 130.1, 127.9, 127.7, 124.1, 123.0, 122.5, 121.0, 118.9, 110.9, 98.5, 12.3. One carbon not observed/coincident. υ_{max} (neat): 3392, 3055, 2980, 1573, 1556 cm^{-1}. HRMS: exact mass calculated for $[M+H]^+$ ($C_{15}H_{13}BrNS$) *m/z* requires 319.9925, *m/z* found 319.9931.

Methyl 3-((2-methyl-1*H*-indol-3-yl)thio)benzoate (92). Prepared according to General Procedure 7 using *trans*-bis(acetato)bis[*o*-(di-*o*-tolylphosphino)benzyl]dipalladium(II) (183 mg, 0.195 mmol, 5 mol%), 3-((3-bromophenyl)thio)-2-methyl-1*H*-indole (**91**) (1.2 g, 3.77 mmol, 1 equiv.), $Mo(CO)_6$ (995 mg, 3.77 mmol, 1 equiv.), [*t*Bu_3PH]BF_4 (219 mg, 0.754 mmol, 20 mol%), and DBU (844 μL, 5.66 mmol, 1.5 equiv.) in MeCN/MeOH (20 mL, 1:4, 0.2 M) to afford the title compound as a brown amorphous solid (1.03 g, 92%). ^{1}H NMR (500 MHz, $CDCl_3$): δ 8.49 (br s, 1H), 7.81 (s, 1H), 7.70 (d, *J* = 7.6 Hz, 1H), 7.51 (d, *J* = 7.8 Hz, 1H), 7.34 (d, *J* = 8.0 Hz, 1H), 7.22-7.09 (m, 4H), 3.86 (s, 3H), 2.50 (s, 3H). ^{13}C NMR (126 MHz, $CDCl_3$): δ 166.9, 141.4, 140.4, 135.6, 130.6, 130.1, 129.8, 128.7, 126.6, 125.8, 122.2, 120.8, 118.8, 110.8, 52.1, 29.1, 12.1. υ_{max} (neat): 3327, 2850, 1710 cm^{-1}. HRMS: exact mass calculated for $[M-H]^-$ ($C_{17}H_{14}NO_2S$) *m/z* requires 296.0751, *m/z* found 296.0753.

Methyl 3-((1,2-dimethyl-1*H*-indol-3-yl)thio)benzoate (93). Prepared according to General Procedure 6 using methyl 3-((2-methyl-1*H*-indol-3-yl)thio)benzoate (**92**) (200 mg, 0.673 mmol,

1 equiv.), NaH 60% w/w (54 mg, 1.35 mmol, 2 equiv.), and MeI (84 μL, 1.35 mmol, 2 equiv.) in THF (3 mL, 0.2 M). Purified using silica chromatography, eluting with 10% EtOAc/petroleum ether, to afford the title compound as a pale yellow amorphous solid (71 mg, 34%). ^{1}H NMR (500 MHz, $CDCl_3$): δ 7.87 (s, 1H), 7.74 (dd, *J* = 7.6, 1.2 Hz, 1H), 7.59 (d, *J* = 7.8 Hz, 1H), 7.38 (d, *J* = 8.2 Hz, 1H), 7.28 (app t, *J* = 7.1 Hz, 1H), 7.24-7.11 (m, 3H), 3.90 (s, 3H), 3.79 (s, 3H), 2.56 (s, 3H). ^{13}C NMR (126 MHz, $CDCl_3$): δ 166.9, 143.1, 140.8, 137.3, 130.7, 129.9, 129.6, 128.8, 126.7, 125.8, 122.0, 120.7, 118.9, 109.3, 97.5, 52.2, 30.5, 11.0. υ_{max} (neat): 2949, 1722, 1572, 1527 cm^{-1}. HRMS: exact mass calculated for $[M+H]^+$ ($C_{18}H_{18}NO_2S$) *m/z* requires 312.1053, *m/z* found 312.1055.

Ethyl 3-((6-chloro-2-methyl-1*H*-indol-3-yl)oxy)benzoate (94). Prepared according to General Procedure 1 using (3-chlorophenyl)hydrazine hydrochloride (1.6 g, 9.01 mmol, 1 equiv.) and ethyl 3-(2-oxopropoxy)benzoate (**59**) (2 g, 9.01 mmol, 1 equiv.) in *t*BuOH (90 mL, 0.1 M) with additional 1 M HCl in Et_2O (27 mL) and AcOH (10 mL). Purified by silica chromatography, eluting with 10% EtOAc/petroleum ether, to afford the title compound as a pale brown amorphous solid (845 mg, 28%). ^{1}H NMR (600 MHz, $CDCl_3$): δ 7.72-7.65 (m, 2H), 7.62 (dd, *J* = 2.5, 1.6 Hz, 1H), 7.31 (app t, *J* = 8.0 Hz, 1H), 7.29 (d, *J* = 1.6 Hz, 1H), 7.13 (d, *J* = 8.4 Hz, 1H), 7.10 (dd, *J* = 8.3, 2.6 Hz, 1H), 6.98 (dd, *J* = 8.4, 1.8 Hz, 1H), 4.34 (q, *J* = 7.1 Hz, 2H), 2.32 (s, 3H), 1.36 (t, *J* = 7.1 Hz, 3H). NH proton not observed. ^{13}C NMR (151 MHz, $CDCl_3$): δ 166.4, 159.2, 133.6, 132.2, 129.6, 129.4, 127.9, 125.1, 123.1, 120.7, 120.3, 119.8, 118.2, 116.6, 111.0, 61.2, 14.4, 10.4. υ_{max} (neat): 3350, 2982, 1713, 1701, 1585 cm^{-1}. HRMS: exact mass calculated for $[M+H]^+$ ($C_{18}H_{17}ClNO_3$) *m/z* requires 332.0862, *m/z* found 332.0867.

3-(3-Bromobenzyl)-6-chloro-2-methyl-1*H*-indole (95). Prepared according to General Procedure 8 using 3-bromobenzaldehyde (442 mg, 2.39 mmol, 1.1 equiv.), 6-chloro-2-methyl-

1*H*-indole (**65**) (360 mg, 2.17 mmol, 1 equiv.), Et_3SiH (451 μL, 2.83 mmol, 1.3 equiv.), and TFA (249 μL, 3.26 mmol, 1.5 equiv.) in CH_2Cl_2 (10 mL, 0.2 M). Purified using silica chromatography, eluting with 0-5% EtOAc/petroleum ether, to afford the title compound as a white amorphous solid (587 mg, 73%). ^{1}H NMR (600 MHz, $CO(CD_3)_2$): δ 10.10 (br s, 1H), 7.38 (s, 1H), 7.34-7.28 (m, 3H), 7.23 (d, *J* = 7.7 Hz, 1H), 7.18 (app t, *J* = 7.8 Hz, 1H), 6.93 (dd, *J* = 8.5, 1.8 Hz, 1H), 4.06 (s, 2H), 2.42 (s, 3H). ^{13}C NMR (151 MHz, $CO(CD_3)_2$): δ 145.7, 134.5, 131.9, 131.0, 129.5, 128.3, 128.1, 126.8, 122.8, 119.9, 119.7, 111.1, 110.2, 30.0, 11.6. One carbon not observed/coincident. υ_{max} (neat): 3409, 3053, 2911, 2850, 1692, 1613, 1593, 1567 cm^{-1}. HRMS: exact mass calculated for $[M+H]^+$ ($C_{16}H_{14}BrClN$) *m/z* requires 337.9948, *m/z* found 337.9947.

Methyl 3-((6-chloro-2-methyl-1*H*-indol-3-yl)methyl)benzoate (96). Prepared according to General Procedure 7 using *trans*-bis(acetato)bis[*o*-(di-*o*-tolylphosphino)benzyl] dipalladium(II) (77 mg, 0.0821 mmol, 5 mol%), 3-(3-bromobenzyl)-6-chloro-2-methyl-1*H*-indole (**95**) (551 mg, 1.65 mmol, 1 equiv.), $Mo(CO)_6$ (436 mg, 1.65 mmol, 1 equiv.), $[tBu_3PH]BF_4$ (96 mg, 0.330 mmol, 20 mol%), and DBU (370 μL, 2.48 mmol, 1.5 equiv.) in MeCN/MeOH (10 mL, 1:4, 0.2 M). Purified using silica chromatography, eluting with 0-15% EtOAc/petroleum ether, to afford the title compound as a pale yellow amorphous solid (348 mg, 67%). ^{1}H NMR (400 MHz, $CO(CD_3)_2$): δ 10.11 (br s, 1H), 7.89 (s, 1H), 7.81-7.78 (m, 1H), 7.53-7.44 (m, 1H), 7.37 (app t, *J* = 7.7 Hz, 1H), 7.33-7.28 (m, 2H), 6.91 (dd, *J* = 8.4, 1.9 Hz, 1H), 4.13 (s, 2H), 3.83 (s, 3H), 2.43 (s, 3H). ^{13}C NMR (101 MHz, $CO(CD_3)_2$): δ 167.3, 143.5, 137.2, 134.4, 133.8, 131.2, 129.9, 129.3, 128.4, 127.7, 126.8, 119.9, 119.8, 111.2, 110.6, 52.2, 30.3, 11.7. υ_{max} (neat): 3328, 2945, 2896, 1705, 1621, 1608 cm^{-1}. HRMS: exact mass calculated for $[M+H]^+$ ($C_{18}H_{17}ClNO_2$) *m/z* requires 316.0913, *m/z* found 316.0914.

3-((6-Bromopyridin-2-yl)methyl)-6-chloro-2-methyl-1-(1-methyl-1*H*-pyrazol-4-yl)-1*H*-indole (97). Prepared according to General Procedure 8 using 6-bromopyridine-2-carbaldehyde (91 mg, 0.489 mmol, 1.2 equiv.), 6-chloro-2-methyl-1-(1-methyl-1*H*-pyrazol-4-yl)-1*H*-indole (**66**) (100 mg, 0.406 mmol, 1 equiv.), Et_3SiH (84 µL, 0.529 mmol, 1.3 equiv.), and TFA (47 µL, 0.610 mmol, 1.5 equiv.) in CH_2Cl_2 (2 mL, 0.2 M). Purified using silica chromatography, eluting with 0-50% EtOAc/petroleum ether, to afford the title compound as a yellow oil (94 mg, 56%). ^{1}H NMR (400 MHz, $CO(CD_3)_2$): δ 7.96 (s, 1H), 7.60 (s, 1H), 7.57 (app t, *J* = 7.7 Hz, 1H), 7.51 (d, *J* = 8.4 Hz, 1H), 7.39 (d, *J* = 7.8 Hz, 1H), 7.22 (d, *J* = 7.2 Hz, 1H), 7.08 (d, *J* = 1.6 Hz, 1H), 7.02 (dd, *J* = 8.4, 1.9 Hz, 1H), 4.23 (s, 2H), 4.01 (s, 3H), 2.33 (s, 3H). ^{13}C NMR (101 MHz, $CDCl_3$): δ 163.8, 141.9, 140.4, 139.5, 137.3, 137.1, 128.9, 127.6, 126.2, 122.4, 120.8, 120.2, 119.9, 110.5, 110.3, 39.8, 33.5, 11.1. One carbon not observed/coincident. υ_{max} (neat): 3114, 2921, 1612, 1582, 1554 cm^{-1}. HRMS: exact mass calculated for $[M+H]^+$ ($C_{19}H_{17}BrClN_4$) *m/z* requires 417.0297, *m/z* found 417.0294.

2-Methyl-1-(1-methyl-1*H*-pyrazol-4-yl)-1*H*-indole (98). Prepared according to General Procedure 4 using 2-methyl-1*H*-indole (1 g, 7.63 mmol, 1 equiv.), 4-bromo-1-methyl-1*H*-pyrazole (1.2 mL, 11.4 mmol, 1.5 equiv.), CuO (1.2 g, 15.3 mmol, 2 equiv.), and K_2CO_3 (1.4 g, 9.92 mmol, 1.3 equiv.) in pyridine (10 mL, 0.8 M). Purified using silica chromatography, eluting with 0-30% EtOAc/petroleum ether, to afford the title compound as a brown amorphous solid (679 mg, 42%). ^{1}H NMR (400 MHz, $CDCl_3$): δ 7.58 (s, 1H), 7.57-7.52 (m, 1H), 7.50 (s, 1H), 7.17-7.07 (m, 3H), 6.37 (s, 1H), 4.01 (s, 3H), 2.31 (s, 3H). ^{13}C NMR (101 MHz, $CDCl_3$): δ 138.9, 137.7, 137.4, 128.3, 127.4, 121.2, 120.3, 120.2, 119.7, 110.0, 101.2, 39.8, 13.3. υ_{max} (neat): 3114, 3051, 2984, 2941, 2919, 1612, 1586, 1560 cm^{-1}. HRMS: exact mass calculated for $[M+H]^+$ ($C_{13}H_{14}N_3$) *m/z* requires 212.1182, *m/z* found 212.1182.

3-(3-Bromobenzyl)-2-methyl-1-(1-methyl-1*H*-pyrazol-4-yl)-1*H*-indole (99). Prepared according to General Procedure 8 using 2-bromobenzaldehyde (90 mg, 0.486 mmol, 1.02 equiv.), 2-methyl-1-(1-methyl-1*H*-pyrazol-4-yl)-1*H*-indole (**98**) (100 mg, 0.474 mmol, 1 equiv.), Et_3SiH (84 μL, 0.529 mmol, 1.1 equiv.), and TFA (47 μL, 0.610 mmol, 1.3 equiv.) in CH_2Cl_2 (2 mL, 0.2 M). Purified using silica chromatography, eluting with 20-50% EtOAc/petroleum ether, to afford the title compound as a yellow gum (165 mg, 89%). ^{1}H NMR (400 MHz, $CDCl_3$): δ 7.60 (s, 1H), 7.53 (s, 1H), 7.46-7.38 (m, 2H), 7.30 (d, *J* = 7.8 Hz, 1H), 7.21-7.04 (m, 5H), 4.09 (s, 2H), 4.02 (s, 3H), 2.26 (s, 3H). ^{13}C NMR (101 MHz, $CDCl_3$): δ 144.1, 138.3, 137.5, 134.6, 131.4, 130.0, 129.1, 128.1, 127.6, 127.1, 122.6, 121.5, 120.4, 120.0, 118.2, 110.5, 109.9, 39.8, 30.3, 11.1. υ_{max} (neat): 3116, 3053, 2986, 2941, 2919, 1614, 1582, 1569 cm^{-1}. HRMS: exact mass calculated for $[M+H]^+$ ($C_{20}H_{19}BrN_3$) *m/z* requires 382.0736, *m/z* found 382.0737.

Methyl 3-((2-methyl-1-(1-methyl-1*H*-pyrazol-4-yl)-1*H*-indol-3-yl)methyl) benzoate (100). Prepared according to General Procedure 7 using *trans*-bis(acetato)bis[*o*-(di-*o*-tolylphosphino)benzyl]dipalladium(II) (19 mg, 0.0202 mmol, 5 mol%), 3-(3-bromobenzyl)-2-methyl-1-(1-methyl-1*H*-pyrazol-4-yl)-1*H*-indole (**99**) (150 mg, 0.395 mmol, 1 equiv.), $Mo(CO)_6$ (104 mg, 0.395 mmol, 1equiv.), [*t*Bu_3PH]BF_4 (23 mg, 0.0793 mmol, 20 mol%), and DBU (88 μL, 0.593 mmol, 1.5 equiv.) in MeCN/MeOH (2.5 mL, 1:4, 0.2 M). Purified using silica chromatography, eluting with 50-70% EtOAc/petroleum ether, to afford the title compound as a yellow oil (111 mg, 78%). ^{1}H NMR (400 MHz, $CDCl_3$): δ 7.99 (s, 1H), 7.85 (d, *J* = 7.8 Hz, 1H), 7.59 (s, 1H), 7.53 (s, 1H), 7.41 (app t, *J* = 8.0 Hz, 2H), 7.31 (app t, *J* = 7.7 Hz, 1H), 7.18-7.01 (m, 3H), 4.16 (s, 2H), 4.01 (s, 3H), 3.90 (s, 3H), 2.27 (s, 3H). ^{13}C NMR (101 MHz, $CDCl_3$): δ 167.4, 142.1, 138.3, 137.5, 134.5, 133.1, 130.3, 129.6, 128.6, 128.1, 127.6, 127.3, 121.5, 120.4, 120.0, 118.2, 110.8, 109.9, 52.2, 39.8, 30.6, 11.1. υ_{max} (neat): 3116, 3051, 2949, 2919, 1718,

1608, 1584 cm^{-1}. HRMS: exact mass calculated for $[M+H]^+$ ($C_{22}H_{22}N_3O_2$) *m/z* requires 360.1707, *m/z* found 360.1705.

3-((6-Bromopyridin-2-yl)methyl)-2-methyl-1-(1-methyl-1*H*-pyrazol-4-yl)-1*H*-indole (101). Prepared according to General Procedure 8 using 6-bromopyridine-2-carbaldehyde (91 mg, 0.489 mmol, 1.03 equiv.), 2-methyl-1-(1-methyl-1*H*-pyrazol-4-yl)-1*H*-indole (**98**) (100 mg, 0.474 mmol, 1 equiv.), Et_3SiH (84 µL, 0.529 mmol, 1.1 equiv.), and TFA (47 µL, 0.610 mmol, 1.3 equiv.) in CH_2Cl_2 (2 mL, 0.2 M). Purified using silica chromatography, eluting with 20-60% EtOAc/petroleum ether, to afford the title compound as a yellow gum (158 mg, 85%). ^{1}H NMR (400 MHz, $CDCl_3$): δ 7.58 (s, 1H), 7.52 (s, 1H), 7.44 (dd, *J* = 6.6, 1.5 Hz, 1H), 7.34 (app t, *J*= 7.7 Hz, 1H), 7.27 (d, *J* = 8.7 Hz, 1H), 7.19-7.05 (m, 3H), 6.98 (dd, *J* = 7.5, 0.7 Hz, 1H), 4.29 (s, 2H), 4.01 (s, 3H), 2.27 (s, 3H). ^{13}C NMR (101 MHz, $CDCl_3$): δ 163.2, 141.3, 138.9, 138.3, 137.5, 135.2, 128.0, 127.5, 125.4, 121.7, 121.2, 120.3, 120.2, 118.2, 110.0, 109.1, 39.8, 33.2, 11.1. υ_{max} (neat): 3114, 3051, 2921, 1616, 1582, 1554 cm^{-1}. HRMS: exact mass calculated for $[M+H]^+$ ($C_{19}H_{18}BrN_4$) *m/z* requires 383.0689, *m/z* found 383.0686.

Methyl 6-((2-methyl-1-(1-methyl-1*H*-pyrazol-4-yl)-1*H*-indol-3-yl)methyl)picolinate (102). Prepared according to General Procedure 7 using *trans*-bis(acetato)bis[*o*-(di-*o*-tolylphosphino)benzyl] dipalladium(II) (17 mg, 0.0181 mmol, 5 mol%), 3-((6-bromopyridin-2-yl)methyl)-2-methyl-1-(1-methyl-1*H*-pyrazol-4-yl)-1*H*-indole (**101**) (140 mg, 0.367 mmol, 1 equiv.), $Mo(CO)_6$ (97 mg, 0.367 mmol, 1 equiv.), [*t*Bu_3PH]BF_4 (21 mg, 0.0724 mmol, 20 mol%), and DBU (82 µL, 0.550 mmol, 1.5 equiv.) in MeCN/MeOH (2.5 mL, 1:4, 0.1 M). Purified using silica chromatography, eluting with 50-100% EtOAc/petroleum ether, to afford the title compound as a yellow oil (55 mg, 42%). ^{1}H NMR (400 MHz, $CDCl_3$): δ 7.94 (d, *J* = 7.6 Hz, 1H), 7.62 (app t, *J* = 7.8 Hz, 1H), 7.59 (s, 1H), 7.53 (s, 1H), 7.42 (d, *J* = 7.4 Hz, 1H), 7.22-

7.04 (m, 4H), 4.44 (s, 2H), 4.04 (s, 3H), 4.02 (s, 3H), 2.27 (s, 3H). ^{13}C NMR (101 MHz, $CDCl_3$): δ 166.2, 162.2, 147.4, 138.4, 137.5, 135.2, 128.1, 127.5, 125.9, 122.8, 121.7, 120.4, 120.2, 118.3, 110.0, 109.3, 53.1, 39.9, 33.6, 11.1. One carbon not observed/coincident. υ_{max} (neat): 3118, 3090, 3001, 2943, 2919, 2855, 1716, 1617, 1591 cm^{-1}. HRMS: exact mass calculated for $[M+H]^+$ ($C_{21}H_{21}N_4O_2$) *m/z* requires 361.1659, *m/z* found 361.1660.

Bis-*p*NPP Inhibition Assay. Molecules were tested for their ability to inhibit autotaxin activity using the Autotaxin Inhibitor Screening Kit (Cayman Chemical) with modifications to the manufacturer's protocol. Briefly, in a 96 well plate 20 ng/mL autotaxin was incubated with 1 mM bis-*p*NPP at 30 °C for 30 min in 50 mM Tris-HCl buffer (pH 8.5) containing 10 mM $CaCl_2$ and 0.02% triton X. Liberated bis-*p*-nitrophenol was measured using a Wallac Victor2 1420 multilabel counter (Perkin Elmer, Beaconsfield, UK) in absorbance mode at 405 nm. The background was determined by incubating bis-*p*NPP in the absence of enzyme. Activity of the compounds was determined by subtracting the average background optical density from all results and expressing the compound activity as a percentage of the enzyme-substrate reaction in the absence of compound. Compounds were screened against autotaxin at a single concentration or using a dose response curve. Single concentration screens were carried out at an inhibitor concentration of 30 μM; samples which showed inhibition of 60% or greater were considered to be active and progressed to further testing. Dose response curves were performed in the concentration range of 30 nM to 30 μM, or 2 nM to 50 μM, ten point curves. Compounds which showed inhibition of less than 60% at 30 μM or a IC_{50} value greater than 30 μM were considered inactive. Data was expressed as mean ± SEM, plotted, and the IC_{50} values were calculated using Graph Pad Prism version 6.00 for Windows, GraphPad Software, La Jolla California USA, www.graphpad.com.

LPC Choline Release Assay. All biochemical studies were performed with hATX. ATX lysoPLD activity was measured by choline release from LPC. 20 nM ATX (prepared from HEK 293 Flp-In cells) was incubated with 150 μM LPC(18:1) in a final volume of 100 μL buffer containing 50 mM Tris pH 7.4, 0.01% Triton X-100, 50 mM $CaCl_2$, 1 Unit ml^{-1} choline oxidase, 2 Unit ml^{-1} HRP, 2 mM homovanilic acid (HVA). The relative amount of released choline was measured by HVA fluorescence in a 96-well plate (Corning). Fluorescent intensity was determined at λex/λem = 320/450 nm every 30 seconds for 90 minutes with a Fluorostar plate reader (BMG Labtech). All compounds were screened initially from 400 nM to 100 μM, n = 3, and categorized into one of four IC_{50} categories: (i) <1 μM; (ii) 1-10 μM; (iii) 10-20 μM; (iv) >30 μM. Further screening of active compounds was then carried out from 0.5 nM to 10 μM, n = 2. Data analysis was performed using GraphPad Prism version 6.00 for Windows, GraphPad Software, La Jolla California USA, www.graphpad.com.

ATX production and crystallization. ATX from rat (rATX) and human (hATX) was produced in HEK293 Flip-In cells as described previously.[40] For co-crystallization of rATX with **51**, **51** was first mixed with a 10M excess of rATX (3.5mg ml^{-1}) and incubated for 30 min. Crystals were obtained at room temperature (293 K) in a 24-well optimization screen (18-22% PEG 3350, 01-04 M NaSCN and 0.1-0.4 M NH_4I) by mixing 1 μl of protein:inhibitor solution and 1 μl of reservoir solution. The structure presented here is from a crystal obtained from a 24-well containing the following conditions: 20% PEG 3350, 0.2 M NH_4I, 0.1 M NaSCN.

Crystallographic data and methods.

X-ray diffraction data was collected at SLS on beamline PXIII. The crystallographic diffraction data was recorded on a PILATUS detector to a resolution of 2.4 Å for the ATX-**51** complex, PDB reference 5LQQ. The data was processed and integrated with XDS,[41] and scaled with AIMLESS.[42] The structure was determined by molecular replacement using PHASER[43] with the structure of ATX (PDB 2XR9) as the search model. Model building and subsequent refinement were performed iteratively with COOT,[35] REFMAC,[44] and PDB_REDO.[45]

CORRESPONDING AUTHOR

*craig.jamieson@strath.ac.uk, +44 (0)141 548 4830.

*allan.watson.100@strath.ac.uk, +44 (0)141 548 2439.

SUPPORTING INFORMATION

Supporting Information Available: Experimental and analytical methods, characterization data, assay data, physicochemical data, molecular modelling data, crystallographic data.

ABBREVIATIONS

ATX, Autotaxin; bis-*p*NPP, bis-(*p*-nitrophenol) phosphate; CLND, chemiluminescent nitrogen detection; ENPP, ectonucleotide pyrophosphatase and phosphodiesterase family; FRET, Förster resonance energy transfer; GPCR, G-protein coupled receptor; LEI, ligand efficiency index; LLE, liphophilic ligand efficiency; LPA, lysophosphatidic acid; LPC, lysophosphatodyl choline; MW, molecular weight; *p*NP-TMP, thymidine 5'monophosphate *p*-nitrophenyl ester; PSA, polar surface area; SAR, structure-activity relationship.

ACKNOWLEDGEMENTS

We thank Tatjana Heidebrecht and Robbie Joosten for help with crystallization and structure refinement. We thank GlaxoSmithKline for the Ph.D. studentships (L.M.M., D.C., E.L.D., and F.P.), as well as chemical and analytical resources. We also thank the EPSRC UK National Mass Spectrometry Facility at Swansea University for analyses. L.M.M. thanks BMCS-RSC (Travel Grant 2016) and SAGES (PEER Grant 2016) for funding.

REFERENCES

[1] Strackes, M. L.; Krutzsch, H. C.; Unsworth, E. J.; Arestad, A.; Cioce, V.; Schiffmann, E.; Liotta, L. A. Identification, purification, and partial sequence analysis of autotaxin, a novel motility-stimulating protein. *J. Biol. Chem.* **1992**, *267*, 2524–2529.

[2] Tokumura, A.; Majima, E.; Kariya, Y.; Tominaga, K.; Kogure, K.; Yasuda, K.; Fukuzawa, K. Identification of human plasma lysophospholipase D, a lysophosphatidic acid-producing enzyme, as autotaxin, a multifunctional phosphodiesterase. *J. Biol. Chem.* **2002**, *277*, 39436–39442.

[3] Yung, Y. C.; Stoddard, N. C.; Chun, J. LPA receptor signaling: pharmacology, physiology, and pathophysiology. *J. Lipid Res.* **2014**, *55*, 1192–1214.

[4] Mutoh, T.; Rivera, R.; Chun, J. Insights into the pharmacological relevance of lysophospholipid receptors. *Br. J. Pharmacol.* **2012**, *165*, 829–844.

[5] Nam, S. W.; Clair, T.; Kim, Y. S.; McMarlin, A.; Schiffmann, E.; Liotta, L. A.; Stracke, M. L. Autotaxin (NPP-2), a metastasis-enhancing motogen, is an angiogenic factor. *Cancer Res.* **2001**, *61*, 6938–6944.

[6] Zahednasab, H.; Balood, M.; Harirchian, M. H.; Mesbah-Namin, S. A.; Rahimian, N.; Siroos, B. Increased autotaxin activity in multiple sclerosis. *J. Neuroimmunol.* **2014**, *273*, 120–123.

[7] Gotoh, M.; Fujiwara, Y.; Yue, J.; Liu, J.; Lee, S.; Fells, J.; Uchiyama, A.; Murakami-Murofushi, K.; Kennel, S.; Wall, J.; Patil, R.; Gupte, R.; Balazs, L.; Miller, D. D.; Tigyi, G. J. Controlling cancer through the autotaxin-lysophosphatidic acid receptor axis. *Biochem. Soc. Trans*. **2012**, *40*, 31–36.

[8] Tager, A. M.; LaCamera, P.; Shea, B. S.; Campanella, G. S.; Selman, M.; Zhao, Z.; Polosukhin, V.; Wain, J.; Karimi-Shah, B.; Kim, N. D.; Hart, W. K.; Pardo, A.; Blackwell, T. S.; Xu, Y.; Chun, J.; Luster, A. D. The lysophosphatidic acid receptor LPA1 links pulmonary fibrosis to lung injury by mediating fibroblast recruitment and vascular leak. *Nat. Med.* **2008**, *14*, 45–54.

[9] Kanda, H.; Newton, R.; Klein, R.; Morita, Y.; Gunn, M.; Rosen, S. Autotaxin, an ectoenzyme that produces lysophosphatidic acid, promotes the entry of lymphocytes into secondary lymphoid organs. *Nat. Immunol.* **2008**, *9*, 415–423.

[10] Awada, R.; Rondeau, P.; Grès, S.; Saulnier-Blache, J. S.; Lefebvre d'Hellencourt, C.; Bourdon, E. Autotaxin protects microglial cells against oxidative stress. *Free Radical Biol. Med*. **2012**, *52*, 516–526.

[11] Castagna, D.; Budd, D. C.; Macdonald, S. J. F.; Jamieson, C.; Watson, A. J. B. Development of autotaxin inhibitors: an overview of the patent and primary literature. *J. Med. Chem.* **2016**, *59*, 5604−5621.

[12] Albers, H. M. H. G.; Ovaa, H. Chemical evolution of autotaxin inhibitors. *Chem. Rev.* **2012**, *112*, 2593–2603.

[13] (a) Hutchinson, J. H.; Lonergan, D.; Huang, F.; Rowbottom, M.; Calderon, I. Autotaxin inhibitor compounds. International Patent Application WO2015/048301 A1, **2015**, PharmAkea, Inc.; (b) Stein, A. J.; Bain, G.; Prodanovich, P.; Santini, A. M.; Darlington, J.; Stelzer, N. M.;

Sidhu, R. S.; Schaub, J.; Goulet, L.; Lonergan, D.; Calderon, I.; Evans, J. F.; Hutchinson, J. H. Structural basis for inhibition of human autotaxin by four potent compounds with distinct modes of binding. *Mol. Pharmacol.* **2015**, *88*, 982–992.

[14] (a) Prestwich, G.; Tigyi, G.; Jiang, G.; Zhang, G.; Gajewiak, J.; Zhang, H.; Xu, X. α-Chloro and α-bromo phosphonate analogs of lysophosphatidic acid and methods of making and using thereof. WO2008157361A1, **2008**; (b) Zhang, H.; Xu, X.; Gajewiak, J.; Tsukahara, R.; Fujiwara, Y.; Liu, J.; Fells, J. I.; Perygin, D.; Parrill, A. L.; Tigyi, G.; Prestwich, G. D. Dual activity lysophosphatidic acid receptor pan-antagonist/autotaxin inhibitor reduces breast cancer cell migration *in vitro* and causes tumor regression *in vivo*. *Cancer Res.* **2009**, *69*, 5441–5449.

[15] (a) Ferry, G.; Moulharat, N.; Pradère, J. P.; Desos, P.; Try, A.; Genton, A.; Giganti, A.; Beucher-Gaudin, M.; Lonchampt, M.; Bertrand, M.; Saulnier-Blache, J. S.; Tucker, G. C.; Cordi, A.; Boutin, J. A. S32826, a nanomolar inhibitor of autotaxin: discovery, synthesis and applications as a pharmacological tool. *J. Pharmacol. Exp. Ther.* **2008**, *327*, 809–819; (b) Jiang G, Madan D, Prestwich GD. Aromatic phosphonates inhibit the lysophospholipase D activity of autotaxin. *Bioorg. Med. Chem. Lett.* **2011**, *21*, 5098–5101.

[16] Gierse, J.; Thorarensen, A.; Beltey, K.; Bradshaw-Pierce, E.; Cortes-Burgos, L.; Hall, T.; Johnston, A.; Murphy, M.; Nemirovskiy, O.; Ogawa, S.; Pegg, L.; Pelc, M.; Prinsen, M.; Schnute, M.; Wendling, J.; Wene, S.; Weinberg, R.; Wittwer, A.; Zweifel, B.; Masferrer, J. A novel autotaxin inhibitor reduces lysophosphatidic acid levels in plasma and the site of inflammation. *J. Pharmacol. Exp. Ther.* **2010**, *334*, 310–317.

[17] Albers, H. M. H. G.; van Meeteren, L. A.; Egan, D. A.; van Tilburg, E. W.; Moolenaar, W. H.; Ovaa, H. Discovery and optimization of boronic acid based inhibitors of autotaxin. *J. Med. Chem.* **2010**, *53*, 4958–4967.

[18] (a) Hutchinson, J. H.; Parr, T. A.; Roppe, J. R.; Stock, N. S.; Volkots, D. Heterocyclic autotaxin inhibitors and uses thereof. International Patent Application WO/2012/024620-A2, **2012**, Amira Pharmaceuticals, Inc.; (b) Roppe, J. R.; Parr, T. A.; Hutchinson, J. H. Heterocyclic autotaxin inhibitors and uses thereof. International Patent Application WO/2012/166415-A1, **2012**, Amira Pharmaceuticals, Inc.; (c) Roppe, J. R.; Parr, T. A.; Hutchinson, J. H. Heterocyclic autotaxin inhibitors and uses thereof. United States Patent Application US/2013/029948-A1, **2012**, Amira Pharmaceuticals, Inc.

[19] (a) Murph, M.; Tanaka, T.; Pang, J.; Felix, E.; Liu, S.; Trost, R.; Godwin, A. K.; Newman, R.; Mills, G. Liquid chromatography mass spectrometry for quantifying plasma lysophospholipids: potential biomarkers for cancer diagnosis. *Methods Enzymol*. 2007, *433*, 1–25. (b) Umezu-Goto, M.; Kishi, Y.; Taira, A.;Hama, K.; Dohmae, N.; Takio, K.; Yamori, T.; Mills, G. B.; Inoue, K.; Aoki, J.; Arai, H. Autotaxin has lysophospholipase D activity leading to tumor cell growth and motility by lysophosphatidic acid production. *J. Cell. Biol.* 2002, *158*, 227–233. (c) Imamura, S.; Horiuti, Y. Enzymatic determination of phospholipase D activity with choline oxidase. *J. Biochem.* 1978, *83*, 677–680. (d) Gijsbers, R.; Aoki, J.; Arai, H.; Bollen, M. The hydrolysis of lysophospholipids and nucleotides by autotaxin (NPP2) involves a single catalytic site. *FEBS Lett.* 2003, *538***,** 60–64.

[20] Takakusa, H.; Kikuchi, K.; Urano, Y.; Sakamoto, S.; Yamaguchi, K.; Nagano, T. Design and synthesis of an enzyme-cleavable sensor molecule for phosphodiesterase activity based on fluorescence resonance energy transfer. *J. Am. Chem. Soc.* **2002**, *124*, 1653–1657.

[21] Ferguson, C.; Bigman, C.; Richardson, R.; van Meeteren, L. A.; Moolenaar, W. H.; Prestwich, G. Fluorogenic phospholipid substrate to detect lysophospholipase D/autotaxin activity. *Org. Lett.* **2006**, *8*, 2023–2026.

[22] Kawaguchi, M.; Okabe, T.; Okudaira, S.; Nishimasu, H.; Ishitani, R.; Kojima, H.; Nureki, O.; Aoki, J.; Nagano. T. Screening and X-ray crystal structure-based optimization of autotaxin (ENPP2) inhibitors, using a newly developed fluorescence probe. *ACS Chem. Biol.* **2013**, *8*, 1713−1721.

[23] North, E. J.; Howard, A. L.; Wanjala, I. W.; Pham, T. C. T.; Baker, D. L.; Parrill, A. L. Pharmacophore development and application toward the identification of novel, small-molecule autotaxin inhibitors. *J. Med. Chem.* **2010**, *53*, 3095–3105.

[24] GVK Biosciences Private Limited, Plot No. 28 A, IDA, Nacharam Hyderabad – 500076, India.

[25] Fells, J. I.; Lee, S. C.; Fujiwara, Y.; Norman, D. D.; Lim, K. G.; Tsukahara, R.; Liu, J.; Patil, R.; Miller, D. D.; Kirby, R. J.; Nelson, S.; Seibel, W.; Papoian, R.; Parrill, A. L.; Baker, D. L.; Bittman, R.; Tigyi, G. Hits of a high-throughput screen identify the hydrophobic pocket of autotaxin/lysophospholipase D as an inhibitory surface. *Mol Pharmacol*. **2013**, *84*, 415–424.

[26] Fells, J. I.; Lee, S. C.; Norman, D. D.; Tsukahara, R.; Kirby, R. J.; Nelson, S.; Seibel, W.; Papoian, R.; Patil, R.; Miller, D. D.; Parrill, A. L.; Pharm, T. C.; Baker, D. L.; Bittman, R.; Tigyi, G. Targeting the hydrophobic pocket of autotaxin with virtual screening of inhibitors identifies a common aromatic sulfonamide structural motif. *FEBS J.* **2014**, *281*, 1017–1028.

[27] Hausmann, J.; Kamtekar, S.; Christodoulou, E.; Day, J. E.; Wu, T.; Fulkerson, Z.; Albers, H. M.; van Meeteren, L. A.; Houben, A. J.; van Zeijl, L.; Jansen, S.; Andries, M.; Hall, T.; Pegg, L. E.; Benson, T. E.; Kasiem, M.; Harlos, K.; Kooi, C. W.; Smyth, S. S.; Ovaa, H.; Bollen, M.; Morris, A. J.; Moolenaar, W. H.; Perrakis, A. Structural basis of substrate discrimination and integrin binding by autotaxin. *Nat. Struct. Mol. Biol.* **2011**, *18*, 198–204.

[28] Nishimasu, H.; Okudaira, S.; Hama, K.; Mihara, E.; Dohmae, N.; Inoue, A.; Ishitani, R.; Takagi, J.; Aoki, J.; Nureki, O. Crystal structure of autotaxin and insight into GPCR activation by lipid mediators. *Nat. Struct. Mol. Biol.* **2011**, *18*, 205–212.

[29] Keune, W.; Hausmann, J.; Bolier, R.; Tolenaars, D.; Kremer, A.; Heidebrecht, T.; Joosten, R. P.; Sunkara, M.; Morris, A. J.; Matas-Rico, E.; Moolenaar, W. H.; Oude Elferink, R. P.; Perrakis, A**.** Steroid binding to Autotaxin links bile salts and lysophosphatidic acid signalling. *Nat. Commun.* **2016**, *7*, article number 11248.

[30] Cole, J. C.; Nissink, J. W. M.; Taylor, R. *Protein-Ligand Docking and Virtual Screening with GOLD. Virtual Screening in Drug Discovery*, Shoichet, B., Alvarez, J., Eds., Taylor & Francis CRC Press, Boca Raton, Florida, USA, **2005**.

[31] Dassault Systèmes BIOVIA, *Discovery Studio Modelling Environment*, Release 4.5, San Diego: Dassault Systèmes, **2015**.

[32] Brooks, H. B.; Geeganage, S.; Kahl, S. D.; Montrose, C.; Sittampalam, S.; Smith, M. C.; Weidner, J. R. Basics of Enzymatic Assays for HTS In: *Assay Guidance Manual* [Online], Sittampalam, G. S.; Coussens, N. P.; Nelson, H., Eds., Eli Lilly & Company and the National Center for Advancing Translational Sciences, Bethesda, **2004**. Available from: https://www.ncbi.nlm.nih.gov/books/NBK53196/. Accessed December 8, 2016.

[33] van Meeteren, L. A.; Ruurs, P.; Christodoulou, E.; Goding, J. W.; Takakusa, H.; Kikuchi, K.; Perrakis, A.; Nagano, T.; Moolenaar, W. H. Inhibition of autotaxin by lysophosphatidic acid and sphingosine 1-phosphate. *J. Biol. Chem.* **2005**, *280*, 21155–21161.

[34] Copeland, R. A. *Evaluation of Enzyme Inhibitors in Drug Discovery: A Guide for Medicinal Chemists and Pharmacologists*. Wiley, New York, 2005. Chapter 3.2, page 53.

[35] Emsley, P.; Lohkamp, B.; Scott, W. G.; Cowtan, K. Features and development of Coot. *Acta Crystallogr., Sect. D: Struct. Chem.* **2010**, *66*, 486–501.

[36] Potterton, L.; McNicholas, S.; Krissinel, E.; Gruber, J.; Cowtan, K.; Emsley, P.; Murshudov, G. N.; Cohen, S.; Perrakis, A.; Noble, M. Developments in the CCP4 molecular-graphics project. *Acta Crystallogr., Sect. D: Biol. Crystallogr.* **2004**, *60*, 2288–2294.

[37] Perrin, D. D.; Armarego, W. L. F. *Purification of Laboratory Chemicals*. 3rd ed., Pergamon Press, Oxford, **1988**, 391.

[38] Huang, W. H.; Jia, W. L.; Wang, S., 7-Azaindolyl- and indolyl-functionalized starburst molecules with a 1,3,5-triazine or a benzene core – syntheses and luminescence. *Can. J. Chem.* **2006,** *84*, 477–485.

[39] Li, M.; Yamato, K.; Ferguson, J. S.; Gong, B. Sequence-specific association in aqueous media by integrating hydrogen bonding and dynamic covalent interactions. *J. Am. Chem. Soc.* **2006**, *128*, 12628–12629.

[40] Hausmann, J.; Christodoulou, E.; Kasiem, M.; De Marco, V.; van Meeteren, L. A.; Moolenaar, W. H.; Axford, D.; Owen, R. L.; Evans, G.; Perrakis, A. Mammalian cell expression, purification, crystallization and microcrystal data collection of autotaxin/ENPP2, a secreted mammalian glycoprotein. *Acta Crystallogr. Sect. F. Struct. Biol. Cryst. Commun.* **2010**, *66*, 1130–1135.

[41] Kabsch, W. XDS. *Acta Crystallogr., Sect. D: Biol. Crystallogr.* **2010**, *66*, 125–132.

[42] Evans, P. R. An introduction to data reduction: space-group determination, scaling and intensity statistics. *Acta Crystallogr., Sect. D: Biol. Crystallogr.* **2011**, *67*, 282–292.

[43] McCoy, A. Solving structures of protein complexes by molecular replacement with Phaser. *Acta Crystallogr., Sect. D: Biol. Crystallogr.* **2007**, *63*, 32–41.

[44] Murshudov, G. N.; Skubák, P.; Lebedev, A. A.; Pannu, N. S.; Steiner, R. A.; Nicholls, R. A.; Winn, M. D.; Long, F.; Vagin, A. A. REFMAC5 for the refinement of macromolecular crystal structures. *Acta Crystallogr., Sect. D: Biol. Crystallogr.* **2011**, *67*, 355–367.

[45] Joosten, R. P.; Long, F.; Murshudov, G. N.; Perrakis, A. The PDB_REDO server for macromolecular structure model optimization. *IUCrJ* **2014**, *1*, 213–220.[

[46] For details of this assay, see: Castagna, D.; Duffy, E. L.; Semann, D.; Young, L. C.; Pritchard, J. M.; MacDonald, S. J. F.; Budd, D. C.; Jamieson, C.; Watson, A. J. B. Identification of a novel class of autotaxin inhibitors through cross-screening. *Med. Chem. Commun.* **2015**, *6*, 1149–1155.

TABLE OF CONTENTS GRAPHIC